Dissertation

submitted to the

Combined Faculties for the Natural Sciences and for Mathematics

of the Ruperto-Carola University of Heidelberg, Germany

for the degree of

Doctor of Natural Sciences

presented by

Diplom-Biologe Hans-Martin Herz

born in: Ludwigsburg, Germany

Oral-examination: 8/29/2008

Control of non-autonomous cell survival and overgrowth and autonomous apoptosis by members of the ESCRT-II complex

Referees

PD Dr. Jörg Großhans

Prof. Dr. Andreas Bergmann

Acknowledgements

First of all, I want to express my gratitude to my boss Prof. Dr. Andreas Bergmann for allowing me to do my graduate work under his supervision in Houston. Considering the fact that I almost knew nothing about *Drosophila* genetics when I started, I really have come a far way in my understanding and appreciation of the importance of elucidating developmental mechanisms by powerful genetic approaches. Andreas was especially there in the beginning when my lack of experience and understanding of genetic principles did not allow me to see the big picture of my research, but later on also gave me plenty of opportunity to experiment on my own. These experiments were not all necessarily very effective or even successful, but they helped me to mature step by step. Looking back, I can see clearly how over the last four years Andreas raised me to scientific independence and that is probably the greatest recommendation that one can give to one's scientific supervisor.

Work in Andreas' lab was made particularly easy because of the cordial atmosphere among all the lab members. Everybody is willing to help out, discuss ongoing projects and to chat about all kinds of different topics. This contributed strongly to creating a positive working environment and enhanced the output of everybody considerably. Particularly, I am very thankful for the help I got from Zhihong Chen and Clare Bolduc. Zhihong taught me how to dissect imaginal discs from larvae and contributed herself significantly to many of my projects when especially in the beginning I was not fast enough yet or later on my schedule became to busy. Both Zhihong and Clare are highly esteemed for their organizational talent to keep the lab running smoothly. Clare is especially cherished for updating the stock list on a regular basis and for her support in injecting my *vps25* rescue constructs.

Namely, I want to thank all of the past and current lab members besides those already mentioned who made this time as a graduate student a very enjoyable one. These include Christian Antonio, Peter Cashio, Audrey Christiansen, Tian Ding, Tania Dutta, Yun Fan, Melinda Lackey, Tom Lee, Vani Rajendran, Vildan Sahin, Mayank Srivastava, Yuan Wang, Regina Willecke, Sarah Woodfield and Dongbin Xu.

Moreover, I want to take a step back and thank PD Dr. Jörg Großhans and his lab for making all that possible, specifically for opening up a way to perform my graduate studies outside Germany and officiate nevertheless as first supervisor for my PhD thesis. Starting out with cooking fly food, being incorporated into the lab and ultimately being able to finish my diploma thesis on a biochemical project certainly laid the ground work for my decision to move on and get some experience on *Drosophila* genetics as well. Having tasted the benefits of both, in the future my plan is to balance biochemical and genetic approaches.

Finally, my deepest gratitude is to my parents Wilhelm and Annegret Herz. I am very much aware of their continual love and support for me in all matters including my graduate work. Even though recently there was little chance to see each other in person the regular phone conversations largely contributed to make myself a partaker of the family life in my absence.

Summary

Appropriate cell-cell signaling is critical for proper tissue homeostasis. Protein sorting of cell surface receptors at the early endosome is important for both the delivery of the signal and the inactivation of the receptor, and its alteration can cause malignancies including cancer. In a genetic screen for suppressors of the pro-apoptotic gene *hid* in *Drosophila*, we identified two alleles of *vps25*, a component of the ESCRT machinery required for protein sorting at the early endosome. Paradoxically, although *vps25* mosaics were identified as suppressors of *hid*-induced apoptosis, *vps25* mutant cells die. However, we provide evidence that non-autonomous increase of Diap1 protein levels, an inhibitor of apoptosis, accounts for suppression of *hid*. Furthermore, before they die, *vps25* mutant clones trigger non-autonomous proliferation through a failure to down-regulate Notch signaling which activates the mitogenic JAK/STAT pathway. The apoptotic phenotype of *vps25* mutant tissue is the result of autonomous activation of at least two cell death pathways. Both Hid and JNK contribute to apoptosis of *vps25* mutant cells. Inhibition of cell death in *vps25* clones causes dramatic overgrowth phenotypes. In addition, Hippo signaling is increased in *vps25* clones, and *hippo* mutants completely block apoptosis in *vps25* clones.

Furthermore, we genetically analyze the remaining ESCRT-II components *vps22* and *vps36*. Like *vps25*, mutants in *vps22* and *vps36* display endosomal defects causing increased Notch and JAK/STAT signaling and autonomous cell death. However, while *vps22* mutants cause strong non-autonomous overgrowth, they do not affect non-autonomous apoptotic resistance. *vps36* mutants display the reciprocal phenotype and increase the apoptotic resistance, but have little effect on non-

autonomous proliferation. Therefore, despite their intimate physical relationship, the ESCRT-II components *vps22*, *vps25* and *vps36* display distinct genetic properties. In summary, the phenotypic analysis of *vps22*, *vps25* and *vps36* mutants highlights the importance of receptor down-regulation by endosomal protein sorting for appropriate tissue homeostasis, and may serve as a model for a better understanding of the mechanisms causing tumorigenesis in humans.

Zusammenfassung

Die Aufrechterhaltung der Integrität für die Signalübertragung zwischen Zellen ist eine notwendige Voraussetzung für die Homöostase im Organismus. Die Sortierung von Proteinen als Rezeptoren am frühen Endosom spielt dabei eine wichtige Rolle sowohl für die Übertragung des Signals als auch die Inaktivierung des Rezeptors. Regulatorische Veränderungen in diesem Prozess können unter anderem zur Entstehung von Krankheiten wie unter anderem auch der Krebsentwicklung beitragen.

In einem genetischen Screen für Suppressoren des proapoptotischen Gens *hid* in *Drosophila* haben wir zwei Allele von *vps25* identifiziert. Vps25 ist eine Komponente der ESCRT Maschinerie, die für die Sortierung von Proteinen am frühen Endosom benötigt wird. Paradoxerweise wurden *vps25* Mosaike als Suppressoren von *hid*-induzierter Apoptose identifiziert obwohl Zellen, die mutant für *vps25* sind, sterben. Wir zeigen jedoch, daß die nichtautonome Erhöhung von Diap1 Protein, einem Apoptoseinhibitor, für die Suppression von *hid* verantwortlich ist. Darüberhinaus lösen Klone die mutant fuer *vps25* sind nichtautonome Proliferation durch eine Störung im Abbau des Notch Rezeptors aus, dessen ektopische Aktivierung zur Stimulation des mitogenen JAK/STAT Signalweges führt. Der apoptotische Phänotyp von mutantem *vps25* Gewebe ist das Resultat autonomer Aktivierung von mindestens zwei Zelltod Signalwegen. Sowohl Hid als auch JNK tragen zur Apoptose von *vps25* mutanten Zellen bei. Eine Inhibition von Zelltod in *vps25* Klonen verursacht starke Überwachstumsphänotypen. Desweiteren ist die Signalübertragung durch den Hippo Signalweg in *vps25* Klonen erhöht und *hippo* Mutanten blockieren Apoptose vollständig in *vps25* Klonen.

Wir führen auch eine Analyse der anderen ESCRT-II Komponenten *vps22* und *vps36* durch. Wie im Fall von *vps25* zeichnen sich *vps22* und *vps36* Mutanten durch endosomale Defekte aus, die in erhöhter Notch und JAK/STAT Signalübertragung und automomem Zelltod resultieren. Überraschenderweise haben *vps22* Mutanten keine Auswirkung auf nichtautonome apoptotische Resistenz, verursachen aber starkes nichtautonomes Überwachstum. *vps36* Mutanten weisen hingegen einen reziproken Phänotyp auf, der sich durch eine Erhöhung der apoptotischen Resistenz auszeichnet, aber kaum nichtautonome Proliferation beeinflusst. Obwohl also *vps22*, *vps25* und *vps36* eine innige physikalische Verwandtschaft als ESCRT-II Komponenten teilen, haben sie verschiedenartige genetische Eigenschaften.

Zusammenfassend lässt sich sagen, dass die phänotypische Analyse von *vps22*, *vps25* und *vps36* Mutanten die Notwendigkeit der Regulation von Rezeptoren durch Sortierung von Proteinen am frühen Endosom hervorhebt, um eine adaequate Gewebshomöostase zu gewährleisten und ein Modell zu einem besseren Verständnis der Mechanismen bereitstellt, die zur Krebsentstehung im Menschen beitragen.

1 Index

2 Summary

Appropriate cell-cell signaling is critical for proper tissue homeostasis. Protein sorting of cell surface receptors at the early endosome is important for both the delivery of the signal and the inactivation of the receptor, and its alteration can cause malignancies including cancer. In a genetic screen for suppressors of the pro-apoptotic gene *hid* in *Drosophila*, we identified two alleles of *vps25*, a component of the ESCRT machinery required for protein sorting at the early endosome. Paradoxically, although *vps25* mosaics were identified as suppressors of *hid*-induced apoptosis, *vps25* mutant cells die. However, we provide evidence that non-autonomous increase of Diap1 protein levels, an inhibitor of apoptosis, accounts for suppression of *hid*. Furthermore, before they die, *vps25* mutant clones trigger non-autonomous proliferation through a failure to down-regulate Notch signaling which activates the mitogenic JAK/STAT pathway. The apoptotic phenotype of *vps25* mutant tissue is the result of autonomous activation of at least two cell death pathways. Both Hid and JNK contribute to apoptosis of *vps25* mutant cells. Inhibition of cell death in *vps25* clones causes dramatic overgrowth phenotypes. In addition, Hippo signaling is increased in *vps25* clones, and *hippo* mutants completely block apoptosis in *vps25* clones.

Furthermore, we genetically analyze the remaining ESCRT-II components *vps22* and *vps36*. Like *vps25*, mutants in *vps22* and *vps36* display endosomal defects causing increased Notch and JAK/STAT signaling and autonomous cell death. However, while *vps22* mutants cause strong non-autonomous overgrowth, they do not affect non-autonomous apoptotic resistance. *vps36* mutants display the reciprocal phenotype

and increase the apoptotic resistance, but have little effect on non-autonomous proliferation. Therefore, despite their intimate physical relationship, the ESCRT-II components *vps22*, *vps25* and *vps36* display distinct genetic properties. In summary, the phenotypic analysis of *vps22*, *vps25* and *vps36* mutants highlights the importance of receptor down-regulation by endosomal protein sorting for appropriate tissue homeostasis, and may serve as a model for a better understanding of the mechanisms causing tumorigenesis in humans.

3 Introduction

Regulation of tissue homeostasis involves the concerted action of several signaling pathways. An imbalance in this fine-tuned signaling network leads to overgrowth or apoptosis, and patterning defects in developing organisms. Hence, it is of exorbitant importance for the cell to hold excessive signaling in check for proper regulation of tissue homeostasis.

3.1 The significance of endosomal trafficking

Appropriate cell/cell signaling requires both coordinated activation and inactivation of cell surface signaling receptors. Usually, the receptors are bound by their respective ligands on the cell surface upon which they induce an intra-cellular response. An intrinsic part of this response is the recruitment of specific ubiquitin ligases that trigger ubiquitinylation of the receptor's cytoplasmic domain, usually mono-ubiquitinylation, which provides the signal for receptor internalization by endocytosis (reviewed in Hicke and Dunn, 2003; Haglund and Dikic, 2005; Hicke et al., 2005; Duncan et al., 2006; Huang et al., 2006). Endocytosis is regulated by Dynamin (*shibire* in *Drosophila*) which facilitates the formation of endocytic vesicles (reviewed in Hinshaw, 2000). Subsequently, the ubiquitinylated cargo is transported via these vesicles to an endosomal compartment and there undergoes Rab5-mediated fusion with the early endosome (Gorvel et al., 1991; Bucci et al., 1992). Recently, evidence has been accumulating that ascribes the early endosome a major function in regulating receptor sorting and signaling. The early endosome seems to form a hub for controlling the steady-state levels of cell surface receptors as well as their activation

by several mechanisms. First, the receptors may be recycled back to the cell surface which applies mostly to unliganded receptors. Second, the environment at the early endosome appears to be required for several signaling molecules as it brings the receptor/ligand complex in close proximity to intracellular signaling components and is thus required for regulation of receptor activation (Seto and Bellen, 2006) (reviewed in Gonzalez-Gaitan, 2003; Seto and Bellen, 2004; Le Roy and Wrana, 2005b). Third, it is also needed to turn off signaling (Urbanowski and Piper, 2001). This is achieved by the assembly of ubiquitinylated protein cargo into vesicles that pinch off from the limiting membrane of the early endosome into the lumen of emerging multi-vesicular bodies (MVB) (Felder et al., 1990; Odorizzi et al., 1998) (reviewed in Katzmann et al., 2002; Raiborg et al., 2003; Gruenberg and Stenmark, 2004; Babst, 2005; Hurley and Emr, 2006; Slagsvold et al., 2006; Saksena et al., 2007; Williams and Urbe, 2007; Hurley, 2008; Tanaka et al., 2008). In the process, MVBs mature to become late endosomes by fusing with vesicles that are derived from the trans-Golgi network (TGN) and contain the precursors of lysosomal enzymes. These hydrolases themselves are enzymatically tagged with mannose-6-phosphate in the *cis*-Golgi network and subsequently bind to mannose-6-phosphate receptors in the *trans*-Golgi network. The binding of the tagged hydrolases is released upon fusion of the *trans*-Golgi derived vesicles with the MVB due to a decreased luminal pH in the late endosome which is the result of acquisition of proton pumps (Nishi and Forgac, 2002). This allows for a recycling of the mannose-6-phosphate receptors back to the Golgi to be reused for additional transport cycles to the MVB. The dissociated hydrolases of the late endosome continue onward to the lysosome where they perform the degradation of internalized proteins (Luzio et al., 2007).

3.2 The ESCRT machinery is involved in receptor turnover at the early endosome

The sorting process of ubiquitinylated proteins at the early endosome into MVBs is highly regulated and requires class E Vps (Vacuolar Protein Sorting) proteins, first identified in *Saccharomyces cerevisiae* (Raymond et al., 1992). So far, fifteen class E Vps proteins have been described to participate in the formation of four ESCRT (Endosomal Sorting Complex Required for Transport) complexes: ESCRT-0, -I, -II and -III (reviewed in Katzmann et al., 2002; Gruenberg and Stenmark, 2004; Babst, 2005; Hurley and Emr, 2006; Slagsvold et al., 2006; Saksena et al., 2007; Williams and Urbe, 2007; Hurley, 2008; Tanaka et al., 2008). Besides many accessory proteins they are the major constituents in sorting the ubiquitinylated receptors into MVBs.

3.3 Function of ESCRT complexes on the early endosome

ESCRT-0, ESCRT-I and ESCRT-II bind ubiquitinylated receptors on early endosomes. According to the current model ESCRT-0 initiates the recruitment of the receptors and subsequently passes them on to the other ESCRT complexes in their numerical order. ESCRT-III catalyzes the internalization of the ubiquitinylated cargo into MVBs (reviewed in Babst, 2005; Hurley and Emr, 2006; Slagsvold et al., 2006; Saksena et al., 2007; Williams and Urbe, 2007; Hurley, 2008). This process separates the intracellular domain of activated signaling receptors from the cytosolic environment and thus, inactivates them.

3.3.1 Subunits of ESCRT complexes

ESCRT-0 is constituted by Vps27 (Hrs in metazoans) and Hse1 (STAM in metazoans) (Lohi and Lehto, 2001; Bilodeau et al., 2002). Vps23 (Tsg101 in metazoans), Vps28, Vps37 and Mvb12 form the 104 kD heterotetramer ESCRT-I (Katzmann et al., 2001; Kostelansky et al., 2007). ESCRT-II (Babst et al., 2002b) consists of the three subunits Vps22, Vps25 and Vps36. Vps2, Vps20, Vps24, Vps32 (synonymous: Snf7), Vps60 and Did2 associate to form the largest complex, ESCRT-III (Amerik et al., 2000; Howard et al., 2001; Kranz et al., 2001; Babst et al., 2002a; Nickerson et al., 2006).

3.3.1.1 ESCRT-0

Due to the current model the process of receptor internalization at the early endosome is initialized by the recruitment of GGA (Golgi-associated, γ-adaptin homologs, Arf-binding) proteins (Bonifacino and Traub, 2003; Bonifacino, 2004) and ESCRT-0 to the early endosomal membrane. The structures of the N-terminal VHS (Vps27, Hrs and STAM) and FYVE (Fab1, YOTB, Vac1 and EEA1) domains of Vps27 have been resolved to atomic scale (Mao et al., 2000). VHS domains are commonly found with proteins that are involved in intracellular trafficking. Vps27 binds to the endosome through the interaction of its FYVE domain with phospatidylinositol-3-phosphate (PtdIns3P) (Burd and Emr, 1998; Misra and Hurley, 1999; Raiborg et al., 2001b) which is highly enriched on early endosomal membranes. Vps27 and Hse1 form a heterodimer through their intertwined GAT domains (Prag et al., 2007) and both interact with ubiquitinylated receptors through their UIM (ubiquitin interaction motif) domains, respectively (Bilodeau et al., 2002; Raiborg et

al., 2002; Shih et al., 2002; Raiborg et al., 2003). Both, Vps27 with its C-terminus and Hse1 interact with Clathrin resulting in a flat Clathrin coat on the early endosome (ter Haar et al., 2000; Raiborg et al., 2001a; Raiborg et al., 2002; Sachse et al., 2002). This Clathrin coat is thought to act as an organizer or condensation point for ubiquitinylated cargo to allow for the proper initialization of subsequent ESCRT complex recruitment.

3.3.1.2 ESCRT-I

Vps27 then binds to the ESCRT-I complex through its interaction with the ESCRT-I subunit Vps23 (Bache et al., 2003a; Bilodeau et al., 2003; Katzmann et al., 2003; Lu et al., 2003). Involved in this interaction is a short amino acid motif of Vps27 (P(S/T)XP) and the UEV (ubiquitin E2 variant) domain of Vps23 (Pornillos et al., 2002a; Pornillos et al., 2002b; Pornillos et al., 2003) that also recognizes ubiquitinylated cargo . The ESCRT-I core has been crystallized and forms a fan-like structure with Vps23 in the middle and Vps37 and Vps28 on its sides (Kostelansky et al., 2006; Teo et al., 2006). A newly discovered ESCRT-I member Mvb12 seems to help stabilizing the complex and allows ESCRT-I oligomer formation, thus contributing to a higher efficiency of cargo sorting (Chu et al., 2006; Curtiss et al., 2007; Gill et al., 2007; Kostelansky et al., 2007; Oestreich et al., 2007).

3.3.1.3 ESCRT-II

In yeast ESCRT-I is directly connected to ESCRT-II by the association of the C-terminus of Vps28 (ESCRT-I) with a zinc finger-like domain (NZF1) of Vp36 (ESCRT-II) (Teo et al., 2006; Gill et al., 2007), which is not conserved in mammals.

Therefore, no direct link between ESCRT-I and ESCRT-II has been established in mammalian systems, yet. It should also be noted that ESCRT-I and –II in the yeast cytosol seem to co-exist as separate complexes suggesting the prerequisite of endosomal recruitment for their physical association (Katzmann et al., 2001; Babst et al., 2002b). Human Vps36 is also required for the binding of ESCRT-II to ubiquitinylated receptors and PtdIns3P by means of its N-terminal GLUE (Gram-like ubiquitin-binding in EAP45) domain in mammals. The binding of the GLUE domain to PtdIns3P is conserved in yeast as well. However, in yeast the association with ubiquitin is mediated by the NZF1 domain (Alam et al., 2004; Slagsvold et al., 2005; Alam et al., 2006; Hirano et al., 2006; Teo et al., 2006). Nonetheless, a general conservation of ESCRT-II in its ability to bind ubiquitinylated cargo and PtdIns3P can be observed. The core of the ESCRT-II complex has the shape of a Y and is a heterotetramer with one copy each of Vps36 and Vps22 and two copies of Vps25. The arms of the Y are formed by one of the Vps25 subunits and the stalk by Vps36 and Vps22. Each of the ESCRT-II subunits contains two tandem repeats of a winged helix domain that are involved in the protein interactions of the respective subunits (Hierro et al., 2004; Teo et al., 2004; Wernimont and Weissenhorn, 2004).

3.3.1.4 ESCRT-III

ESCRT-II is associated with ESCRT-III through the cooperative interaction of the C-terminus of Vps25 with Vps20, a myristoylated subunit of ESCRT-III (Hierro et al., 2004; Teo et al., 2004; Yorikawa et al., 2005). Vps20 with Vps32 and Vps2 and Vps24 are thought to form two subcomplexes (Babst et al., 2002a). Much of what is known about the structure of ESCRT-III is derived from crystallization studies on Vps24 (Muziol et al., 2006). Generally, all ESCRT-III-like proteins can be subdivided

in a basic N-terminal core with four α-helices (α1-α4) and an acidic C-terminal auto-inhibitory region that contains α-helix 5 and a MIR (MIT-interacting region) domain which prevents hetero- and homo-dimerization of individual ESCRT-III subunits by interacting with their respective core. It is inferred from the resolved structure of Vps24 that upon activation the release from the auto-inhibitory interaction of the MIR domain on the core of ESCRT-III components results in the formation of a flat lattice-like array of dimericing subunits along the endosomal membrane (von Schwedler et al., 2003; Tsang et al., 2006; Zamborlini et al., 2006). Upon release from its binding to the basic core the MIR domain is now free to recruit MIT-domain containing proteins such as deubiquitinylases (DUBs: Doa4 in yeast, AMSH and UBPY in mammals) (McCullough et al., 2004; Agromayor and Martin-Serrano, 2006; McCullough et al., 2006; Kyuuma et al., 2007; Ma et al., 2007; Row et al., 2007) or the AAA+ ATPase Vps4 (Babst et al., 1997; Babst et al., 1998; Scott et al., 2005b). These DUBs catalyze the removal of ubiquitin moieties from cargo proteins at the formation of the MVB (Luhtala and Odorizzi, 2004). This allows ubiquitin to be reused in other cellular contexts without undergoing proteolysis in the lysosome. Another *vps* protein Bro1 (ALIX in mammals) (Odorizzi et al., 2003) also seems to be involved in the activation of these DUBs (Richter et al., 2007) by forming a linker that binds to ESCRT-III (Luhtala and Odorizzi, 2004), but also interacts with ESCRT-I and Vps4 (Martin-Serrano et al., 2003a; von Schwedler et al., 2003; Bowers et al., 2004; Nikko and Andre, 2007).

3.3.2 Disassembly of ESCRT complexes

Vps4 with another protein Vta1 forms a complex that is involved in the disassembly of the ESCRT-III lattice from the endosomal membrane (Azmi et al.,

2006; Lottridge et al., 2006; Haas et al., 2007; Vajjhala et al., 2007; Azmi et al., 2008). Vta1 stimulates the ATPase activity of Vps4 by promoting the assembly of a double hexameric Vps4 ring. Furthermore, the binding of the ESCRT-III subunits Did2 and Vps2 to Vps4 suggest a cooperative regulation of Vps4 activity (Obita et al., 2007; Stuchell-Brereton et al., 2007). Based on structural and mechanistic studies of Vps4 the current model favors the idea that the Vps4 is involved in the disassembly of the ESCRT-III complex by pumping ESCRT-III monomers through the pore of its hexameric ring (Scott et al., 2005a).

3.3.3 Models of ESCRT function

Until recently the mode of action of individual ESCRT complexes at the early endosome was considered to be sequential. From the first step of recognition of ubiquitinylated cargo by ESCRT-0 a "conveyor belt" model was suggested in which the ubiquitinylated cargo would be passed on from complex to complex to be finally fed into the forming vesicles of the MVB (reviewed in Hurley and Emr, 2006). However, an explosion of data over the last few years now seems to paint a picture in which some of the obtained information is apparently hard to reconcile with a classical conveyor belt mechanism. It seems to become more and more apparent that a network of interactions between subunits of different ESCRT complexes and ESCRT-related proteins exists. Among others, this could be shown by different yeast two-hybrid analyses (Martin-Serrano et al., 2003a; von Schwedler et al., 2003; Bowers et al., 2004; Tsang et al., 2006) and it was already mentioned before that Bro1 forms a connection between ESCRT-I and –III (Luhtala and Odorizzi, 2004). Therefore, another model has recently gained attraction in which ESCRT-0, -I and –II would co-assemble to cluster multiple ubiquitinylated receptors together. The assembly of

ESCRT-III at the perimeter of this ESCRT-0/I/II supercomplex would recruit the disassembly machinery (Bro1, Doa4 and Vps4) and after dissociation of the supercomplex catalyze the removal of ubiquitin from receptors and disassemble ESCRT-III from the endosomal membrane resulting in scission of the intraluminal vesicles of the MVB (Kostelansky et al., 2007; Nickerson et al., 2007).

3.4 *vps* mutant phenotypes

As crucial regulators of receptor turnover at the early endosome it is easy to imagine that interfering with the process of intraluminal vesicle formation by abolishing the function of individual members of the ESCRT machinery one might expect profound effects on the cell's ability to keep excessive signaling in check. Mutants of ESCRT genes have been first described by their characteristic mutant phenotype in yeast. Interference with their function in MVB formation on the early endosome results in aberrantly shaped class E compartments (Raymond et al., 1992). Class E compartments represent malformed endosomal structures which are located adjacent to the yeast vacuole and accumulate ubiquitinylated cargo on their limiting membrane (reviewed in Katzmann et al., 2002). Mutations in genes with this phenotype consequently were termed *vacuolar protein sorting* (*vps*) implying their important function in regulating MVB formation. Compared to their spherical wild-type counterparts MVBs in *vps* mutants consist of cisternae-like structures that form unconnected sheets of membrane which lie on top of each other (Nickerson et al., 2006). Biochemical studies in mammalian cell lines have revealed a similar function for endosomal protein sorting (Scheuring et al., 1999; Babst et al., 2000; Bishop and Woodman, 2000; Yoshimori et al., 2000; Howard et al., 2001; Scheuring et al., 2001;

Bache et al., 2003a; Bache et al., 2003b; Fujita et al., 2003; Bache et al., 2004; Peck et al., 2004). In *Drosophila*, among class E *vps* genes only mutations in *hrs* have been reported (Lloyd et al., 2002; Jekely and Rorth, 2003). Loss of *hrs* leads to accumulation of the epidermal growth factor receptor (EGFR), PVR (PDGF/VEGF receptor), Notch, Patched, Smoothened, and Thickveins on enlarged early endosomes consistent with a conserved role of *hrs* for endosomal protein sorting.

3.5 Endosomal regulation of Notch signaling activity

The regulation of Notch (N) activation through endocytosis has lately become the focus of several studies (reviewed in Le Borgne and Schweisguth, 2003a; Le Borgne et al., 2005; Le Borgne, 2006). The principle of signal transduction in the N pathway appears to be relatively simple on the first sight. N, as a transmembrane receptor is regulated by its ligands Delta (Dl) and Serrate (Ser) in *Drosophila* (Fehon et al., 1990). Upon ligand binding the N receptor undergoes two proteolytic cleavages. The first cleavage (S2 cleavage) occurs in the extracellular space and is catalyzed by the ADAM/TACE/Kuzbanian-family of metalloproteases (Qi et al., 1999; Brou et al., 2000; Mumm et al., 2000). The second cleavage (S3 cleavage) is mediated by γ-secretase, a protein complex that contains the subunits Presenilin, Nicastrin, PEN2 and APH1 (Kopan et al., 1996; Schroeter et al., 1998; De Strooper et al., 1999; Struhl and Greenwald, 1999; Wolfe et al., 1999; Ye et al., 1999) (reviewed in Mumm and Kopan, 2000; Fortini, 2002; Selkoe and Kopan, 2003) which releases the intracellular domain of N for translocation into the nucleus. Once there, the intracellular domain of N forms a complex with the DNA-binding protein Suppressor of Hairless (Su(H)) (Fortini and Artavanis-Tsakonas, 1994; Tamura et al., 1995), the co-factor Mastermind (Mam) (Petcherski and Kimble, 2000; Wu et al., 2000; Zhou et al., 2000)

and additional other co-factors and replaces certain co-repressors to activate transcription of various N target genes (reviewed in Schweisguth, 2004; Bray, 2006; Fiuza and Arias, 2007) among which are *Enhancer of Split* (*E(spl))* (Jennings et al., 1994; Bailey and Posakony, 1995) and *cut* (de Celis et al., 1996; Micchelli et al., 1997).

Despite the simplicity of this pathway the roles that the N pathway plays in development are very diverse and in many cases just poorly understood. This is largely due to the fact that the N pathway is controlled at many levels which allows for its great diversity in regulation. Therefore, it is not surprising that N signaling has been described to be involved in a multitude of developmental decisions. The N pathway mainly operates by regulating cell fate decisions, cell proliferation and cell death. However, the misregulation of these processes is the cause for the development of various cancers. The oncogenic potential of N was first described in studies on T-cell acute lymphoblastic leukemias (Reynolds et al., 1987; Ellisen et al., 1991; Weng et al., 2004), but later also for epithelial tumors (Gallahan and Callahan, 1987; Uyttendaele et al., 1996) such as human breast cancers (Weijzen et al., 2002) and other cancers (reviewed in Allenspach et al., 2002; Radtke and Raj, 2003; Grabher et al., 2006; Miele et al., 2006).

More recently as mentioned above there has been accumulating evidence that endocytosis plays a prominent role in the regulation of Notch signaling (reviewed in Le Borgne and Schweisguth, 2003a; Le Borgne et al., 2005; Le Borgne, 2006). The first report opening a link to the control of N signaling through endocytosis was described by the analysis of temperature-sensitive *shibire* mutants which encode the

Drosophila homolog of Dynamin, a GTPase that is required to catalyze the pinching off of vesicles from the plasma membrane (Poodry, 1990; Chen et al., 1991; van der Bliek and Meyerowitz, 1991). Shibire has been shown to be required in both signal sending and receiving cells in Dl-dependent N signaling (Seugnet et al., 1997). The presence of Dl and Ser in intracellular vesicles which are absent in *shibire* mutants (Kramer and Phistry, 1996) and their uptake into living cells (Le Borgne and Schweisguth, 2003b) further supported the involvement of the endocytic machinery. Mutations in *liquid facets* (*lqf*, homolog of *epsin*), an ubiquitin binding protein, *neuralized* and *mindbomb* have been demonstrated to interfere with Dl (for *mindbomb* also Ser) internalization and signaling. *epsin* mutants result in the accumulation of Dl at the cell surface because of reduced levels of endocytosis (Overstreet et al., 2004; Tian et al., 2004; Wang and Struhl, 2004). Neuralized (Deblandre et al., 2001; Lai et al., 2001; Pavlopoulos et al., 2001; Yeh et al., 2001) and Mindbomb (Itoh et al., 2003; Lai et al., 2005) are E3 ubiquitin ligases that bind and ubiqutinylate Dl (Ser) and thus promote its endocytosis. Consistent with their role in regulating Dl all three have been shown to control N signaling non-autonomously (Pavlopoulos et al., 2001; Itoh et al., 2003; Le Borgne and Schweisguth, 2003b). Besides the requirement of endocytosis for N ligands recent data also suggests that endocytosis precedes S3 cleavage of S2 cleaved N and that endocytois as well as S3 cleavage of N are regulated by its mono-ubiquitinylation on the intracellular domain (Gupta-Rossi et al., 2004). However, controversial data exist on this issue (Struhl and Adachi, 2000). Therefore, as of now, no conclusive inferences can be drawn as to whether the S3 cleavage of N occurs at the plasma membrane or after endocytosis in an endocytic compartment. One reason to explain the difference in these apparently contradicting findings might be the fact that ligand-dependent S3 cleavage of N occurs at another cellular location

(plasmamembrane) (Tarassishin et al., 2004) than a postulated ligand-independent S3 cleavage (endocytic compartment) (Vetrivel et al., 2004). However, there is no doubt that the endocytic pathway plays an important role in the degradation of the N receptor. One of the mediators of targeting N to lysosomal compartments is Cbl, an E3 ubiquitin ligase (Jehn et al., 2002) and also two other E3 ubiquitin ligases, Nedd4 (Sakata et al., 2004; Wilkin et al., 2004) and Suppressor of Deltex (Fostier et al., 1998; Cornell et al., 1999). Both, Nedd4 and Supressor of Deltex antagonize Deltex a third E3 ubiquitin ligase which positively regulates N signaling (Diederich et al., 1994; Matsuno et al., 1995; Cornell et al., 1999; Sakata et al., 2004). This seems to imply that ubiquitinylation represents a significant regulatory mechanism to target N for endocytic degradation. Furthermore as already mentioned above, in *hrs* mutant clones N also co-localizes with a marker that recognizes ubiquintinylated prtoteins (Jekely and Rorth, 2003).

3.6 Non-endosomal functions of ESCRT components

In addition to their function in endosomal trafficking ESCRT subunits also have been reported to be involved in various other cellular processes. These include topologically related processes such as the regulation of virus budding (reviewed in Pornillos et al., 2002c; Demirov and Freed, 2004; Morita and Sundquist, 2004; Fujii et al., 2007; Martin-Serrano, 2007; Welsch et al., 2007) and the regulation of cytokinesis (Spitzer et al., 2006; Carlton and Martin-Serrano, 2007; Morita et al., 2007; Dukes et al., 2008). However, there is no direct requirement for the ESCRT machinery in exosome secretion -another analogous event- as has been previously suggested (Trajkovic et al., 2008) (reviewed in Thery et al., 2002; de Gassart et al., 2004). This seems to imply that the cell utilizes other factors besides ESCRT which

convey the recruitment of protein cargo for recycling to the plasma membrane or the shedding into the extracellular lumen through MVBs.

Surprisingly, more and more evidence has been accumulating that ascribes unique functions to the ESCRT machinery that apparently appear to be independent of its 'classical' role of catalyzing scission events on membranes. Some of these are the regulation of transcription (Shilatifard, 1998; Sun et al., 1999; Feng et al., 2000; Kamura et al., 2001; Burgdorf et al., 2004), regulation of chromatin modification (Stauffer et al., 2001), regulation of mRNA localization (Irion and St Johnston, 2007) and regulation of the cytoskeleton (Xie et al., 1998; Feng et al., 2000; Schmidt et al., 2003; Sevrioukov et al., 2005).

3.6.1 Endosome-related functions of ESCRT components

3.6.1.1 Virus budding

In order to be able to bud from their host cells some retroviruses need to hijack the cellular ESCRT machinery (Garrus et al., 2001; Martin-Serrano et al., 2003b; Stuchell et al., 2004). The release of virions from the cell is mediated by Late (L) domain-containing proteins. L domains contain a short amino acid motif with the consensus P(T/S)XP (X can be any amino acid) (Demirov and Freed, 2004) that is identical to the tetrapeptide in Vps27 (ESCRT-0) which mediates the interaction with Vps23 (ESCRT-I) (Pornillos et al., 2003; Bouamr et al., 2007). The PTAP sequence of the HIV-1 Gag protein can mimic this recruitment step by interacting with Vps23 allowing HIV-1 to bud out of the host cytosol through the ESCRT machinery (Pornillos et al., 2003). This budding process is analogous in its function to the events

that lead to receptor internalization on the early endosome and is also used in the same way by other viruses such as Hepatitis B virus (Lambert et al., 2007), Ebola virus (Martin-Serrano et al., 2001; Licata et al., 2003), Rous sarcoma virus (Johnson et al., 2005; Medina et al., 2005), Bluetonge virus or African horse sickness virus (Wirblich et al., 2006). However, the virus egress of at least HIV-1 does not seem to require ESCRT-II suggesting context- or even subunit-specific requirements for ESCRT components (Langelier et al., 2006).

3.6.1.2 Cytokinesis

A subunit-specific requirement of ESCRTs has also been suggested for cytokinesis. In dividing cells Tsg101 (Vps23) and ALIX (Bro1) are initially concentrated at the centrosome but are subsequently recruited to the midbody by interaction with Centrosome protein 55 (Cep55). Cep55 is essential for the abscission event of the two daughter cells at the midbody a structure that contains proteins that are required for cell cleavage. Over-expression of either ESCRT-I or –III components or Vps4 results in multinucleated cells. Yet, this phenotype cannot be observed when ESCRT-II subunits are over-expressed (Carlton and Martin-Serrano, 2007; Morita et al., 2007). Cytokinesis is a topologically related event to virus budding and shows obvious parallels regarding the mechanisms that have been established to successfully achieve membrane scission events.

3.6.2 Endosome-independent functions of the ESCRT machinery

3.6.2.1 Regulation of transcription and chromatin modification

Strikingly, mammalian ESCRT-II components were first described to be involved in modifying RNA polymerase II activity (Shilatifard, 1998; Kamura et al., 2001). The transcription elongation factor ELL was purified as a multiprotein complex containing three additional proteins which turned out to be ELL-associated protein 45 (EAP45), EAP30 and EAP20 which are the mammalian homologues of Vps36, Vps22 and Vps25. Together with ELL they form an 'holo-ELL' complex which increases the efficiency of transcription elongation *in vitro* (Shilatifard, 1998). In addition, Tsg101 (Vps23) a mammalian ESCRT-I member has been described to control androgen receptor-mediated transcription (Sun et al., 1999; Burgdorf et al., 2004). Depending on the context it either activates (Burgdorf et al., 2004) or represses (Sun et al., 1999) androgen receptor-controlled target genes. Furthermore, the ESCRT-III component CHMP1 (Did2) was originally identified as a nuclear matrix interactor and has been shown to be involved in chromatin regulation by recruiting the Polycomb group (PcG) protein BMI1 to heterochromatic regions of the genome (Stauffer et al., 2001). This suggests that ESCRT subunits also play a crucial role beyond the regulation of MVB formation and topologically related processes such as virus budding and cytokinesis.

3.6.2.2 Regulation of mRNA localization

One further example of an endosomal-independent function of ESCRT members is their role in the localization of *bicoid* mRNA in the *Drosophila* egg. *bicoid* mRNA is localized to the anterior part of the embryo and results in a smooth

Bicoid morphogen gradient that sets up the patterning of the head and thorax of the *Drosophila* embryo. All three ESCRT-II components have been shown to be necessary for this localization step (Irion and St Johnston, 2007). Interestingly, the interaction with the 3' untranslated region of *bicoid* mRNA is mediated by the GLUE domain of Vps36. This implies a dual function of Vps36 in binding to ubiquitinylated cargo at the endosome on the one hand and on the other hand its ability to mediate an association with *bicoid* mRNA. It is striking that the interaction with *bicoid* mRNA solely relies on ESCRT-II subunits and is independent of at least Hrs (Vps27, ESCRT-0), Vps23 (Erupted in *Drosophila*) and Vps28 (both ESCRT-I) and Vps32 (ESCRT-III).

3.6.2.3 Regulation of the cytoskeleton

From very early on, studies have been suggesting an involvement of Vps23 (Tsg101) in organizing the microtubule cytoskeleton (Xie et al., 1998; Feng et al., 2000). Additionally, a recent study on *Drosophila* embryos lacking Vps28 reveals cellularization defects as a result of a malfunctioning actin cytoskeleton (Sevrioukov et al., 2005) corroborating the idea of ESCRT involvement in cytoskeletal regulation. However, so far the molecular mechanism that drives those events has not been identified, yet. It is however possible that ALIX (Bro1) might perform a mediating function in this process as it has been proposed as an interactor with both actin and microtubules (Schmidt et al., 2003; Cabezas et al., 2005).

3.7 ESCRT in pathogenesis and disease

The endosomal system is crucial to maintain proper tissue homeostasis by controlling various signaling pathways and mediating the decision of receptor internalization at the forming MVB resulting in receptor recycling or lysosomal degradation (see also: 'The significance of endosomal trafficking'). Therefore, an impairment of the signaling events of various crucial pathways caused by dysfunctional endosomal machinery such as ESCRT might have fatal consequences for an organism. Furthermore, defects in non-endosomal ESCRT-mediated processes can result in apoptosis (Krempler et al., 2002; Wagner et al., 2003; Carstens et al., 2004), autophagy (Filimonenko et al., 2007; Lee et al., 2007; Rusten et al., 2007a; Rusten et al., 2007b; Lee and Gao, 2008), neurodegeneration (Yamada et al., 2001; Sweeney et al., 2006; Filimonenko et al., 2007; Lee et al., 2007; Rusten et al., 2007a; Lee and Gao, 2008) and disruption of cell cycle control (Li et al., 2001; Ruland et al., 2001; Krempler et al., 2002; Oh et al., 2002; Carstens et al., 2004) some of which are the cause of cancer.

Additionally, the central role of the endosomal system has also been used by pathogens to exit or enter the cell. Under 'virus budding' we have already discussed how this is attained by retroviruses through hijacking the ESCRT machinery of the host cell. In order to survive, replicate and evade the immune system many other pathogens besides viruses including bacteria and parasites make use of the cellular machinery that controls the endosomal pathway. However, they have developed remarkable strategies in order to avoid degradation in the lysosome (Gruenberg and van der Goot, 2006). The mechanisms how this is achieved are complex and vary considerably between different species but ultimately serve the purpose of evading the

endosomal pathway before the pathogen enters the lysosome. Now, new evidence also implies the ESCRT machinery as a modulator of the mycobacterial phagosome (Vieira et al., 2004; Philips et al., 2008).

3.7.1 Modulation of the mycobacterial phagosome by the ESCRT machinery

Upon infection with pathogens the host defense of an organism reacts by recruiting macrophages to the infected site. Macrophages are specialized cells that internalize pathogenic invaders and exterminate them by forming pathogen-containing phagosomes which through the endosomal pathway are delivered to the lysosome for degradation. In order to resist the hydrolytic breakdown in the phagolysosome mycobacteria have developed a survival mechanism within macrophages to prevent further maturation of phagosomes. They are able to arrest phagosomal maturation at an early stage as has been determined by the absence of late endosomal markers by co-opting the cellular machinery of their host (Russell, 2001). The family of mycobacteria contains prominent members such as *Mycobacterium tuberculosis* which is the cause of approximately two million deaths every year. Now, ESCRT components are also surfacing as modulators of mycobacterial phagosomes. Earlier studies already suggested a role for Hrs (Vps27) in the arrest of mycobacterial phagosome maturation (Vieira et al., 2004). Furthermore, knockdown experiments with RNAi directed against Vps28, Tsg101 (Vps23) and Vps32 show an increase in mycobacterial proliferation (Philips et al., 2008) ascribing at least some ESCRT members an essential role in restricting bacterial growth.

3.7.2 The ESCRT machinery and cancer

Several regulatory pathways need to be altered for cancer to be initiated, expand and ultimately metastasize. As mentioned above the ESCRT machinery plays a crucial role in controlling essential processes like the cell cycle, autophagy and apoptosis which all have been implicated in various kinds of cancers and other diseases (Abrams, 2002; Hipfner and Cohen, 2004; Kastan and Bartek, 2004; Lowe et al., 2004; Massague, 2004; Mathew et al., 2007; Levine and Kroemer, 2008).

3.7.2.1 Cell cycle control

The versatile potential of Tsg101 (Vps23) to act in various cellular processes could also be extended to its ability to control the cell cycle (Li et al., 2001; Krempler et al., 2002; Oh et al., 2002; Carstens et al., 2004). This is true for two factors –p53 and p21- that take center stage in negatively regulating the progression of the cell cycle (Li et al., 2001; Ruland et al., 2001). Tsg101 affects p53 protein stability by stimulating its proteasomal degradation through the ubiquitin ligase MDM2. This is achieved by binding of Tsg101 to mono-ubiquitinylated MDM2 via its UEV (ubiquitin E2 variant) domain. The formation of a Tsg101/MDM2 complex is believed to prevent further poly-ubiquitinylation and thus to stabilize MDM2 (Li et al., 2001).

3.7.2.2 Autophagy and neurodegeneration

Autophagy is a cellular pathway that is utilized to remove damaged intracellular constituents, turn over organelles or remove protein aggregates but is also required during starvation periods to maintain the basic functions of the cell through

degradation of dispensable proteins or organelles. The mechanisms regulating autophagy are complex but ultimately serve the goal of homeostatic maintenance and viability of the organism (reviewed in Maiuri et al., 2007; Mathew et al., 2007; Mizushima, 2007; Xie and Klionsky, 2007; Levine and Kroemer, 2008). A host of factors is involved in the induction of autophagosome formation. Ultimately, the autophagocytosed material has to be degraded through the lysosomal system. Now, new evidence suggests that this interaction of the autophagosome pathway occurs at the level of the MVB. Recently, several reports have been implicating the ESCRT machinery in the removal of protein aggregates through autophagosome formation, making a functional MVB the key player therein (Filimonenko et al., 2007; Lee et al., 2007; Rusten et al., 2007b; Lee and Gao, 2008). Protein aggregation is one of the hallmarks of neurodegenerative diseases such as frontotemporal dementia linked to chromosome 3 (FTD3) (Skibinski et al., 2005), amyotrophic lateral sclerosis (ALS) (Parkinson et al., 2006), hereditary spastic paraplegia (Reid et al., 2005) or Huntington's disease (Rusten et al., 2007b), all of which could be linked indirectly or directly to impaired ESCRT function in these studies.

3.7.2.3 Apoptosis

There are several reports that suggest an involvement of ESCRT members and related proteins in the regulation of cell death (Krempler et al., 2002; Wagner et al., 2003; Carstens et al., 2004; Mahul-Mellier et al., 2006; Khoury et al., 2007). Programmed cell death or apoptosis is involved in the removal of supernumerary or damaged cells during development of all organisms (Jacobson et al., 1997; Baehrecke, 2002). The cell contains an extrinsic and an intrinsic program to execute apoptosis. The extrinsic program is activated through death receptors that pass the death signal

on by adaptor proteins. Ultimately the executioners of cell death –the caspases- are being activated. Caspases are cysteine proteases which upon activation cleave a set of target proteins at distinct loci after an aspartate residue. The cleavage of caspase targets results either in activation or inactivation of caspase substrates and ensures a regulated disintegration of the cell. Hallmarks of apoptotic cells are a loss of cell shape, membrane blebbing, nuclear condensation and DNA laddering. Ultimately, the dead cells are engulfed by neighboring tissue thus allowing a recycling of residual material. The intrinsic cell death pathway is regulated by pro- and anti-apoptotic proteins which control the integrity of the mitochondrial outer membrane. If for a reason a cell is depleted of survival factors or receives pro-apoptotic insults a cell death response is initiated which results in the release of mitochondrial proteins - among which are cytochrome c, Smac/DIABLO, Omi/Htra2, Endo G and AIF- into the cytoplasm. Smac/DIABLO and Omi/Htra2 bind to Inhibitor of apoptosis proteins (IAPs). This binding releases the inhibitory interaction of IAPs with initiator caspases such as Caspase-9 and results in the formation of the apoptosome. The apoptosome as the major death initiating complex has to be assembled by the association of cytochrome c with the scaffolding protein Apaf-1 and the recruitment of Caspase-9. Activation of the apoptosome in turn induces downstream effector caspases that initiate the afore mentioned regulated destruction of the cell (reviewed in Hengartner, 2000; Meier et al., 2000a; Danial and Korsmeyer, 2004; Hay et al., 2004; Taylor et al., 2008). It has been confirmed that the basic core machinery which is involved in the execution of the apoptotic program is conserved from *Caenorhabditis elegans*, over *Drosophila melanogaster* to mammals (reviewed in Jacobson et al., 1997; Meier et al., 2000a; Baehrecke, 2002; Hay et al., 2004).

Cell death in *Drosophila* is under control of the pro-apoptotic genes *reaper* (White et al., 1994), *head involution defective* (*hid*) (Grether et al., 1995), and *grim* (Chen et al., 1996; reviewed in Bergmann et al., 2003). Expression of these genes results in caspase activation, most notably Dronc (Dorstyn et al., 1999), the Caspase-9 homolog. In living cells, Dronc is kept inactive by binding to Diap1 (*Drosophila* inhibitor of apoptosis protein 1) to prevent cell death (Meier et al., 2000b; reviewed in Bergmann et al., 2003). Reaper, Hid, and Grim induce cell death through binding to and stimulation of proteolytic degradation of Diap1 (Holley et al., 2002; Ryoo et al., 2002; Yoo et al., 2002). Dronc is released from Diap1 inhibition, and forms with the scaffolding protein Ark (Rodriguez et al., 1999; Zhou et al., 1999; Igaki et al., 2002) the active apoptosome, which activates DrICE (Fraser and Evan, 1997; Fraser et al., 1997) and DCP-1 (Song et al., 1997), Caspase-3-like proteins, inducing cell death.

3.7.2.4 ESCRT members as tumor suppressors

In addition, human *hrs* (*vps27*) and *Tsg101* (*vps23*) have been linked to a number of tumors including cervical, breast, prostate and gastrointestinal cancers (Li and Cohen, 1996; Gayther et al., 1997; Lee and Feinberg, 1997; Li et al., 1997; Steiner et al., 1997; Sun et al., 1997; Lin et al., 1998; Oh et al., 2007; Toyoshima et al., 2007). Most of these studies found genomic deletions or aberrant splicing of *Tsg101* in certain breast cancers. However, the picture becomes increasingly more complex. It turned out that the reported aberrant splicing of *Tsg101* in some tumor cell lines are in fact alternative splice products of *Tsg101* (Steiner et al., 1997). Moreover, *Tsg101* knockout mice die early in embryogenesis, but neither *Tsg101* haploinsufficient nor conditional knockout mice show any signs of tumorous

phenotypes (Wagner et al., 2003). In contrast, a variety of cancers show increased levels of Hrs and Tsg101 and their over-expression result in malignant transformation in mammary glands of ageing female mice (Oh et al., 2007; Toyoshima et al., 2007). In summary, this points toward a mild oncogenic property of Hrs and Tsg101 in mammary glands. Even though the present data seems to imply an involvement of ESCRT in tumor formation and or control a mechanistic model for the tumorous phenotypes associated with *hrs* and *Tsg101* mutations or over-expression has not been brought forward yet.

4 Results

4.1 Control of non-autonomous cell survival and overgrowth and autonomous apoptosis by *vps25*

4.1.1 Identification of *K2* and *N55* as mutants of the *Drosophila vps25* homolog

Over-expression of the pro-apoptotic gene *hid* under control of the eye-specific *Glass Multimer Reporter* (*GMR-hid*) causes a strong eye-ablation phenotype as a result of induction of apoptosis (Fig. 3A) (Grether et al., 1995). Using the recently described *GheF* (*GMR-hid ey-FLP*) method (Xu et al., 2005) we conducted an EMS-mutagenesis screen on chromosome arm 2R aimed at identifying recessive suppressors of the *GMR-hid* eye-ablation phenotype (not performed by me, Fig. 1). The *GheF* method takes advantage of the *ey-FLP*/*FRT* system which induces homozygous mutant clones specifically in the eye by mitotic recombination (Xu and Rubin, 1993; Newsome et al., 2000). Mutants which suppress the *GMR-hid* eye-ablation phenotype were selected for further analysis.

In the *GheF* screen, two mutants, *su*(*GMR-hid*)*K2* and *su*(*GMR-hid*)*N55* (referred to as *K2* and *N55*) were independently recovered as moderately strong recessive suppressors of the *GMR-hid* eye ablation phenotype (Fig. 3B, C). These mutants are homozygous lethal in *trans* to each other, thus affecting the same genetic function. By P-element (Zhai et al., 2003) (Fig. 2) and deficiency mapping, *K2*/*N55* was located to the cytological region 44D4-44D5 on the polytene map. Both alleles failed to complement the lethality of a P-element-induced mutation (l(2)*44Db*^{k08904})

which is inserted in the gene *CG14750*. DNA sequencing of *CG14750* of *K2* revealed a transversion from T to A in the second base of the only intron presumably causing a splicing defect and subsequently premature termination of translation by an in-frame stop codon in the intron (Fig. 3M). *CG14750* of *N55* carries a premature termination codon at amino acid 93 (Fig. 3M). Genomic constructs of *CG14750* rescue the phenotypes associated with *K2* and *N55* mutants (data not shown) suggesting that *K2* and *N55* affect *CG14750* (further details under 'Materials and methods').

A BLAST search identified *CG14750* as the *Drosophila* homologue of *vps25* in *S. cerevisiae*. It is a member of the class E Vps proteins (Raymond et al., 1992), and a component of ESCRT-II, which functions to catalyze the feeding of ubiquitinylated transmembrane receptors into intraluminal vesicles of MVBs, targeting them for degradation in lysosomes. From now on, we refer to *K2* and *N55* as $vps25^{K2}$ and $vps25^{N55}$, respectively. *Drosophila vps25* encodes a protein of 174 amino acids and contains two winged helix (WH) domains, WHA and WHB (Fig. 3M). Because both WHA and WHB are essential for ESCRT-II function (Hierro et al., 2004; Teo et al., 2004) and because of the molecular lesions of $vps25^{K2}$ and $vps25^{N55}$ (Fig. 3M), these alleles are likely to be very strong hypomorphic alleles, if not null alleles. Recently, two papers reported the isolation of *vps25* mutants in entirely different genetic screens (Thompson et al., 2005; Vaccari and Bilder, 2005). Our phenotypic characterization of *vps25* is largely consistent with these studies.

4.1.2 Characterization of *vps25* alleles

To characterize these alleles, we induced $vps25^{K2}$ and $vps25^{N55}$ mosaics via the *ey-FLP*/*FRT* system in the eye (without simultaneous expression of *GMR-hid*). Surprisingly, homozygous mutant clones (marked by absence of red eye pigment, compare to Fig. 3D) were not recovered, although the twin-spots were (Fig. 3E, F) suggesting that the mosaic eyes are composed of wild-type and heterozygous tissue (marked by red eye pigment). Even more surprisingly, $vps25^{K2}$ (Fig. 3E) and $vps25^{N55}$ (Fig. 3F) mosaic eyes were larger than a wild-type control (Fig. 3D). Thus, the mutant clones do not contribute to the adult eye tissue, but appear to be able to induce overgrowth in wild-type tissue. Analysis of third instar eye-antennal $vps25^{K2}$ (Fig.3H) and $vps25^{N55}$ (Fig. 3I) mosaic discs confirms these conclusions. These discs are overgrown and disorganized compared to wild-type (Fig. 3G). At this stage, mutant clones are detectable (marked by absence of GFP labeling in Fig. 3H, I). However, as shown below, they are eliminated by apoptosis.

These results pose an apparent paradox. Although we identified $vps25^{K2}$ and $vps25^{N55}$ as recessive suppressors of *GMR-hid*, the mutant clones do not survive. We determined whether $vps25^{K2}$ and $vps25^{N55}$ mutant clones contribute to the suppression of *GMR-hid* by clonal analysis. However, the *GMR-hid* transgene used for *GheF* screening is marked with w^+, and does not allow a clonal analysis based on red/white pigment selection in eyes. Thus, we generated a *GMR-hid* transgene which has lost w^+, termed $GMR\text{-}hid^{w-}$, allowing the determination of the genetic identity of the rescued tissue of $GMR\text{-}hid^{w-}$ in $vps25^{K2}$ and $vps25^{N55}$ mosaics. As a positive control, the strong suppression of $GMR\text{-}hid^{w-}$ by a mutant of *ark*, an essential component of

the cell death pathway, is largely mediated by *ark* mutant tissue (marked by absence of eye pigment in Fig. 3J). In contrast, in $vps25^{K2}$ and $vps25^{N55}$ mosaics, the rescued tissue of $GMR\text{-}hid^{w-}$ is genetically wild-type or heterozygous (marked by red pigment in Fig. 3K, L), suggesting that $vps25^{K2}$ and $vps25^{N55}$ mutant tissue does not contribute to the suppression of $GMR\text{-}hid^{w-}$. Therefore, because the surviving wild-type tissue is exposed to *GMR*-driven *hid* expression, this tissue may have an increased apoptotic resistance induced by $vps25^{K2}$ and $vps25^{N55}$ mutant clones. Thus, these are unprecedented phenotypes, which merit further analysis.

4.1.3 $vps25^{K2}$ and $vps25^{N55}$ mutant clones die, but induce non-autonomous proliferation

To examine the $vps25^{K2}$ and $vps25^{N55}$ mutant phenotypes in more detail, we performed TUNEL and BrdU labeling as assays for apoptosis and cell proliferation, respectively, in imaginal discs of third instar larvae. TUNEL labeling is increased in $vps25^{N55}$ mutant clones (Fig. 4A), consistent with the observed lack of mutant clones in the adult eye (Fig. 3E, F). $vps25^{N55}$ clones can grow to a fairly large size, suggesting that they are not growth-impaired (Fig. 4A). However, these clones are completely removed by apoptosis during pupal stages (data not shown). Similar data in this and all other figures were obtained for $vps25^{K2}$ (data not shown).

Interestingly, the number of cells in S phase in $vps25^{N55}$ mosaics as demonstrated by BrdU incorporation is significantly increased in tissue adjacent to the mutant clones. This non-autonomous cell proliferation is best visible in wing imaginal

discs, where *vps25*^{N55} clones appear to be the origin for increased proliferation of adjacent tissue (Fig. 4B) whereas wing discs with wild-type clones show a homogenous distribution of proliferating cells both within and outside the clones (Fig. 4C). Similar data were obtained in eye-antennal imaginal discs (Fig. 12C).

In addition to the apoptotic and proliferation phenotypes, *vps25*^{N55} mutant clones fail to differentiate. Elav labeling as neuronal differentiation marker demonstrates that *vps25*^{N55} cells are unable to differentiate (Fig. 4D). In summary, these analyses reveal that the wild-type function of *vps25*^{K2} and *vps25*^{N55} is required for appropriate control of apoptosis, cell proliferation and cell differentiation. The overgrowth phenotype in *vps25*^{K2} and *vps25*^{N55} mosaics (Fig. 3E, F, H, I) might most likely be explained by emission of signaling molecules from the mutant cells initiating non-autonomous proliferation in the adjacent wild-type tissue.

4.1.4 Increased Notch and JAK/STAT signaling in *vps25* mosaics

Cell surface receptors are able to signal after endocytosis as long as they are not incorporated into MVBs (Gonzalez-Gaitan, 2003; Seto and Bellen, 2004) because their intracellular domains are still exposed to the cytosol. As *vps25* mutants likely impair MVB function, these receptors may still continue to signal. Thus, the proliferation phenotype of *vps25* mosaics may be explained by continued signaling activity. Consistently, N protein and its ligand Dl accumulate in *vps25* clones (Fig. 5A, B) resulting in increased N activity as shown by the N reporter *E(spl)m8 2.61-lacz* (Fig. 5C) (Kramatschek and Campos-Ortega, 1994; Thompson et al., 2005;

Vaccari and Bilder, 2005). However, not all known target genes of N are up-regulated in *vps25* clones. The expression of *cut*, another N target (de Celis et al., 1996; Micchelli et al., 1997), is unaltered in *vps25* mutant clones in wing discs or even in some cases seems to be slightly inhibited (data not shown) (Childress et al., 2006). N is able to promote global growth in the developing *Drosophila* eye by inducing *unpaired* (*upd)* expression (Chao et al., 2004; Tsai and Sun, 2004; Reynolds-Kenneally and Mlodzik, 2005). Upd (Harrison et al., 1998) is a ligand of Domeless (Brown et al., 2001) and Master of marelle (Chen et al., 2002), which are receptors of the JAK/STAT signaling pathway and has been demonstrated to promote global growth of up to 20 cell diameters in eye imaginal discs (Tsai and Sun, 2004). Consistently, STAT activity is stimulated in *vps25* mutant clones in eye imaginal discs (Fig. 5D) and can sometimes even be observed non-autonomously in the vicinity of *vps25* mutant tissue. In summary, these data seem to support the previously reported link between N activation and stimulation of the mitogenic JAK/STAT pathway which may be the cause for the non-autonomous proliferation in *vps25* mosaics.

4.1.5 N is required for non-autonomous proliferation in *vps25* mosaics

To determine a genetic requirement of N signaling for non-autonomous proliferation in *vps25* mosaics, we expressed a dominant negative *N* (N^{DN}) transgene (Sen et al., 2003) in *vps25* clones (referred to as *vps25*/N^{DN}) using the MARCM technique (Lee and Luo, 2001). STAT activity in *vps25*/N^{DN} eye mosaics was strongly reduced or absent compared to *vps25* clones (Fig. 6A). Furthermore, BrdU-

incorporation indicates that cell proliferation is not significantly increased in *vps25*/N^{DN} mosaics (Fig. 6B). Consistently, eye imaginal discs obtained from *vps25*/N^{DN} mosaics are normal in shape and size (data not shown). Furthermore, the overgrowth phenotype of *vps25* eye mosaics can be significantly reduced by removing one copy of *N* (Fig. 13 C, G, K, O). These observations suggest that increased N activity in *vps25* clones accounts for the non-autonomous proliferation phenotype of *vps25* mosaics through activation of the JAK/STAT pathway. A similar conclusion was obtained by analyzing *vps25* mosaics in a heterozygous *stat92E* mutant background (Vaccari and Bilder, 2005). Interestingly, Dl protein does not accumulate in *vps25*/N^{DN} clones (Fig. 6C). This observation suggests that N controls Dl protein levels in *vps25* clones.

We wanted to determine whether non-autonomous proliferation mediated by Upd and JAK/STAT signaling is sufficient for suppression of *GMR-hid* as observed for *vps25* mosaics (Fig. 3B, C). However, although over-expression of *upd* in the fly eye gives rise to enlarged eyes (Bach et al., 2003; Muller et al., 2005), it is not sufficient for suppression of *GMR-hid* (Fig.6E, F). Interestingly enough, over-expression of the intracellular domain of *N* (N^{intra}) can completely suppress the *GMR-hid* eye ablation phenotype, even though the surviving tissue displays strong pigmentation defects which are probably due to a failure in differentiation (Fig. 6G). Activating the N pathway by over-expressing a *N* construct that lacks its extracellular domain (N^{NEXT}) and thus mimics S2 cleavage of N can also suppress *GMR-hid* (data not shown). Suppression can not be obtained by solely over-expressing full length N (data not shown). Thus, the suppression of *GMR-hid* in *vps25* mosaics is not caused

by non-autonomous proliferation through Upd signaling. In agreement with our data, the N pathway may provide another postulated non-autonomous signal which results in suppression of *GMR-hid*. Alternatively, N signaling could control apoptosis autonomously and might not be involved in the non-autonomous suppression of cell death as observed in *vps25* mosaics. Therefore it is possible that another mechanism may account for the observed suppression (see below).

In contrast to our findings that the N pathway can inhibit apoptosis, it has also been implicated in inducing cell death in eye imaginal discs (Miller and Cagan, 1998; Yu et al., 2002). Thus, we tested whether increased N signaling accounts for the cell death phenotype of *vps25* clones. However, labeling of *vps25*/N^{DN} clones with activated Caspase-3 antibody is indistinguishable from *vps25* clones (Fig.6D). Similar results were obtained by TUNEL labeling (data not shown). Thus, although N induces non-autonomous proliferation in *vps25* mosaics, it is not responsible for the apoptotic phenotype of *vps25* clones.

We also tested the possibility that activation of cell death might activate N signaling, and thus induces compensatory proliferation (Huh et al., 2004; Perez-Garijo et al., 2004; Ryoo et al., 2004; Wells et al., 2006; Fan and Bergmann, 2008). To address this question we blocked cell death by expression of *diap1* in *vps25* mutant clones (see below). However, pSTAT92E activity (data not shown) and cell proliferation (Fig. 7C) was still evident under these conditions establishing that activation of the N pathway and induction of cell death in *vps25* clones are independent of each other.

4.1.6 Non-autonomous survival through up-regulation of Diap1 protein

Because N signaling does not induce cell death in *vps25* clones, we analyzed the underlying cause of the apoptotic phenotype. *vps25* clones contain increased protein levels of the cell death-inducer Hid (Fig. 7A). Hid, as well as Reaper and Grim, induce apoptosis by stimulating ubiquitin-mediated degradation of Diap1, an inhibitor of the initiator caspase Dronc (Meier et al., 2000b; Holley et al., 2002; Ryoo et al., 2002; Yoo et al., 2002). Indeed, Diap1 protein levels were markedly reduced in *vps25* mutant clones (Fig. 7B) suggesting that Diap1 no longer inhibits Dronc.

Strikingly, however, Diap1 immunoreactivity is increased in wild-type cells immediately abutting *vps25* clones (Fig. 7B) suggesting that *vps25* clones also promote non-autonomous cell survival. *GMR-hid* is sensitive to altered levels of Diap1 (Hay et al., 1995). Thus, the non-autonomous increase of Diap1 protein likely promotes the suppression of *GMR-hid* in *vps25* mosaics (Fig. 3B, C). This activity is independent of Upd signaling because over-expression of *upd* does not alter Diap1 protein levels (data not shown) and does not suppress *GMR-hid* (Fig. 6F) but may be dependent on N signaling (Fig. 6G). It is currently unknown, how the N pathway or another signaling mechanism cause non-autonomous survival by regulating Diap1 protein levels or other apoptotic factors.

4.1.7 Blocking cell death induces massive overgrowth of *vps25* mosaics

It has recently been demonstrated that dying cells are able to induce compensatory proliferation in neighboring cells (Huh et al., 2004; Perez-Garijo et al., 2004; Ryoo et al., 2004; Wells et al., 2006; Fan and Bergmann, 2008). Thus, we tested whether compensatory proliferation contributes to non-autonomous proliferation in *vps25* mosaics. If it does, then inhibition of apoptosis either through expression of Diap1 in *vps25* clones (*vps25*/Diap1) or in *vps25 ark* double mutants (using an *ark* null allele (Srivastava et al., 2007), see also 'Materials and Methods') is expected to reduce proliferation and subsequently to suppress the overgrowth phenotype of *vps25* mosaics. However, non-autonomous proliferation is still observed in *vps25*/Diap1 mosaics (Fig. 7C) and in *vps25 ark* mosaics (data not shown) suggesting that compensatory proliferation does not contribute significantly to non-autonomous proliferation of *vps25* mosaics. In contrast, eye-antennal discs of *vps25*/Diap1 mosaics are extremely overgrown and can be up to five times as large as wild-type discs (Fig. 7D). In addition, *vps25*/Diap1 and *vps25 ark* clones occupy a large fraction of the eye disc (Fig. 7D, E) suggesting that *vps25* clones have no intrinsic growth disadvantage over wild-type tissue if cell death is blocked. The adult eye of *vps25 ark* mosaics is severely overgrown and folded (Fig. 7F). However, most of these flies do not eclose, probably due to massive overgrowth of the eye and head capsule. Thus, inhibiting cell death in *vps25* clones gives rise to an even stronger overgrowth phenotype as has also been observed by expression of the caspase inhibitor P35 (Thompson et al., 2005).

4.1.8 Hid and JNK contribute to the elimination of *vps25* mutant clones

Caspase-3 labeling reveals that cell death is completely blocked in *vps25*/Diap1 clones (Fig. 7D). Surprisingly, Caspase-3 activity is still detectable in *vps25 ark* double mutant clones (Fig. 7E), suggesting that although *ark*, an essential component of the cell death pathway, is mutated, *vps25 ark* double mutant cells still die. This is also confirmed by the observation that *vps25 ark* clones (marked by absence of eye pigment) cannot be recovered in adult eyes of *vps25 ark* mosaics (Fig. 7F). Diap1 inhibits both initiator (Dronc) (Meier et al., 2000b) and Caspase-3-like caspases (DrICE, DCP-1) (Kaiser et al., 1998; Hawkins et al., 1999), whereas Ark directly only activates Dronc (Igaki et al., 2002) (reviewed in Cashio et al., 2005). Thus, an alternative cell death pathway is operating in *vps25* clones that can induce Caspase-3-like activity independently of Ark.

We considered Jun N-terminal kinase (JNK, encoded by *basket* in *Drosophila*) signaling as candidate for the alternative cell death pathway (reviewed in Weston and Davis, 2007). JNK activation occurs under stress conditions, and can induce apoptosis (Adachi-Yamada et al., 1999; Adachi-Yamada and O'Connor, 2002). We found increased levels of activated JNK in *vps25* clones (Fig. 8A). It was previously shown that inactivation of Diap1 can induce JNK activation (Kuranaga et al., 2002; Ryoo et al., 2004). Thus, we tested whether this applies to *vps25* clones as well. However, JNK activity is not appreciably altered in *vps25*/Diap1 clones (Fig. 8B) excluding the possibility that JNK activation occurs as a result of Diap1 inactivation. To determine a requirement of JNK for the apoptotic phenotype, we inhibited JNK in *vps25* clones by

over-expression of *puckered* (*vps25*/Puc), a phosphatase that dephosphorylates JNK (Martin-Blanco et al., 1998). However, Caspase-3 activity is still detectable in *vps25*/Puc clones (Fig. 8C). This caspase activity may be derived from Hid activity which is expressed in *vps25*/Puc clones (data not shown). Thus, we expressed *puc* in *vps25 ark* double mutant clones. In *vps25 ark*/Puc clones, Caspase-3 activity is mostly blocked (Fig. 8D), and *vps25 ark*/Puc mosaic discs are severely overgrown (Fig. 8D) similar to *vps25*/Diap1 eye discs (Fig. 7D). Taken together, these observations implicate Hid/Diap1/Dronc/Ark and JNK signaling as contributing factors to the apoptotic phenotype of *vps25* mutant clones. Interestingly, we still detect Caspase-3 activity at the clonal margin of *vps25 ark*/Puc clones suggesting that a third cell death pathway may operate in *vps25* clones or that surrounding wild-type tissue is outcompeted. Alternatively, JNK inhibition by Puc may be incomplete.

4.1.9 Hippo signaling, but not cell competition, controls apoptosis in *vps25* clones

Which process controls the apoptotic phenotype of *vps25* mutants? One possibility is cell competition. Cell competition was originally described in studies using *Minute* (*M*) mutations in which faster growing cells (M^+/M^+) outcompete neighboring slow-growing cells (M^-/M^+) by inducing apoptosis (Morata and Ripoll, 1975; Simpson and Morata, 1981; Moreno et al., 2002) (reviewed in Abrams, 2002).Thus, we analyzed *vps25* clones in a *M* background. However, although *vps25* clones are larger in a *M* background compared to a wild-type background (Thompson et al., 2005), they are still Caspase-3 positive and undergo apoptosis (Fig. 9A). In addition, it was recently shown that dMyc protein levels are critical for cell

competition (de la Cova et al., 2004; Moreno and Basler, 2004). An imbalance of dMyc protein levels between neighboring cells induces cell competition, outcompeting cells with lower dMyc levels by apoptosis. However, expression of dMyc in *vps25* clones (*vps25*/dMyc) does not significantly change Caspase-3 activity (Fig. 9B). These data illustrate that cell competition is not an important contributor for cell death in *vps25* clones.

In recent years, the Hippo signaling pathway has emerged as an important regulator of tissue growth by controlling cell proliferation and apoptosis (Harvey et al., 2003; Pantalacci et al., 2003; Udan et al., 2003; Wu et al., 2003) (reviewed in Edgar, 2006; Harvey and Tapon, 2007; Pan, 2007; Saucedo and Edgar, 2007). Thus, we tested whether Hippo activity is altered in *vps25* clones. Expanded (Ex) is a useful marker for the Hippo pathway and is inversely correlated with Hippo activity, such that low Ex levels at the apical plasma membrane are indicative of high Hippo activity (Hamaratoglu et al., 2006). Ex protein levels are low in *vps25* clones (Fig. 9C, arrow) indicating that they contain high Hippo activity. Interestingly, in *vps25 hippo* double mutants, Caspase-3 is almost completely blocked (Fig. 9D) suggesting that Hippo signaling directly or indirectly controls apoptosis in *vps25* mutant cells. The cause for increased Hippo signaling in *vps25* clones is unknown. It is possible that a putative receptor which controls Hippo activity is deregulated at the *vps25* endosome (see also 'Discussion').

4.2 Shared and distinct genetic properties of ESCRT-II components

4.2.1 Description of *vps* alleles used

In order to obtain a better understanding of the genetic properties of ESCRT components in *Drosophila* we performed a comparative analysis between the members of the ESCRT-II complex. In this analysis the following mutant alleles of ESCRT-II members were used. $vps22^{5F8\text{-}3}$ (also known as $lsn^{5F8\text{-}3}$) was previously described by Irion and St Johnston (2007) (Irion and St Johnston, 2007). It carries a premature termination codon at residue 2, likely encoding a null allele. $vps25^{N55}$ has a premature termination codon at residue 93. Earlier, we have characterized this allele as a null allele (see also 'Identification of *K2* and *N55* as mutants of the *Drosophila vps25* homolog') (Herz et al., 2006). $vps36^{L5212}$ was also characterized by Irion and St Johnston (2007) (Irion and St Johnston, 2007). A P-element insertion in the first exon at nucleotide 59 disrupts the *vps36* transcript. RT-PCR demonstrates that some *vps36* transcript still forms in $vps36^{L5212}$ mutants (Fig. 10, compare lanes 2 and 3) suggesting that it is a hypomorph. Interestingly, transcript levels as detected by primers further downstream of the transcription start site of *vps36* seem to be comparable between a *y w* control and $vps36^{L5212}$ mutants, suggesting that the P-element insertion at the *vps36* locus just disrupts full length transcripts of *vps36*. Transcription from alternative start sites further downstream might not be affected by the P-element insertion and thus result in similar *vps36* mRNA levels (Fig. 10, compare lanes 4 and 5, 6 and 7). Alternative transcripts of ESCRT components have already been reported before for *Tsg101* (*vps23*) and *vps24* (Steiner et al., 1997; Khoury et al., 2007).

4.2.2 *vps22*, *vps25* and *vps36* mutants contain enlarged endosomes accumulating ubiquitinylated proteins

Because *hrs* mutants in *Drosophila* are characterized by enlarged early endosomes (Lloyd et al., 2002; Jekely and Rorth, 2003), we tested whether mutants in the three ESCRT-II components also contain abnormal endosomes. As endosomal marker we used an antibody raised against Hrs (Lloyd et al., 2002). Mutant clones of *vps22*, *vps25* and *vps36* in eye imaginal discs contain enlarged Hrs-positive particles, representing abnormal early endosomes (Fig. 11 A-C). In this study we used FK1 and FK2 antibodies which recognize mono-and poly-conjugated and poly-conjugated ubiquitin respectively, but not unconjugated ubiquitin (Fujimuro et al., 1994; Fujimuro et al., 1997; Lee et al., 2008). Using these FK antibodies, we found that these enlarged Hrs-positive particles accumulate ubiquitin-conjugated proteins (shown for FK1 in Fig. 11A-C; similar data were obtained for FK2 (Fig. 15D-F)). Thus, *vps22*, *vps25*, and *vps36* mutant cells contain abnormally large early endosomes which accumulate ubiquitin-conjugated proteins. The accumulation of ubiquitin-conjugated proteins is consistent with the notion that ubiquitinylation provides the signal for endocytosis into the early endosome (reviewed in Hicke and Dunn, 2003; Haglund and Dikic, 2005; Hicke et al., 2005; Williams and Urbe, 2007). As shown below (Fig. 14A-C), the enlarged Hrs-positive particles contain increased levels of signaling receptors such as Notch.

4.2.3 *vps22* and *vps25*, but not *vps36* mosaics, display strong non-autonomous overgrowth

We have already shown above that *vps25* mutant mosaics cause non-autonomous overgrowth (Fig. 4B) (see also Thompson et al., 2005; Vaccari and Bilder, 2005; Herz et al., 2006). Therefore, we determined whether this applies to *vps22* and *vps36* mosaic flies as well. We performed BrdU labelings to determine the number of cells in S-phase. *vps22* mutant clones do not proliferate very well (Fig. 12B). However, the wild-type tissue immediately adjacent to *vps22* mutant clones shows increased density of BrdU-positive cells (compare Fig. 13B to wild-type in Fig. 13A). Thus, similar to *vps25* mosaics (Fig. 13C), *vps22* controls cell proliferation non-autonomously. However, *vps36* mosaics behave differently. BrdU-positive cells can be observed both within and outside of *vps36* clones with homogeneous density (Fig. 13D).

We also detect strong overgrowth in *vps22* eye mosaics in adult flies (Fig. 13B, J). This is very well visible for *vps22* mosaic heads (Fig. 13J) which are significantly larger than wild-type controls (Fig. 13I). The overgrowth is also detectable in eye-antennal imaginal discs, the larval precursors of the adult eyes, of *vps22* and *vps25* mosaic animals. *vps22* and *vps25* mosaic eye discs are significantly larger compared to wild-type controls (Fig. 13Q-S). This overgrowth is non-autonomous because *vps22* mutant clones which are marked by the absence of red eye pigment are not recovered in mosaic *vps22* eyes (compare Fig. 10B with the wild-type control in Fig. 10A). However, a similar strong overgrowth phenotype was not found for *vps36* mosaic eyes and heads (Fig. 13D, L), although a roughening of the eye can be observed and *vps36* mutant tissue does not survive (Fig. 13D). We also find this

confirmed at the level of eye imaginal discs. *vps36* mosaic eye discs (Fig. 13T) are noticeably smaller than *vps22* and *vps25* mosaic discs (Fig. 13R, S), and are comparable to wild-type (Fig. 13Q). Thus, *vps36* mutant clones appear to be unable to induce strong non-autonomous proliferation or secondly because of their hypomorphic nature still retain some residual activity which is sufficient to maintain the proper control of different signaling pathways, such as N. Our data below reveals that the second scenario is unlikely as it shares all the major endosomal phenotypes with *vps22* and *vps25* mutant clones, which are the reason for increased N signaling (Fig. 14 and 15).

To analyze the absence of *vps22* and *vps36* mutant clones in adult eyes (Fig. 13B, D), we performed Caspase-3 labelings as a marker for apoptosis. In third instar eye imaginal discs, *vps22* and *vps36* clones contain increased Caspase-3 activity explaining the loss of these clones in the adult eye (Fig. 12E, G). A similar apoptotic phenotype has also been observed for *vps25* clones (Fig. 4A and 13F) (see also Thompson et al., 2005; Vaccari and Bilder, 2005; Herz et al., 2006). Thus, as for *vps25*, loss of *vps22* and *vps36* causes the apoptotic death of the affected cells.

In summary, these analyses indicate that, although Vps22, Vps25 and Vps36 are components of the ESCRT-II complex, they do not behave genetically identical. While mutants of all three ESCRT-II components display endosomal defects and are apoptotic, only *vps22* and *vps25* mutant clones trigger strong non-autonomous proliferation. *vps36*, on the other hand, does not display a strong non-autonomous effect on proliferation. We will reveal below that at least one other difference exists.

4.2.4 Up-regulation of Notch protein and JAK/STAT activity in *vps* mosaics

The non-autonomous overgrowth of *vps25* mosaics has been attributed to a failure in down-regulation of N protein and activity in *vps25* mutant endosomes (see also Thompson et al., 2005; Vaccari and Bilder, 2005; Herz et al., 2006). Consistently, removal of one copy of *N*, which does not affect head and eye size of wild-type flies (Fig. 13E, M) can suppress the strong overgrowth phenotypes of *vps22* and *vps25* mosaic eyes and heads (Fig. 13F, G, N, O) and slightly reduces the roughening of *vps36* eye mosaics (Fig. 13H).

Additionally, in *vps22, vps25* and *vps3*6 mutant clones, Hrs-positive enlarged early endosomes accumulate N protein (Fig. 14A-C). Shown in Fig. 14A'''-C''' are immunolabelings with an antibody that recognizes the intracellular domain of N. We also observe accumulation of N in *vps22, vps25* and *vps36* mutant tissue using an antibody against the extracellular domain of N (Fig. 15A-C). In addition, increased abundance of the N-ligand Dl is also detected in *vps22, vps25* and *vps36* clones (Fig. 15G-I).

To determine whether the increased abundance of N correlates with increased activity, we tested the JAK/STAT pathway, a known downstream target of N in eye development (Chao et al., 2004; Tsai and Sun, 2004; Reynolds-Kenneally and Mlodzik, 2005). The accumulation of N protein correlates with increased JAK/STAT activity in *vps22*, *vps25* and *vps36* mosaics, as judged by an antibody recognizing

activated phosphorylated STAT (pSTAT) (Fig. 14D-F). Increased pSTAT activity is predominantly observed in *vps* mutant clones, however, it can also be detected non-autonomously (Fig. 5D and 14D-F) (Herz et al., 2006).

Thus, the observed differences in non-autonomous overgrowth between *vps22*, *vps25* and *vps36* do not correlate with the de-regulation of N signaling. It is unclear why the de-regulation of N and JAK/STAT activity causes overgrowth in *vps22* and *vps25* mosaics, but not in *vps36* mosaics. This observation further supports the notion that there are intrinsic differences between the components of the ESCRT-II complex.

4.2.5 *vps36* mosaics, but not *vps22*, promote strong apoptotic resistance

Paradoxically, despite the fact that *vps25* clones are highly apoptotic, we originally isolated *vps25* mutants based on their ability to suppress apoptosis (Fig. 3B, C) (Herz et al., 2006). Specifically, the eye-ablation phenotype caused by expression of the pro-apoptotic gene *hid* under control of the eye-specific *GMR* promoter (*GMR-hid*) is suppressed in *vps25* mosaics compared to a control (Fig. 16A, C). However, this suppression occurs in a non-autonomous manner through up-regulation of the apoptosis inhibitor Diap1 in neighboring cells (Fig. 7B) (Herz et al., 2006) or another unknown apoptotic factor. Therefore, we tested whether *vps22* and *vps36* have a similar activity. However, to our surprise although *vps22* mosaics cause a strong non-autonomous proliferation phenotype (Fig. 12B and 13B, J) they do not suppress *GMR-hid* (Fig. 16B). In contrast, although *vps36* mosaics display only a mild non-autonomous proliferation phenotype (Fig. 12D and 13D, L), they are very strong

suppressors of *GMR-hid* (Fig. 16D), comparable to *vps25* mosaics (Figure 16C). This observation provides another example of genetic differences between the individual components of ESCRT-II.

5 Figures

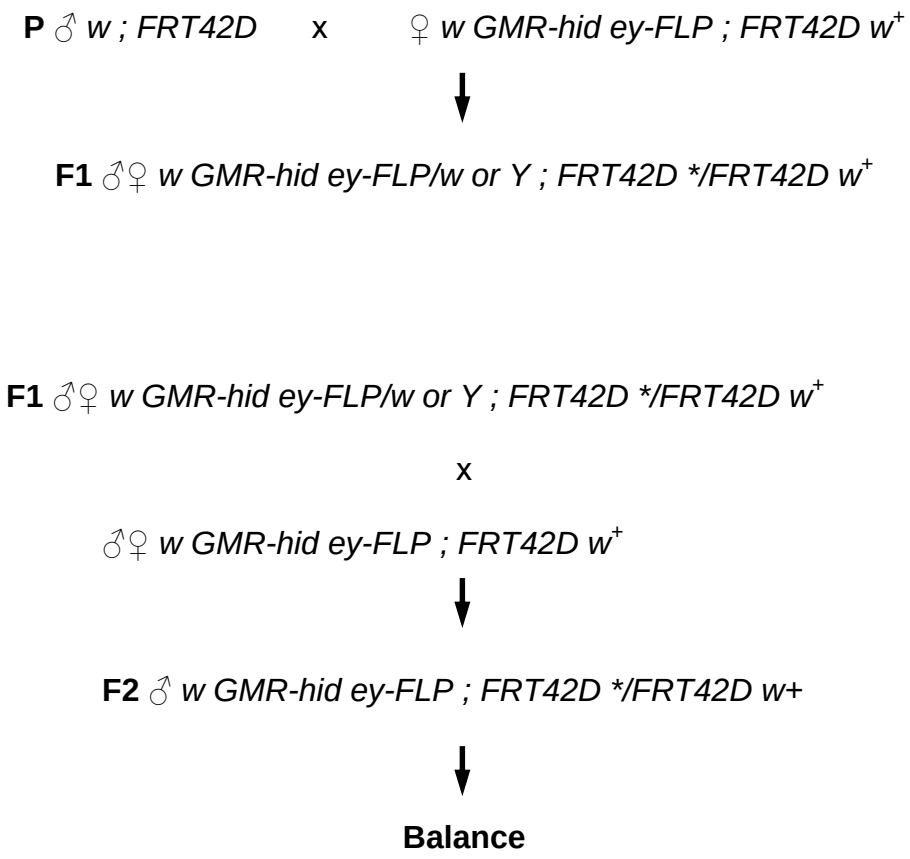

5.1 Fig.1. *GMR-hid ey-FLP* (*GheF*) screen scheme.

P males were mutagenized with EMS and crossed to females of an 'analyzer' line containing *GMR-hid*. Flies in F1 were analyzed for recessive suppression of the *GMR-hid*-induced eye ablation phenotype (Fig. 3A) The star * indicates the introduced mutation on chromomsome arm 2R. Suppressors of *GMR-hid* were retested for germline transformation by backcrossing to the 'analyzer' line and balanced with a *y w ; Sco/CyO* line after confirmation of the *GMR-hid* suppression phenotype.

P ♂ *w ; FRT42D K2/CyO* x ♀ *w ; P[w+]/CyO*

↓

F1 ♀ *w ; FRT42D K2/P[w+]*

P ♂ *w ; FRT42D N55/CyO* x ♀ *w ; Sco/CyO, GMR-hid*

↓

F1 ♂ *w ; FRT42D N55/CyO, GMR-hid*

F1 ♂ *w ; FRT42D N55/CyO, GMR-hid* x ♀ *w ; FRT42D K2/P[w+]*

↓

F2 no recombination

1.	w ; *FRT42D K2/FRT42D N55*	lethal
2.	**w ; *P[w+]/FRT42D N55***	***w+***
3.	w ; *FRT42D K2/CyO, GMR-hid*	*CyO*, small eye
4.	w ; *P[w+]/CyO, GMR-hid*	CyO, small eye

F2 recombination

5.	*K2 P[w+]/FRT42D N55*	lethal
6.	***FRT42D or +/FRT42D N55***	***w***
7.	*FRT42D P[w+] or K2 P[w+]CyO, GMR-hid*	*CyO*, small eye
8.	*FRT42D or +/CyO, GMR-hid*	*CyO*, small eye

P-elements used	Nr. of F2 flies with genotype *P[w+]/FRT42D N55*	Nr. of F2 flies with genotype *FRT42D or +/FRT42D N55*
KG01834 (43E11)	361	5
KG01035 (49D6)	347	33
KG04965 (56D1)	346	169
KG02448 (57A5)	347	187

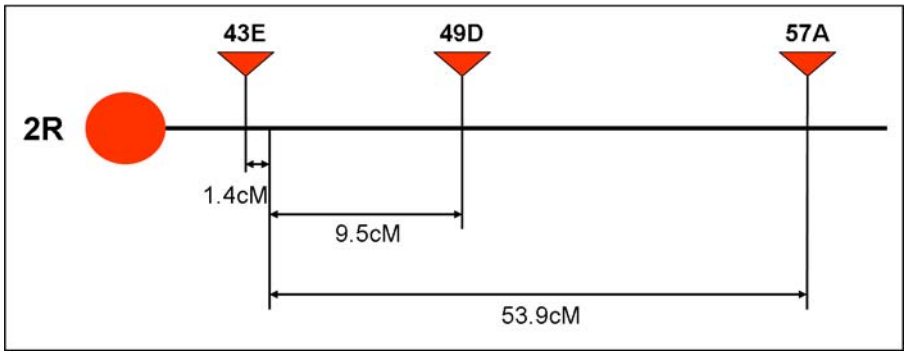

5.2 Fig. 2. Mapping of *K2/N55*.

Crossing scheme used to locate *K2/N55* by P-element mapping. F2 progeny can have eight different genotypes, dependent on whether recombination occurred in F1 females or not. Flies in F2 were counted for recombination between the respective P-element and *K2* by comparing the numbers of red-eyed with white-eyed flies.

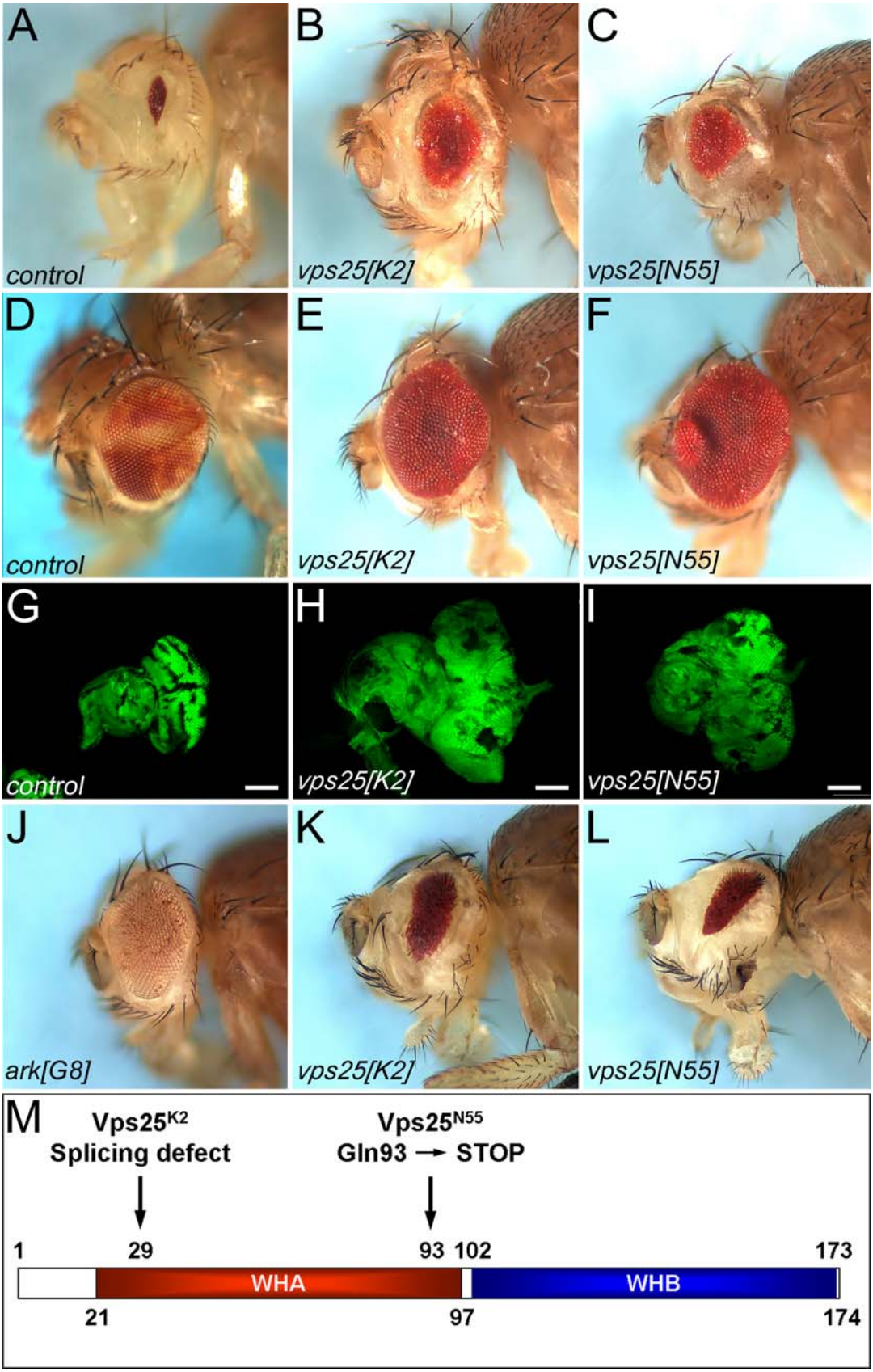
A
control
B
vps25[K2]
C
vps25[N55]
D
control
E
vps25[K2]
F
vps25[N55]
G
control
H
vps25[K2]
I
vps25[N55]
J
ark[G8]
K
vps25[K2]
L
vps25[N55]
M
Vps25K2
Splicing defect
Vps25N55
Gln93 → STOP
1
29
93
102
173
WHA
WHB
21
97
174

5.3 Fig.3. Isolation and characterization of *vps25^{K2}* and *vps25^{N55}* alleles.

(A) The unmodified *GMR-hid ey-FLP* (*GheF*) eye-ablation phenotype.

(B, C) *vps25^{K2}* and *vps25^{K2}* alleles are moderate suppressors of the *GheF*-eye phenotype.

(D-F) Adult eyes of *ey-FLP*-induced mosaics of (D) wild-type, (E) *vps25^{K2}* and (F) *vps25^{N55}*. (E, F) *vps25^{K2}* and *vps25^{N55}* mosaic eyes lack mutant clones (marked by absence of red pigment) and are overgrown.

(G-I) Eye-antennal discs from 3rd instar larvae of (H) *vps25^{K2}* and (I) *vps25^{N55}* mosaics are overgrown and disorganized compared to (G) wild-type. Scale bar: 100μm.

(J-L) Non-autonomous suppression of *GMR-hid^{w-}* in *vps25^{K2}* and *vps25^{N55}* mosaics. (J) Control: in *ark^{G8}* mosaics, largely *ark^{G8}* mutant clones (marked by absence of eye pigment) suppress *GMR-hid^{w-}*. (K, L) In (K) *vps25^{K2}* and (L) *vps25^{N55}* mosaics, the suppression of *GMR-hid^{w-}* is mediated by wild-type tissue (red pigment). *vps25^{K2}* and *vps25^{N55}* clones do not contribute.

(M) Schematic outline of the Vps25 protein and the molecular lesions in Vps25^{K2} and Vps25^{N55}. WHA and WHB are winged-helix domains A and B.

Genotypes: (A) *GMR-hid ey-FLP ; FRT42D y^{+}/FRT42D w^{+}*, (B) *GMR-hid ey-FLP ; FRT42D vps25^{K2}/FRT42D w^{+}*, (C) *GMR-hid ey-FLP ; FRT42D vps25^{N55}/FRT42D w^{+}*, (D) *w ey-FLP ; FRT42D y^{+}/FRT42 w^{+}*, (E) *w ey-FLP ; FRT42D vps25^{K2}/FRT42D w^{+}*, (F) *w ey-FLP ; FRT42D vps25^{N55}/FRT42D w^{+}*, (G) *ey-FLP ; FRT42D y^{+}/FRT42D ubi-GFP*, (H) *ey-FLP ; FRT42D vps25^{K2}/FRT42D ubi-GFP*, (I) *ey-FLP ; FRT42D vps25^{N55}/FRT42D ubi-GFP*, (J) *w ey-FLP ; FRT42D ark^{G8}/FRT42D w^{+} ; GMR-hid^{w-}*, (K) *w ey-FLP ; FRT42D vps25^{K2}/FRT42D w^{+} ; GMR-hid^{w-}*, (L) *w ey-FLP ; FRT42D vps25^{N55}/FRT42D w^{+} ; GMR-hid^{w-}*.

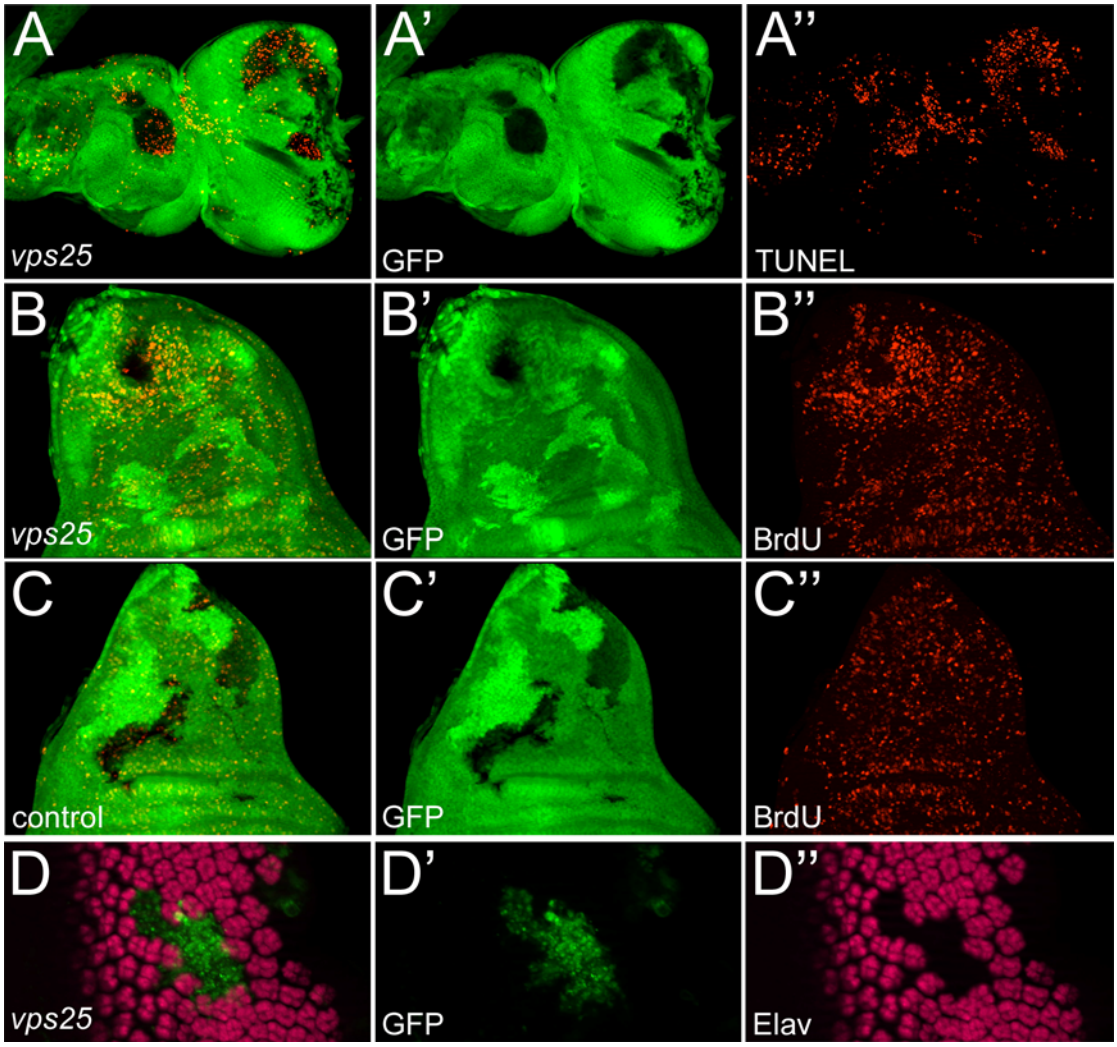

5.4 Fig. 4. TUNEL and BrdU analysis of *vps25*^{N55} mosaics.

(A-A'') Increased TUNEL-positive cell death in *vps25*^{N55} mutant clones of eye-antennal imaginal discs from 3rd instar larvae. *vps25*^{N55} clones are marked by absence of GFP.

(B-B'') BrdU labeling of *vps25*^{N55} mosaic wing imaginal discs. Note increased proliferation in tissue adjacent to *vps25*^{N55} clones.

(C-C'') BrdU labeling of wild-type (control) clones in wing imaginal discs serve as control to (B-B''). BrdU incorporation is homogeneous inside and outside the clones.

(D-D'') Elav labeling of *vps25*^{N55} mutant clones in eye-antennal imaginal discs of third instar larvae. Clones are positively marked with GFP.

Genotypes: (A-A'', B-B'') *ey-FLP* ; *FRT42D vps25*^{N55}*/FRT42D ubi-GFP*. (C-C'') *ey-FLP* ; *FRT42D/FRT42D ubi-GFP*. (D-D'') *hs-FLP UAS-GFP* ; *FRT42D vps25*^{N55}*/FRT42D tub-Gal80* ; *tub-Gal4*.

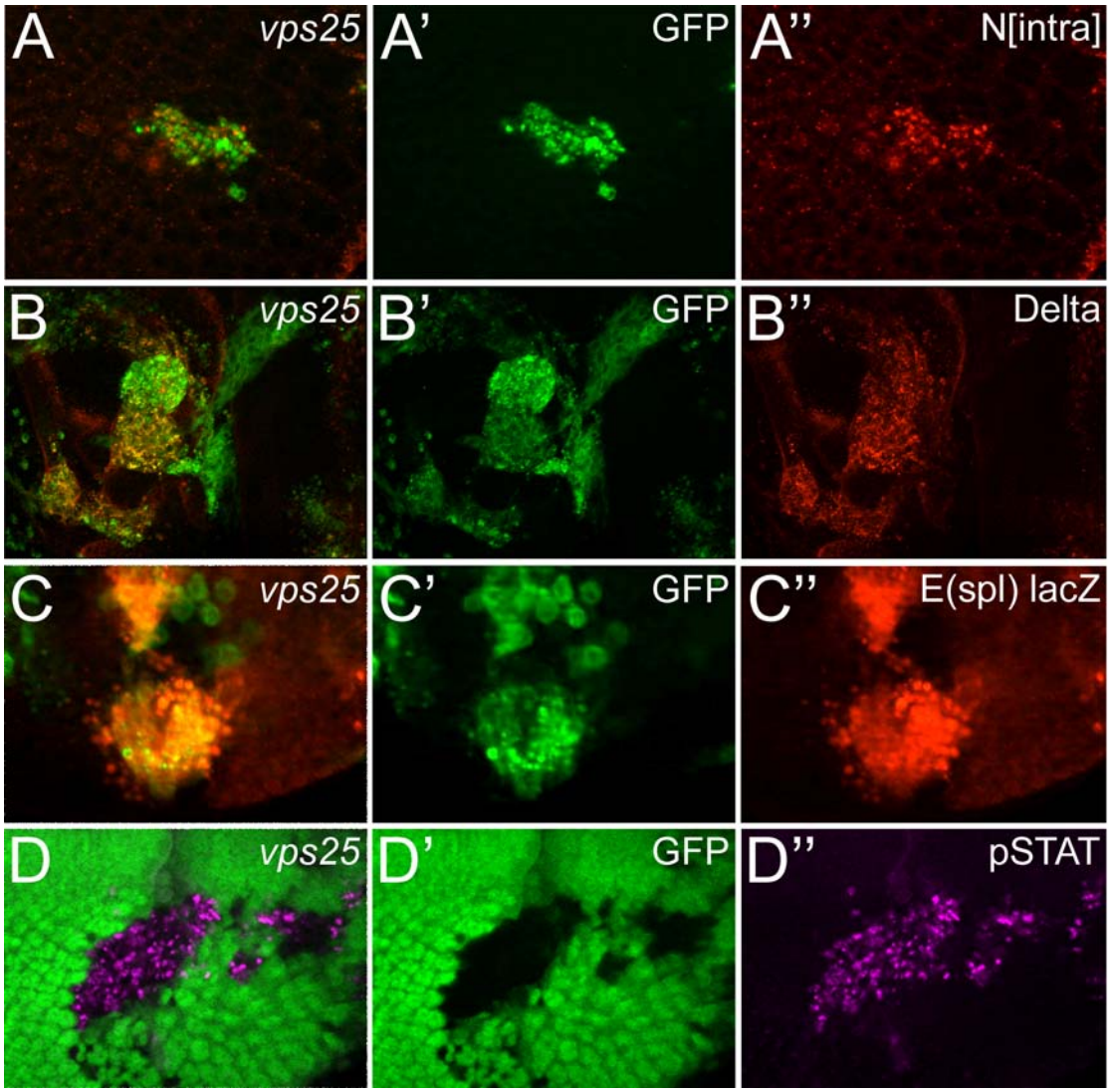

5.5 Fig. 5. Accumulation of N and Dl in *vps25* clones, and increased pSTAT immunoreactivity adjacent to *vps25* clones.

(A-A'') Accumulation of N in GFP-marked $vps25^{N55}$ clones.

(B-B'') Accumulation of Dl in GFP-marked $vps25^{N55}$ clones.

(C-C'') Increased N activity in GFP-marked *vps25* clones.

(D-D'') Increased STAT activity inside and outside of *vps25* clones by anti-pSTAT92E labeling. Clones are marked by absence of GFP.

Genotypes: (A-A'', B-B'', C-C'') Note $vps25^{N55}$ clones are positively marked with GFP using the MARCM technique (Lee and Luo, 2001). (A-A'', B-B'') *hs-FLP UAS-GFP* ; *FRT42D* $vps25^{N55}$*/FRT42D tub-Gal80* ; *tub-Gal4*. (C-C'') *hs-FLP UAS-GFP* ; *E[spl]m8 2.61-lacZ FRT42D* $vps25^{N55}$*/FRT42D tub-Gal80* ; *tub-Gal4*. (D-D'') *ey-FLP* ; *FRT42D* $vps25^{N55}$*/FRT42D ubi-GFP*.

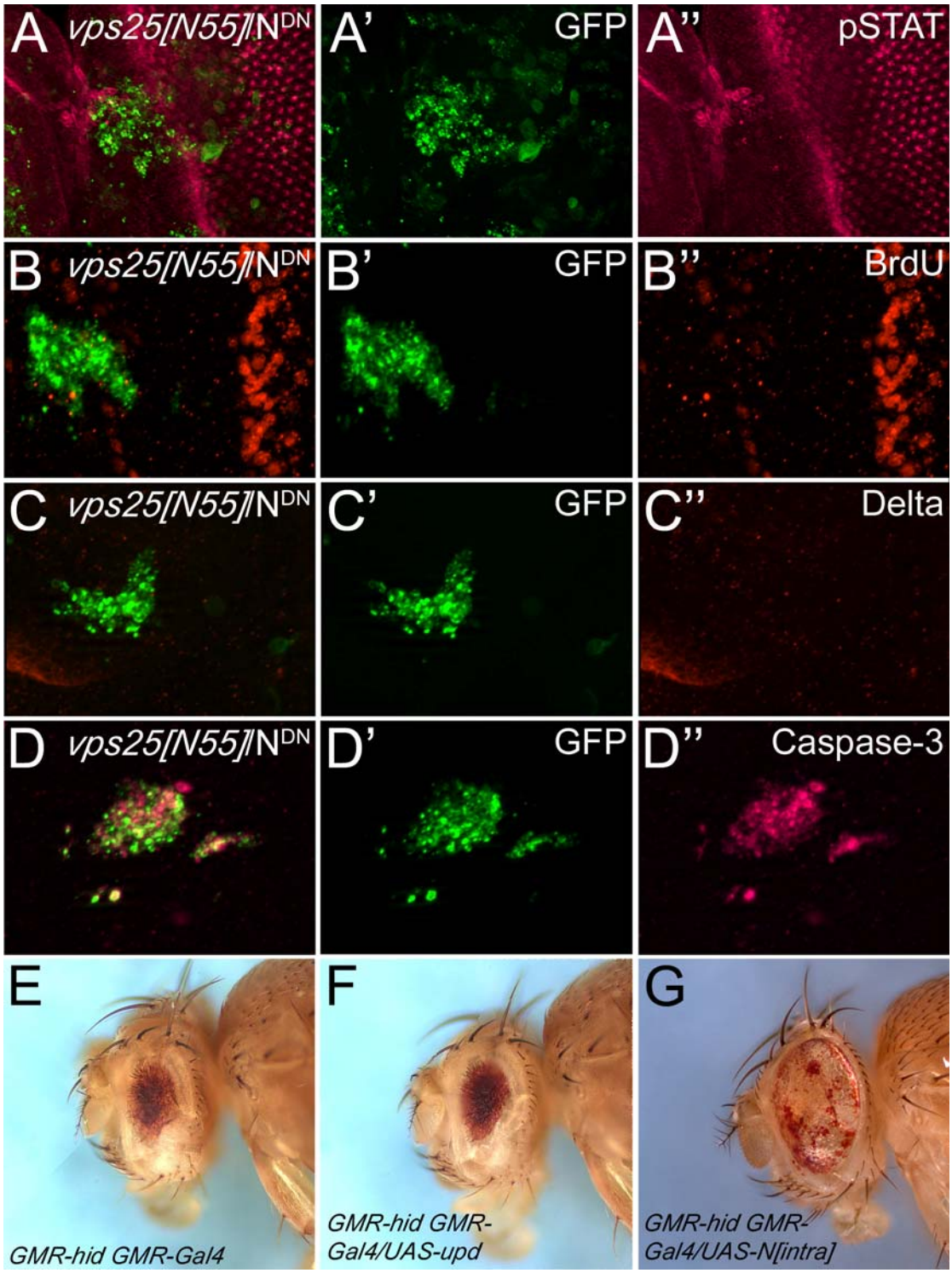
A vps25[N55]/N^DN
A' GFP
A'' pSTAT
B vps25[N55]/N^DN
B' GFP
B'' BrdU
C vps25[N55]/N^DN
C' GFP
C'' Delta
D vps25[N55]/N^DN
D' GFP
D'' Caspase-3
E
GMR-hid GMR-Gal4
F
GMR-hid GMR-Gal4/UAS-upd
G
GMR-hid GMR-Gal4/UAS-N[intra]

5.6 Fig. 6. N is required for non-autonomous proliferation of *vps25* mosaics, but not for apoptosis.

All $vps25^{N55}$ clones expressing N^{DN} ($vps25^{N55}/N^{DN}$) are labeled with GFP using MARCM. (A-A'') $vps25^{N55}/N^{DN}$ clones have reduced levels of pSTAT92E.

(B-B'') $vps25^{N55}/N^{DN}$ clones elicit non-autonomous cell proliferation (BrdU labeling in B and B''). The strong BrdU signal in (B, B'') is due to the second mitotic wave.

(C-C'') $vps25^{N55}/N^{DN}$ clones show reduced levels of Dl.

(D-D'') Caspase-3-positive apoptosis is unchanged in $vps25^{N55}/N^{DN}$ clones.

(E) The unmodified *GMR-hid GMR-Gal4* eye-ablation phenotype.

(F) Over-expression of *upd* is not sufficient to suppress *GMR-hid GMR-Gal4*.

(G) Over-expression of the intracellular domain of *N* strongly suppresses *GMR-hid GMR-Gal4*.

Genotypes: (A-A'', B-B'', C-C'', D-D'') *hs-FLP UAS-GFP* ; *FRT42D* $vps25^{N55}$ *UAS-*N^{DN}*/FRT42D tub-Gal80*; *tub-Gal4*. (E) *GMR-hid GMR-Gal4*. (F) *GMR-hid GMR-Gal4*/*UAS-upd*. (G) *GMR-hid GMR-Gal4*/*UAS-*N^{intra}.

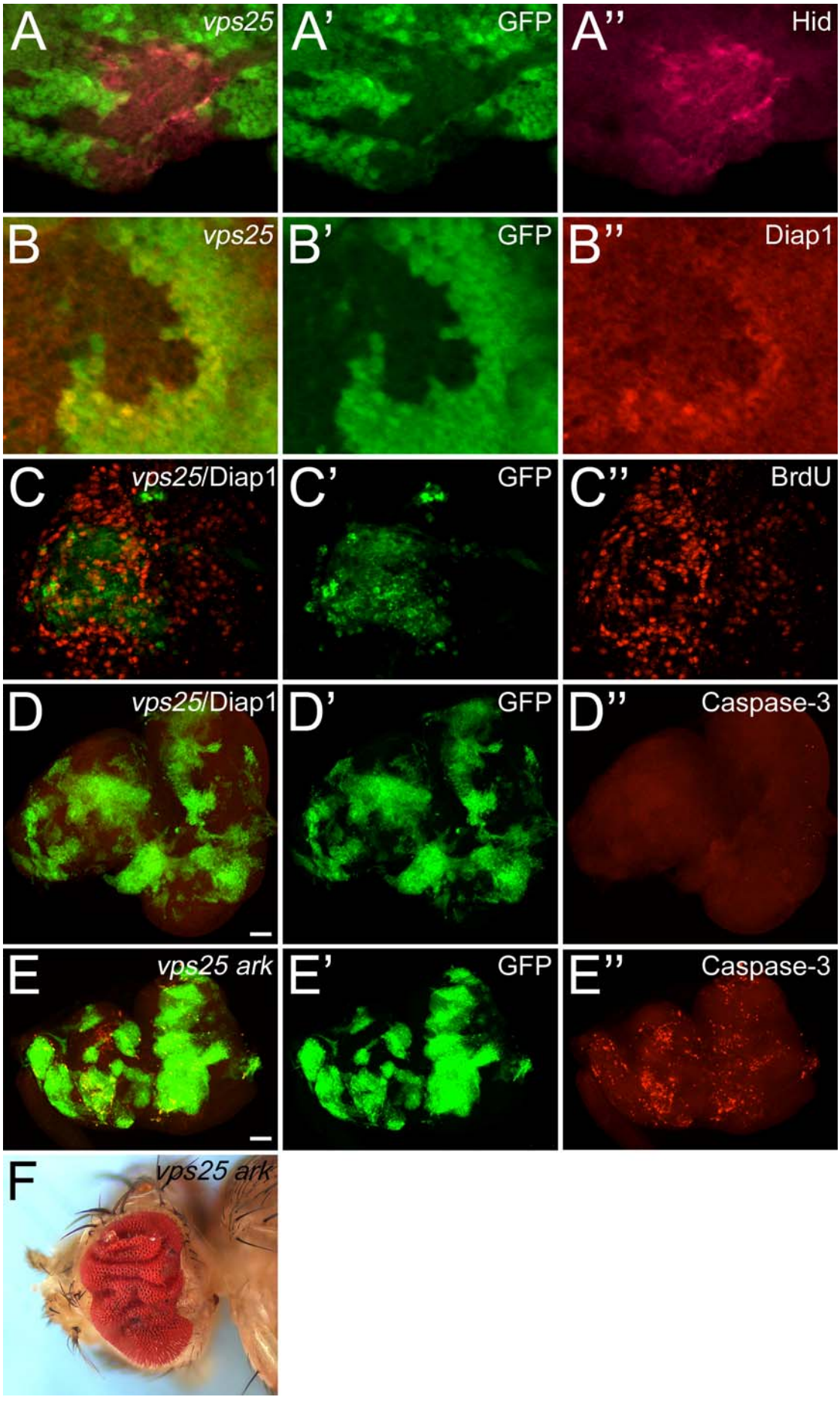
A
vps25
A'
GFP
A''
Hid
B
vps25
B'
GFP
B''
Diap1
C
vps25/Diap1
C'
GFP
C''
BrdU
D
vps25/Diap1
D'
GFP
D''
Caspase-3
E
vps25 ark
E'
GFP
E''
Caspase-3
F
vps25 ark

5.7 Fig. 7. Non-autonomous increase of Diap1 protein levels, and evidence of two cell death pathways.

(A-A'') Increased levels of Hid protein in *vps25*^{K2} clones of 3rd instar eye discs. Clones are marked by absence of GFP.

(B-B'') Diap1 protein levels are reduced in, and increased adjacent to, *vps25*^{K2} clones.

(C-C'') BrdU labeling of GFP-marked *vps25*^{N55}/Diap1 mosaics. Over-expression of Diap1 does not block non-autonomous proliferation.

(D-D'') Caspase-3-labeling of GFP-marked *vps25*^{N55}/Diap1 mosaics. Caspase-3 is completely blocked. Scale bar: 100μm.

(E-E'') Caspase-3-labeling of GFP-marked *vps25*^{N55} *ark*^{H16} double mutant mosaics. Caspase-3-dependent cell death is detectable in *vps25*^{N55} *ark*^{H16} clones. Scale bar: 100μm.

(F) Adult eyes of *ey-FLP*-induced mosaics of *vps25*^{K2} *ark*^{G8} double mutants are severely overgrown and folded. Note: *vps25*^{K2} *ark*^{G8} clones are absent (marked by lack of red pigment).

Genotypes: (A-A'', B-B'') *ey-FLP* ; *FRT42D vps25*^{N55}*/FRT42D ubi-GFP*. (C-C'', D-D'') *hs-FLP UAS-GFP/UAS-Diap1* ; *FRT42D vps25*^{N55}*/FRT42D tub-Gal80* ; *tub-Gal4*. (E-E'') *hs-FLP UAS-GFP* ; *FRT42D vps25*^{N55} *ark*^{H16}*/FRT42D tub-Gal80* ; *tub-Gal4*. (F) *ey-FLP* ; *FRT42D vps25*^{N55} *ark*^{H16}*/FRT42D w*$^{+}$.

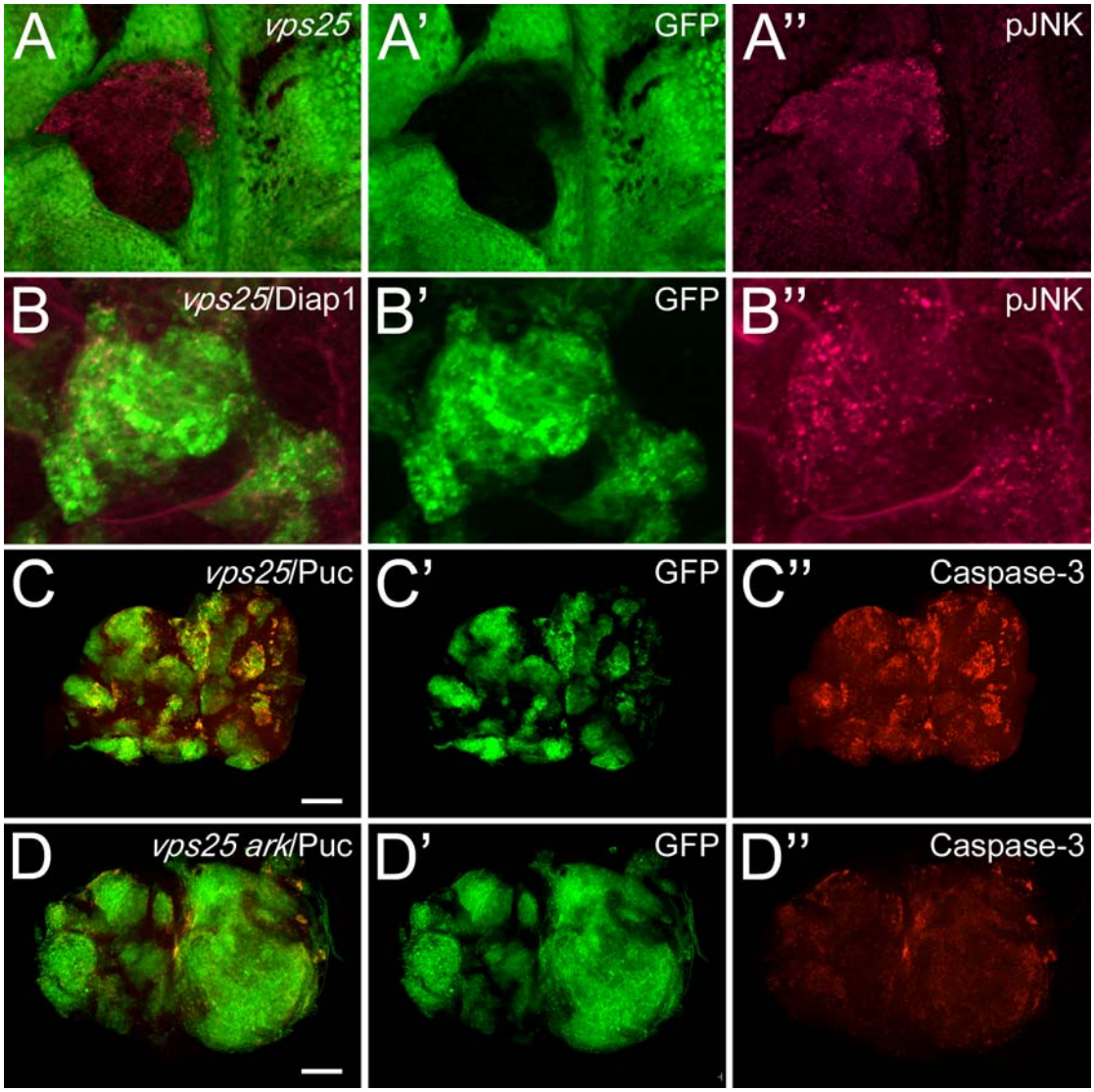

5.8 Fig. 8. JNK contributes to the apoptotic phenotype of *vps25* clones.

(A-A'') Increased JNK activity in *vps25*^{N55} clones by anti-pJNK labeling. Clones are marked by absence of GFP.

(B-B'') pJNK labeling of GFP-marked *vps25*^{N55}/Diap1 mosaics.

(C-C'') Caspase-3-labeling of GFP-marked *vps25*^{N55}/Puc mosaics. Scale bar: 100μm.

(D-D'') Caspase-3-labeling of GFP-marked *vps25*^{N55} *ark*^{G8}/Puc mosaics. Note, the clones marked with GFP are severely enlarged. Scale bar: 100μm.

Genotypes: (A-A'') *ey-FLP* ; *FRT42D vps25*^{N55}*/FRT42D ubi-GFP*. (B-B'') *hs-FLP UAS-GFP/UAS-Diap1* ; *FRT42D vps25*^{N55}*/FRT42D tub-Gal80*; *tub-Gal4*. (C-C'') *hs-FLP UAS-GFP* ; *FRT42D vps25*^{N55}*/FRT42D tub-Gal80*; *tub-Gal4/UAS-puc*. (D-D'') *hs-FLP UAS-GFP* ; *FRT42D vps25*^{N55} *ark*^{G8}*/FRT42D tub-Gal80*; *tub-Gal4/UAS-puc*.

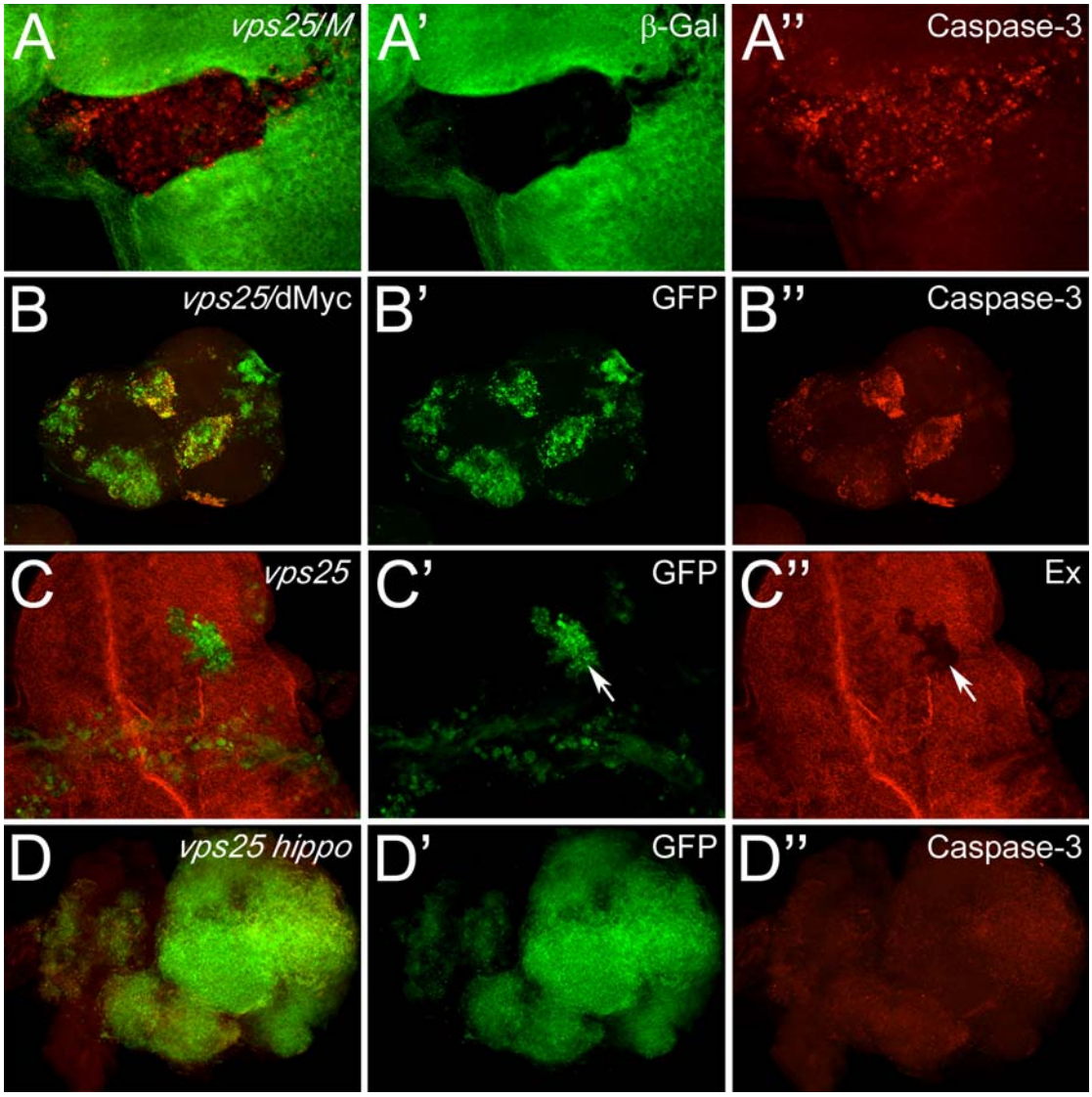

5.9 Fig. 9. Increased Hippo signaling, but not cell competition, controls apoptosis in *vps25* clones.

(A-A'') Caspase-3-labeling of $vps25^{N55}$ mosaics in *Minute* (*M*) background. Caspase-3 activity is unaffected. Clones are marked by the absence of β-Gal staining.

(B-B'') Caspase-3-labeling of GFP-marked $vps25^{N55}$/dMyc mosaics. Caspase-3-activity is unaffected.

(C-C'') Expanded (Ex) labeling of GFP-marked $vps25^{N55}$ mosaics. Ex protein levels are reduced in $vps25^{N55}$ clones (arrow), indicating increased Hippo activity.

(D-D'') Caspase-3-labeling of GFP-marked $vps25^{N55}$ $hippo^{D3}$ double mutant mosaics. Caspase-3 activity is blocked.

Genotypes: (A-A'') *ey-FLP* ; *FRT42D* $vps25^{N55}$/*FRT42D arm-lacZ M(2)*. (B-B'') *hs-FLP UAS-GFP* ; *FRT42* $vps25^{N55}$/*FRT42D tub-Gal80* ; *tub-Gal4*/*UAS-dMyc*. (C-C'') *hs-FLP UAS-GFP* ; *FRT42D* $vps25^{N55}$/*FRT42D tub-Gal80* ; *tub-Gal4*. (D-D'') *hs-FLP UAS-GFP* ; *FRT42D* $vps25^{N55}$ $hippo^{3D}$/*FRT42D tub-Gal80*; *tub-Gal4*.

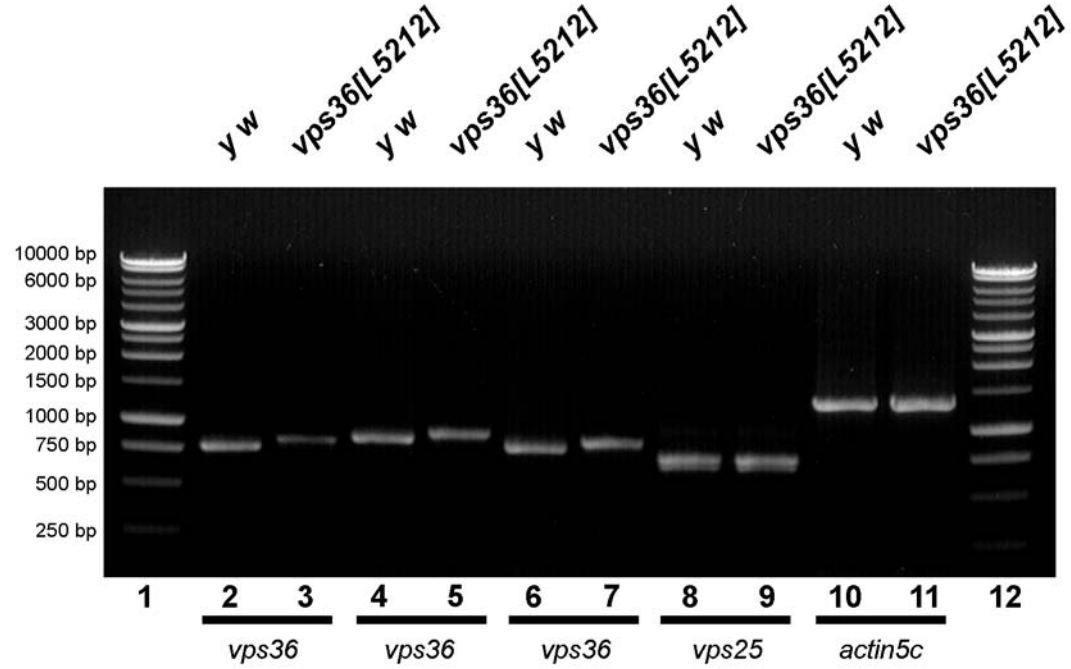

5.10 Fig. 10. RT PCR analysis of *vps36* mutants.

Lanes 1 and 12 depict the 1kb DNA ladder (Promega, G571A). RT PCR with primer pairs directed against a *vps36* transcript (lanes 2-7). RT PCR confirms reduced levels of *vps36* transcript in $vps36^{L5212}$ first instar larvae (lane 3) compared to *y w* controls (lane 2). However, transcript levels as detected with primer pairs targeting *vps36* transcription further downstream appear to be comparable between $vps36^{L5212}$ and *y w* controls (compare lanes 4 and 5, 6 and 7). Comparable levels of *vps25* (compare lanes 8 and 9) and *actin5c* (compare lanes 10 and 11) transcripts are obtained in $vps36^{L5212}$ mutants and *y w* controls.

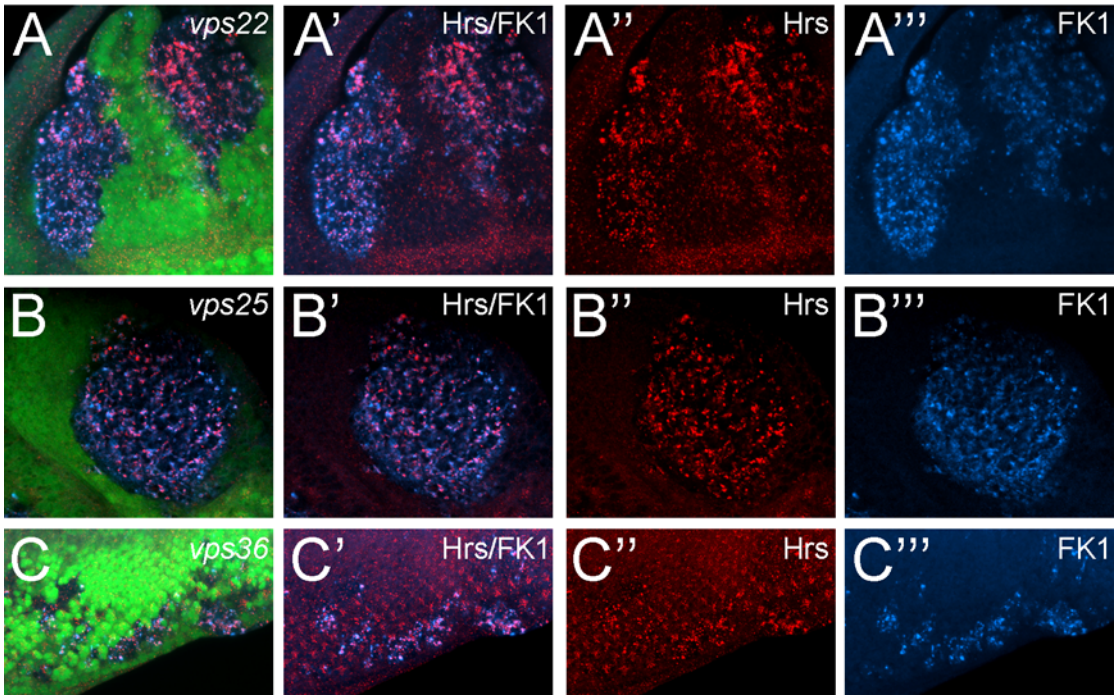

5.11 Fig. 11. Mutant clones of ESCRT-II components display endosomal defects and accumulate ubiquitinylated proteins at the early endosome.

Shown are eye-anntenal imaginal discs of third instar larvae mocaic for ESCRT-II mutants. Mutant clones are marked by the absence of GFP. Mutant clones of ESCRT-II components show changes in the subcellular localization of the early endosomal marker Hrs and accumulation of ubiquitin-conjugated proteins as visualized by the FK1 antibody. Hrs and ubiquitin-conjugated proteins accumulate in foci which co-localize frequently.

(A, B, C) GFP/Hrs/FK1 co-labelings of (A) $vps22^{5F8\text{-}3}$, (B) $vps25^{N55}$ and (C) $vps36^{L5212}$ eye mosaics.

(A', B', C') Hrs/FK1 co-labelings of (A') $vps22^{5F8\text{-}3}$, (B') $vps25^{N55}$ and (C') $vps36^{L5212}$ eye mosaics.

(A’’, B’’, C’’) Hrs labeling of (A’’) *vps22*$^{5F8\text{-}3}$, (B’’) *vps25*^{N55} and (C’’) *vps36*^{L5212} eye mosaics.

(A’’’, B’’’, C’’’) FK1 labeling of (A’’’) *vps22*$^{5F8\text{-}3}$, (B’’’) *vps25*^{N55} and (C’’’) *vps36*^{L5212} eye mosaics.

Areas of increased Ubiquitin concentration co-localize with increased levels of the Notch receptor (antibody against the extracellular domain of Notch) in ESCRT-II mutant tissue.

(D, E, F) GFP/Ubiquitin/N^{extra} co-labeling of (A) *vps22*$^{5F8\text{-}3}$, (B) *vps25*^{N55} and (C) *vps36*^{L5212} eye mosaics.

(D’, E’, F’) Ubiquitin/N^{extra} co-labeling of (D’) *vps22*$^{5F8\text{-}3}$, (E’) *vps25*^{N55} and (F’) *vps36*^{L5212} eye mosaics.

(D’’, E’’, F’’) Ubiquitin labeling of (D’’) *vps22*$^{5F8\text{-}3}$, (E’’) *vps25*^{N55} and (F’’) *vps36*^{L5212} eye mosaics.

(D’’’, E’’’, F’’’) N^{extra} labeling of (D’’’) *vps22*$^{5F8\text{-}3}$, (E’’’) *vps25*^{N55} and (F’’’) *vps36*^{L5212} eye mosaics.

Genotypes: (A-A’’’, D-D’’’) *ey-FLP ; FRT82B vps22*$^{5F8\text{-}3}$*/FRT82B ubi-GFP*, (B-B’’’, E-E’’’) *ey-FLP ; FRT42D vps25*^{N55}*/FRT42D ubi-GFP* and (C-C’’’, F-F’’’) *ey-FLP ; vps36*^{L5212} *FRT2A/ubi-GFP FRT2A*.

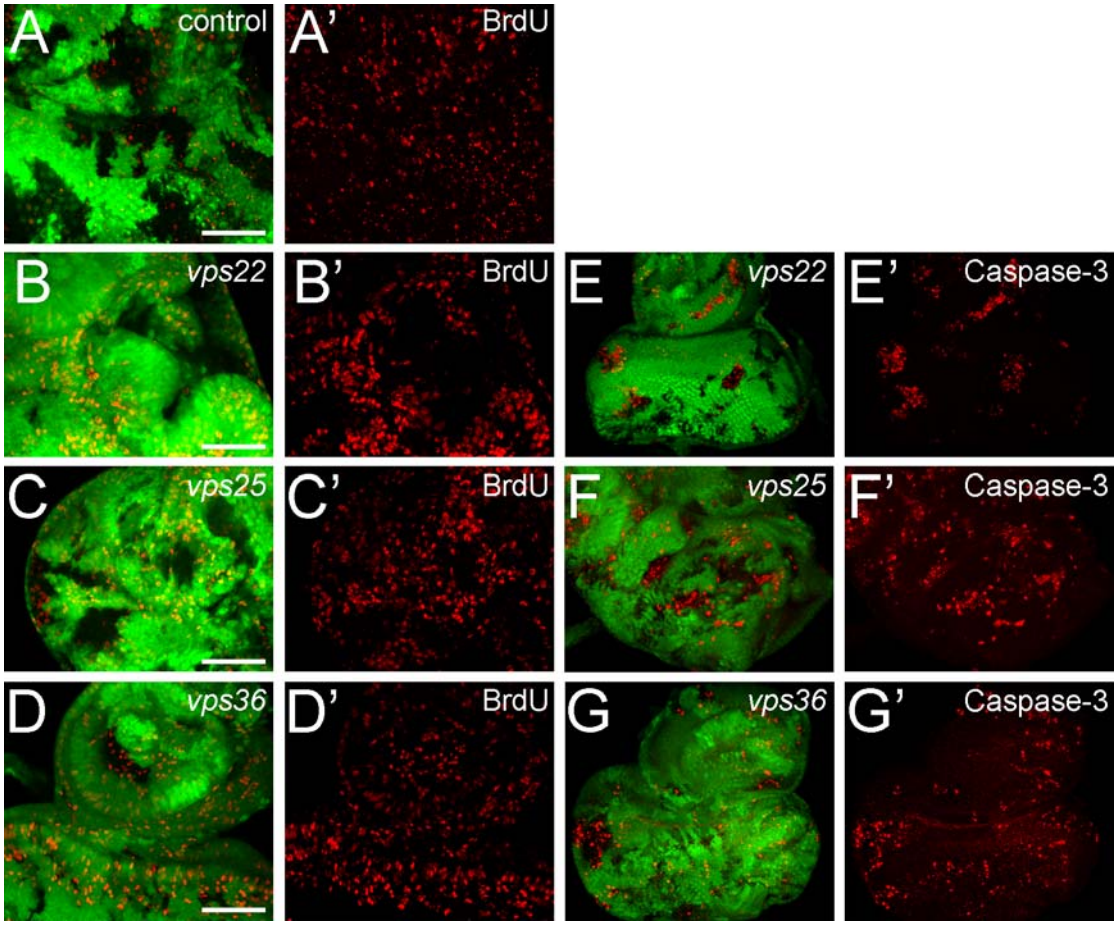

5.12 Fig. 12. Proliferation and apoptosis phenotypes of ESCRT-II mosaics.

(**A-D**) Non-autonomous regulation of proliferation in *vps22* and *vps25* eye mosaics as depicted by BrdU incorporation. Compared to control discs *vps36* mutants do not affect the proliferation pattern significantly.

(A-D) GFP/BrdU co-labelings of (A) control, (B) $vps22^{5F8\text{-}3}$, (C) $vps25^{N55}$ and (D) $vps36^{L5212}$ eye mosaics. The scale bar represents 50µm.

(A'-D') BrdU labeling of (A') control, (B') $vps22^{5F8\text{-}3}$, (C') $vps25^{N55}$ and (D') $vps36^{L5212}$ eye mosaics.

(**E-G**) Labeling of *vps22*, *vps25* and *vps36* eye-antennal imaginal discs with cleaved Caspase-3 (Cas-3) antibody as apoptotic marker.

(E-G) GFP/Caspase-3 co-labelings of (E) *vps22*$^{5F8-3}$, (F) *vps25*^{N55} and (G) *vps36*^{L5212} eye mosaics.

(E'-G') Caspase-3 labeling of (E') *vps22*$^{5F8-3}$, (F') *vps25*^{N55} and (G') *vps36*^{L5212} eye mosaics.

Genotypes: (A-A') *ey-FLP ; FRT42B/FRT42B ubi-GFP*, (B-B', E-E') *ey-FLP ; FRT82B vps22*$^{5F8-3}$*/FRT82B ubi-GFP*, (C-C', F-F') *ey-FLP ; FRT42D vps25*^{N55}*/FRT42D ubi-GFP* and (D-D', G-G') *ey-FLP ; vps36*^{L5212} *FRT2A/ubi-GFP FRT2A*.

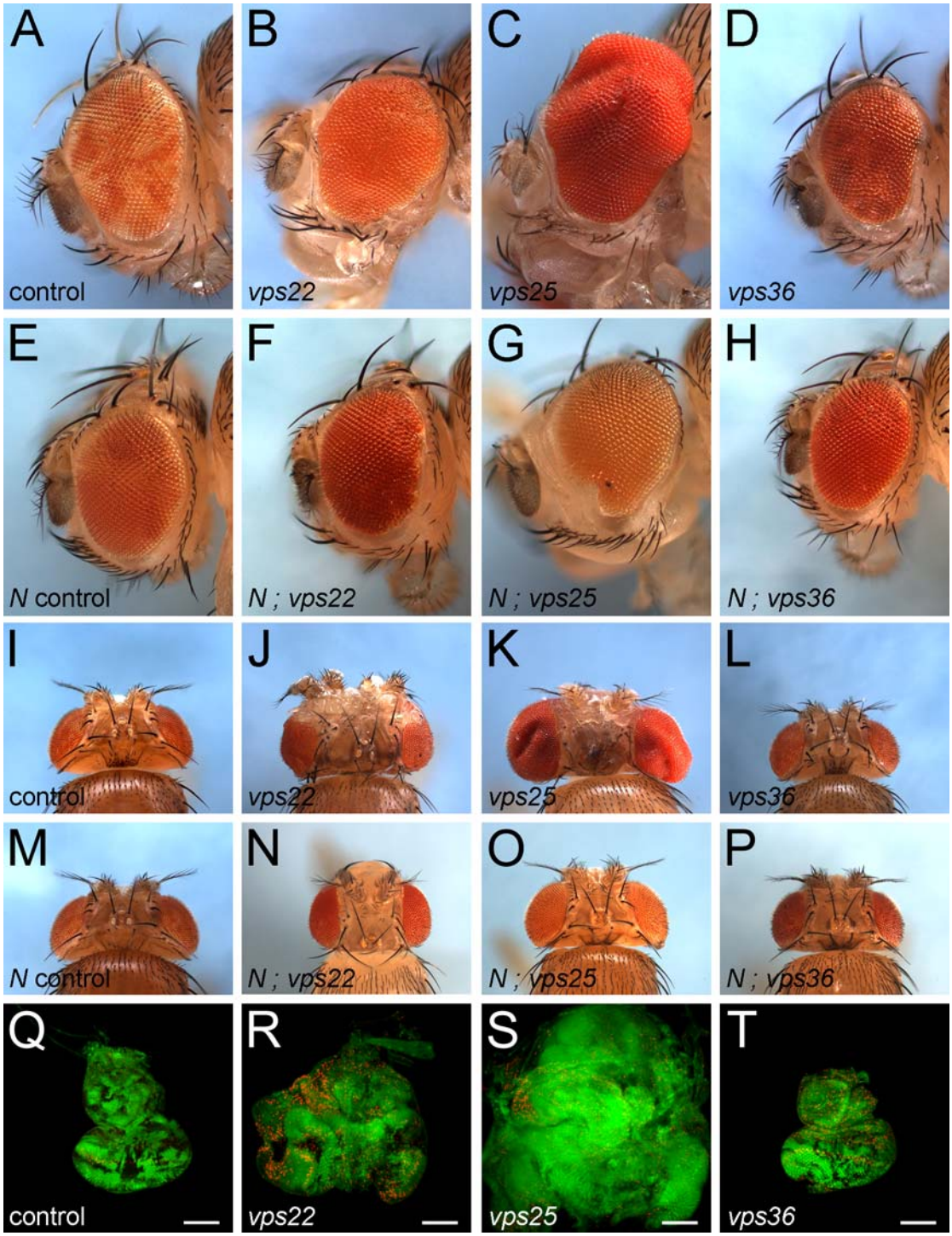

5.13 Fig. 13. Growth phenotypes of ESCRT-II mosaics.

vps22 and *vps25* mosaics display strong overgrowth phenotypes of the adult eyes and heads and the larval eye imaginal discs. In contrast, *vps36* mutants show just mild proliferation phenotypes such as a roughening of the adult eye. Removing one copy of

N in *vps22* and *vps25* mosaics reduces the overgrowth phenotypes of eyes and heads significantly and a weak effect can be observed on the roughening of *vps36* mosaics.

(A-D) Side view of genetic eye mosaics of (A) control flies, (B) $vps22^{5F8-3}$, (C) $vps25^{N55}$ and (D) $vps36^{L5212}$ mutants.

(E-H) Side view of genetic eye mosaics of (E) N^{264-39} control flies, (F) N^{264-39} ; $vps22^{5F8-3}$, (G) N^{264-39}; $vps25^{N55}$ and (H) N^{264-39} ; $vps36^{L5212}$ mutants.

(I-L) Top view of genetic eye mosaics of (I) control flies, (J) $vps22^{5F8-3}$, (K) $vps25^{N55}$ and (L) $vps36^{L5212}$ mutants.

(M-P) Top view of genetic eye mosaics of (E) N^{264-39} control flies, (F) N^{264-39} ; $vps22^{5F8-3}$, (G) N^{264-39} ; $vps25^{N55}$ and (H) N^{264-39} ; $vps36^{L5212}$ mutants.

(Q-T) Size comparison between eye imaginal discs of (Q) control, (R) $vps22^{5F8-3}$, (S) $vps25^{N55}$ and (T) $vps36^{L5212}$ mutants. The scale bar represents 100μm.

Genotypes: (A, I, Q) *y w ey-FLP ; FRT82B/ FRT82B P[w$^+$]*, (B, J, R) *y w ey-FLP ; FRT82B* $vps22^{5F8-3}$*/FRT82B P[w$^+$],* (C, K, S) *y w ey-FLP ; FRT42D* $vps25^{N55}$*/FRT42D P[w$^+$]*, and (D, L, T) *y w ey-FLP ;* $vps36^{L5212}$ *FRT2A/P[w$^+$] FRT2A*, (E, M) *y w ey-FLP/*N^{264-39} *; FRT82B/ FRT82B P[w$^+$]*, (F, N) *y w ey-FLP/*N^{264-39} *; FRT82B* $vps22^{5F8-3}$*/FRT82B P[w$^+$]*, (G, O) *y w ey-FLP/*N^{264-39} *; FRT42D* $vps25^{N55}$*/FRT42D P[w$^+$]*, (H, P) *y w ey-FLP/*N^{264-39} *;* $vps36^{L5212}$ *FRT2A/P[w$^+$] FRT2A*.

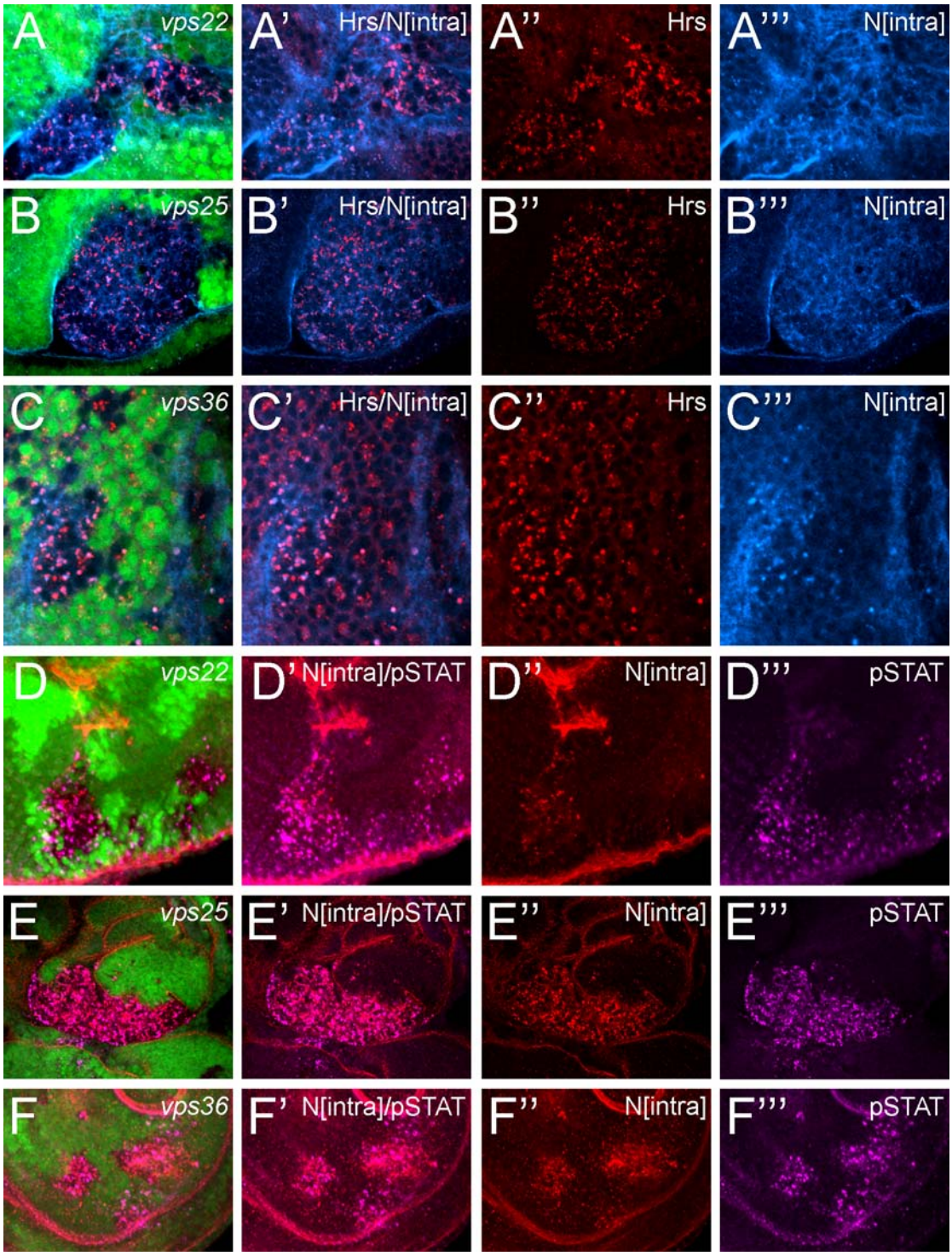
A
vps22
A'
Hrs/N[intra]
A''
Hrs
A'''
N[intra]
B
vps25
B'
Hrs/N[intra]
B''
Hrs
B'''
N[intra]
C
vps36
C'
Hrs/N[intra]
C''
Hrs
C'''
N[intra]
D
vps22
D'
N[intra]/pSTAT
D''
N[intra]
D'''
pSTAT
E
vps25
E'
N[intra]/pSTAT
E''
N[intra]
E'''
pSTAT
F
vps36
F'
N[intra]/pSTAT
F''
N[intra]
F'''
pSTAT

5.14 Fig. 14. Accumulation of Notch protein and JAK/STAT activity in ESCRT-II mosaics.

(**A-C**) The Notch receptor (detected with an antibody against the intracellular domain of Notch) co-localizes with the early endosomal marker Hrs in distinct punctae in mutant tissue of ESCRT-II components.

(A, B, C) GFP/Hrs/N^{intra} co-labelings of (A) $vps22^{5F8-3}$, (B) $vps25^{N55}$ and (C) $vps36^{L5212}$ eye mosaics.

(A', B', C') Hrs/N^{intra} co-labelings of (A') $vps22^{5F8-3}$, (B') $vps25^{N55}$ and (C') $vps36^{L5212}$ eye mosaics.

(A'', B'', C'') Hrs labeling of (A'') $vps22^{5F8-3}$, (B'') $vps25^{N55}$ and (C'') $vps36^{L5212}$ eye mosaics.

(A''', B''', C''') N^{intra} labeling of (A''') $vps22^{5F8-3}$, (B''') $vps25^{N55}$ and (C''') $vps36^{L5212}$ eye mosaics.

(**D-F**) Co-localization of accumulated Notch protein (using an antibody detecting the intracellular domain of Notch) and increased STAT activity, as visualized using anti-pSTAT antibody, a readout of JAK/STAT pathway activity.

(D, E, F) GFP/N^{intra}/pSTAT92E co-labelings of (D) $vps22^{5F8-3}$, (E) $vps25^{N55}$ and (F) $vps36^{L5212}$ eye mosaics.

(D', E', F') N^{intra}/pSTAT92E co-labelings of (D') $vps22^{5F8-3}$, (E') $vps25^{N55}$ and (F') $vps36^{L5212}$ eye mosaics.

(D'', E'', F'') N^{intra} labeling of (D'') $vps22^{5F8-3}$, (E'') $vps25^{N55}$ and (F'') $vps36^{L5212}$ eye mosaics.

(D''', E''', F''') pSTAT92E labeling of (D''') $vps22^{5F8-3}$, (E''') $vps25^{N55}$ and (F''') $vps36^{L5212}$ eye mosaics.

Genotypes: (A-A’’’, D-D’’’) *ey-FLP ; FRT82B vps22*$^{5F8\text{-}3}$*/FRT82B ubi-GFP*, (B-B’’’, E-E’’’) *ey-FLP ; FRT42D vps25*^{N55}*/FRT42D ubi-GFP* and (C-C’’’, F-F’’’) *ey-FLP ; vps36*^{L5212} *FRT2A/ubi-GFP FRT2A*.

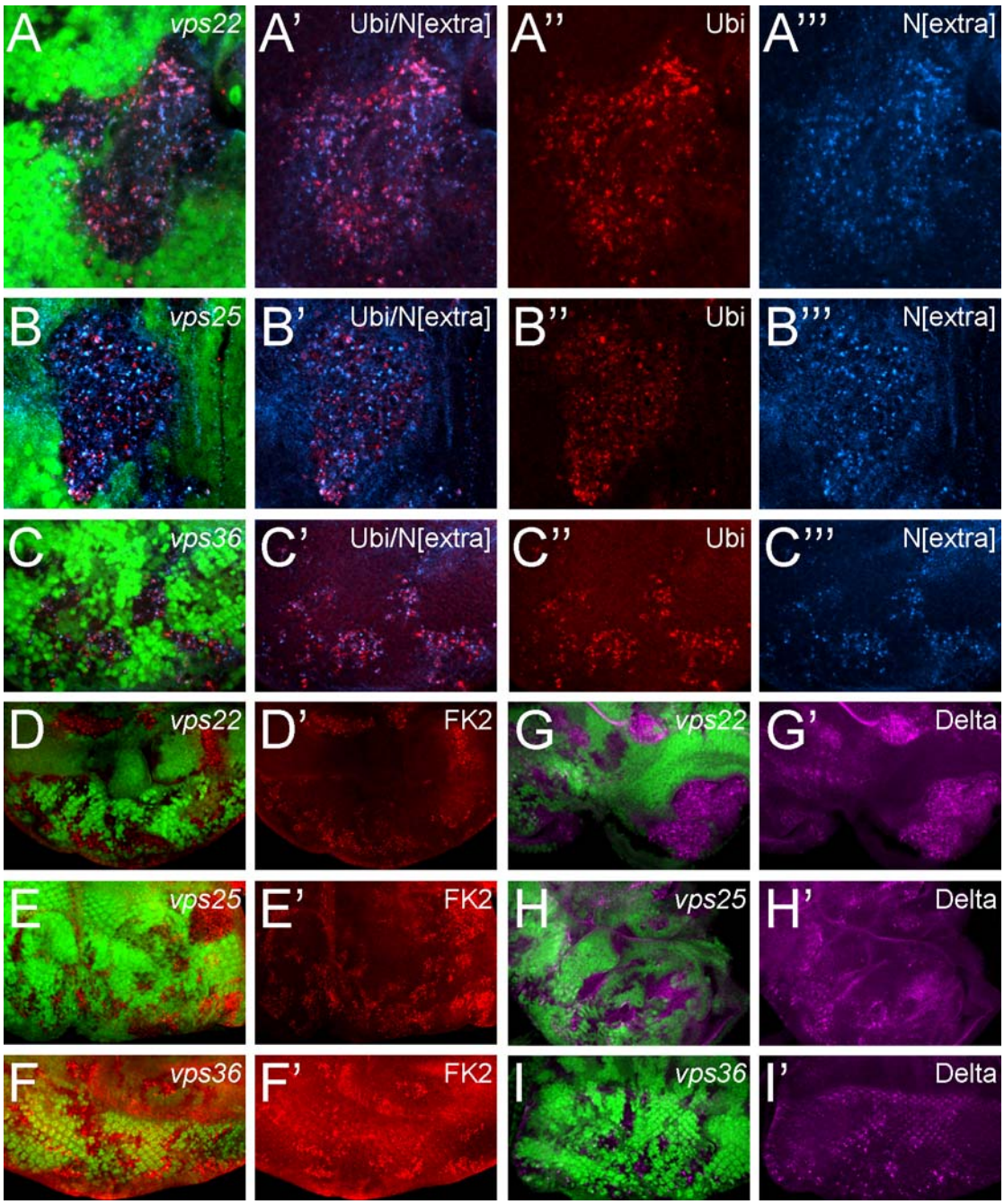

5.15 Fig. 15. The Notch receptor and its ligand Delta accumulate at the early endosome in ESCRT-II mosaics

(**A-C**)Areas of increased Ubiquitin concentration co-localize with increased levels of the Notch receptor (antibody against the extracellular domain of Notch) in ESCRT-II mutant tissue.

(A, B, C) GFP/Ubiquitin/N^{extra} co-labelings of (A) *vps22*$^{5F8-3}$, (B) *vps25*^{N55} and (C) *vps36*^{L5212} eye mosaics.

(A', B', C') Ubiquitin/N^{extra} co-labeling of (A') *vps22*$^{5F8-3}$, (B') *vps25*^{N55} and (C') *vps36*^{L5212} eye mosaics.

(A'', B'', C'') Ubiquitin labeling of (A'') *vps22*$^{5F8-3}$, (B'') *vps25*^{N55} and (C'') *vps36*^{L5212} eye mosaics.

(A''', B''', C''') N^{extra} labeling of (A''') *vps22*$^{5F8-3}$, (B''') *vps25*^{N55} and (C''') *vps36*^{L5212} eye mosaics.

(**D-F**) Aggregation of mono- and poly-ubiquitinylated proteins (detected by the FK2 antibody) in ESCRT-II mutant tissue.

(D, E, F) GFP/FK2 co-labeling of (D) *vps22*$^{5F8-3}$, (E) *vps25*^{N55} and (F) *vps36*^{L5212} eye mosaics.

(D', E', F') FK2 labeling of (D') *vps22*$^{5F8-3}$, (E') *vps25*^{N55} and (F') *vps36*^{L5212} eye mosaics.

(**G-I**) The Notch ligand Delta accumulates in foci that are reminiscent of the phenotype which is observed for the Notch receptor.

(G, H, I) GFP/Delta co-labeling of (G) *vps22*$^{5F8-3}$, (H) *vps25*^{N55} and (I) *vps36*^{L5212} eye mosaics.

(G', H', I') Delta labeling of (G') *vps22*$^{5F8-3}$, (H') *vps25*^{N55} and (I') *vps36*^{L5212} eye mosaics.

Genotypes: (A-A’’’, D-D’, G-G’) *ey-FLP ; FRT82B vps22*$^{5F8\text{-}3}$*/FRT82B ubi-GFP*, (B-B’’’, E-E’, H-H’) *ey-FLP ; FRT42D vps25*^{N55}*/FRT42D ubi-GFP* and (C-C’’’, F-F’, I-I’) *ey-FLP ; vps36*^{L5212} *FRT2A/ubi-GFP FRT2A*.

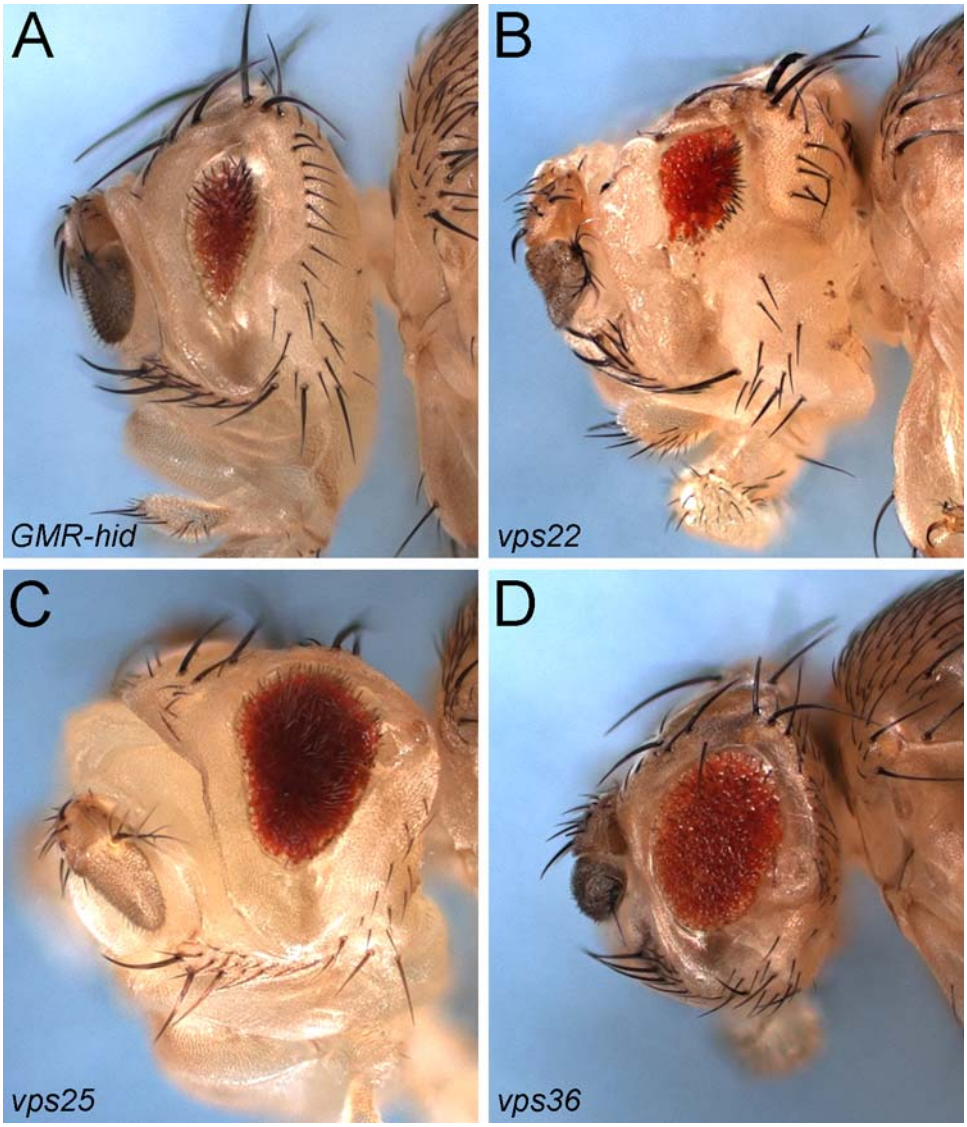

5.16 Fig. 16. Suppression of the *GMR-hid* eye ablation phenotype by ESCRT-II mosaics.

(**A**) Expression of the pro-apoptotic gene hid under control of the eye-specific *GMR* enhancer (*GMR-hid*) gives rise to a strong eye ablation phenotype due to excessive apoptosis.

(**B-D**) *vps25* (C) and *vps36* (D) eye mosaics are strong suppressors the *GMR-hid*-induced eye ablation phenotype in adult flies. *vps22* mosaics (B) which cause a strong overgrowth phenotype similar to *vps25* do not suppress the *GMR-hid*-eye ablation phenotype.

Genotypes: (A) *y w ey-FLP ; GMR-hid ; FRT82B/FRT82B P[w^{+}]*, (B) *y w ey-FLP ; GMR-hid ; FRT82B vps22^{5F8-3}/FRT82B P[w^{+}],* (C) *y w GMR-hid ey-FLP ; FRT42D vps25^{N55}/FRT42D P[w^{+}]* and (D) *y w ey-FLP ; GMR-hid ; vps36^{L5212} FRT2A/P[w^{+}] FRT2A*.

6 Discussion

The inactivation of signaling pathways is as important for appropriate tissue homeostasis as its activation. Interference with the inactivation process often gives rise to malignant phenotypes, including cancer. Several strategies to restrict signaling exist, including receptor sequestration, receptor inactivation, production of inhibitory signaling proteins, and inactivation of intracellular signaling proteins (reviewed in Sorkin and Von Zastrow, 2002; Le Roy and Wrana, 2005a). The phenotypic analysis of *vps22*, *vps25* and *vps36* mutants highlights the importance of receptor down-regulation by endosomal protein sorting. Lack of *vps25* function causes at least three phenotypes: non-autonomous proliferation, non-autonomous resistance to cell death, and autonomous apoptosis. Vps22 loss results just in two phenotypes: non-autonomous proliferation and autonomous apoptosis while disrupting *vps36* function leads to non-autonomous resistance to cell death and autonomous apoptosis. The differences and the cause of these combined phenotypes in mutations of different ESCRT-II members and the potential role of class E Vps proteins for tumorigenesis will be discussed below.

6.1 Endosomal phenotypes in *vps22*, *vps25* and *vps36* mosaics

So far, a systematic genetic analysis of class E *vps* genes has only been performed in yeast (Raymond et al., 1992) (reviewed in Katzmann et al., 2002). Endosomal defects in these mutants in yeast are genetically very similar. Vps22, Vps25 and Vps36 are components of the ESCRT-II complex required for internalization of cell surface receptors into MVBs at the early endosome (Babst et

al., 2002b). The signal for protein sorting into MVBs is provided by mono-ubiquitinylation (reviewed in Hicke and Dunn, 2003; Haglund and Dikic, 2005; Duncan et al., 2006; Huang et al., 2006). In yeast, mutations in ESCRT-II components cause aberrant endosomal structures and accumulation of ubiquitinylated proteins (Babst et al., 2002b) (reviewed in Katzmann et al., 2002). However, the consequences of the loss of appropriate endosomal sorting in multi-cellular organisms have only recently been described. In *Drosophila*, mutants of *hrs* display enlarged endosomes that accumulate ubiquitin-conjugated receptors on their limiting membrane (Lloyd et al., 2002; Jekely and Rorth, 2003). Our studies confirm these findings for *vps22*, *vps25* and *vps36* mosaics as well. Interference with the function of all three ESCRT-II members results in accumulation of ubiquitinylated protein cargo on Hrs positive endosomal compartments (Fig. 11A-C) confirming a role of ESCRT-II in MVB formation. This also implies that Hrs must act upstream of ESCRT-II function consistent with the studies that have been performed in yeast.

6.2 Shared and distinct genetic properties of ESCRT-II components

Our analysis and comparison of the mutant phenotypes of the ESCRT-II components *vps22*, *vps25* and *vps36* show that *vps22* mosaics are characterized by strong non-autonomous proliferation (Fig. 12B), but not an increase in apoptotic resistance (Fig. 16B). *vps36* mosaics exhibit the reverse phenotype, i.e. increased apoptotic resistance (Fig. 16D) and no or only weak non-autonomous proliferation (Fig. 12D). As shown before (Herz et al., 2006), *vps25* mosaics combine both phenotypes (Fig. 3B, C; 12C and 16C). Nonetheless, mutant tissue of all three

ESCRT-II members fails to survive (Fig. 4A and 12E-G). Furthermore, mutant larvae of all three ESCRT-II alleles tested in this study die at around the same developmental stage in the first or second instar suggesting that they affect larval development to a similar extend. Thus, this analysis shows that although these components are part of the same structural complex and in many aspects show great similarity, especially for endosomal phenotypes, they are not genetically equivalent and display distinct properties.

There are at least two reasons that might account for the differences in phenotypes. One will be discussed under 'Non autonomous proliferation by Notch signaling in vps mosaics'. The other reason simply considers the possibility that class E *vps* genes have also been reported to function outside of endosomal protein sorting. As such they appear to be involved in diverse processes like virus budding (reviewed in Martin-Serrano, 2007), cytokinesis (Spitzer et al., 2006; Carlton and Martin-Serrano, 2007), transcriptional control (Shilatifard, 1998; Sun et al., 1999), chromatin modification (Stauffer et al., 2001), mRNA localization (Irion and St Johnston, 2007), cell cycle progression (Li et al., 2001; Ruland et al., 2001) and apotosis (Krempler et al., 2002; Wagner et al., 2003) (for a more detailed overview see 'Introduction'). Therefore, it is possible that the observed genetic differences of the ESCRT-II components may be caused by distinct requirements in addition to and independently of endosomal function and possibly independently of the ESCRT-II complex and the remaining ESCRT machinery. Future work will be necessary to dissect the roles of the ESCRT-II components in processes unrelated to endosomal processing.

6.3 Non-autonomous proliferation by Notch signaling in *vps* mosaics

As we have shown in this study, the lack of appropriate protein sorting at the early endosome in *vps22*, *vps25* and *vps36* mutant tissue in *Drosophila* causes accumulation of N and its ligand Dl at an early endosomal compartment (Fig. 5A, B and Fig. 14A-C) which leads to increased activation of the N pathway (Fig. 5C). Even though we find evidence for altered regulation of various pathways in *vps25* mutant clones and embryos such as EGF receptor, Dpp and Wg signaling (data not shown) it appears that deregulation of the N pathway largely accounts for the observed overgrowth phenotype of *vps25* mosaics. For this reason we will focus on N signaling and related processes in the discussion to follow.

Others have shown that N signaling plays an important role in inducing non-autonomous proliferation through activation of the JAK/STAT pathway (Harrison et al., 1998; Chao et al., 2004; Tsai and Sun, 2004; Reynolds-Kenneally and Mlodzik, 2005). Consistently, our data support these findings as *vps22*, *vps25* and *vps36* mutant clones display increased pSTAT activity, a readout for JAK/STAT signaling (Fig. 5D and Fig. 14D-F). Furthermore, our genetic analysis using a dominant negative N transgene (N^{DN}, Fig. 6) suggests that the strong overgrowth phenotype of *vps25* mosaics is largely due to inappropriate N signaling (Fig. 6B) and that the observed increase in pSTAT immunoreactivity in *vps25* mutant clones is the result of elevated N activity (Fig. 6A). Our findings largely correspond with the results of others (Thompson et al., 2005; Vaccari and Bilder, 2005) who observe similar phenotypes in *vps25* clones, suggesting the conserved function of *vps25* in *Drosophila*. Additionally,

mutations in *erupted*, the *vps23* homolog which encodes a component of ESCRT-I, give rise to similar phenotypes as observed for *vps22* and *vps25* (Moberg et al., 2005). Astonishingly, a puzzling scenario is created by the analysis of *vps36* mosaics. *vps36* mutant clones exhibit the same levels of accumulated N receptors at the early endosome and display a similar level of activation of the JAK/STAT pathway as *vps22* and *vps25* mutant tissue (Fig. 14D-F) but show a much weaker overgrowth phenotype (Fig. 13). It is therefore possible that the strength in activation of the N and JAK/STAT pathway cannot be measured by comparing the endosomal phenotypes of the different ESCRT-II components alone and that the weaker overgrowth effect in *vps36* mosaics are the consequence of the hypomorphic nature of the *vps36* allele. Alternatively, the overgrowth phenotypes might be the result of at least two pathways acting synergistically. One of these could be the JAK/STAT pathway which may be more susceptible to alterations in regulation than a postulated second pathway. In *vps36* mosaics this susceptibility threshold might not have been reached for the putative second pathway yet and thus results in a weaker overgrowth phenotype that is only mediated by the activation of the JAK/STAT pathway.

However, in *hrs* mosaics in *Drosophila*, non-autonomous cell proliferation has not been observed although signaling receptors including N and Dl accumulate in *hrs* mutant tissue (Lloyd et al., 2002; Jekely and Rorth, 2003). This is a puzzling observation as *hrs* encodes a class E Vps protein acting as a member of the ESCRT-0 complex. It is possible that N and Dl are not in an environment in the *hrs* endosome which permits signaling. Alternatively, Jekely and Rørth (2003) showed that *hrs* controls the steady-state levels of non-activated receptors at the plasmamembrane.

Although this function may apply to *vps25*, it may also indicate that there are inherent differences between different class E proteins regarding protein sorting at the early endosome. Further support to the idea that N needs to be in a particular milieu at the early endosome in order to be activated comes from a study that analyses genes which act upstream of the ESCRT machinery in the endosomal pathway, namely *shibire*, *avalanche* and *Rab5*. Mutations in these genes result in accumulation of N on an early endosomal compartment but do surprisingly not activate the pathway (Vaccari et al., 2008). Additionally, mutations in the tumor suppressor *lethal giant discs* (*lgd*) have been demonstrated to cause very strong activation of N signaling (Childress et al., 2006; Gallagher and Knoblich, 2006; Jaekel and Klein, 2006). In *lgd* mutant clones Hrs co-localizes with N. Surprisingly, in contrast to *lgd* single mutant clones *hrs lgd* double mutant tissue did not show ectopic N activation (Childress et al., 2006; Jaekel and Klein, 2006). Furthermore, Lgd does not accumulate in *hrs* mutant clones but co-localizes with N in aberrant early endosomes in *vps25* mutant tissue (Childress et al., 2006). In summary, this places Lgd between Hrs and Vps25 at the early endosome. However, as Lgd does not seem to be required for controlling the activity of many other pathways which is the case for Hrs and Vps25 (Lloyd et al., 2002; Jekely and Rorth, 2003; Thompson et al., 2005), it probably is not part of the core machinery that regulates MVB formation but rather represents a specific modulator of N activation at the early endosome (Childress et al., 2006).

Currently, it is unclear whether N exerts its function in a ligand-dependent manner in *vps25* mosaics. Dl protein also accumulates in *vps25* clones (Fig. 5B), and endocytosis of Dl is required for N activation (Lai et al., 2001; Pavlopoulos et al.,

2001; Yeh et al., 2001; Itoh et al., 2003; Le Borgne and Schweisguth, 2003b) (reviewed in Le Borgne and Schweisguth, 2003a; Le Borgne et al., 2005; Le Borgne, 2006). Thus, blocking MVB formation in *vps25* clones may lead to accumulation of active Dl, resulting in increased N activity. However, we also show that N is required for Dl accumulation in *vps25* clones (Fig. 6C). There are two possibilities to explain these results. First, Dl accumulation is directly or indirectly the result of increased N activity in *vps25* clones. This conclusion infers that N activation occurs before Dl accumulation and would argue in favor of a ligand-independent mechanism for N activation in *vps25* clones, although Dl may be required for maintaining N activity. Ligand-independent activation of N has also been proposed for *erupted* (*vps23*) (Vaccari et al., 2008) and *lgd* (Childress et al., 2006; Jaekel and Klein, 2006). Alternatively, the use of a dominant-negative form of N in our study may result in cell autonomous '*cis*-inhibition' of Dl through N^{DN} at the plasmamembrane or another location. *'Cis*-inhibition' is a process that describes the cell autonomous binding of Dl and Ser to N to inactivate the pathway. It is currently not known where exactly in the cell this inhibition occurs (de Celis and Bray, 1997; Klein et al., 1997; Micchelli et al., 1997; Panin et al., 1997; Jacobsen et al., 1998; Sakamoto et al., 2002; Li and Baker, 2004; Ladi et al., 2005; Glittenberg et al., 2006). As a result of '*cis*-inhibition' Dl would be trapped and could no longer be shuttled to the early endosome.

As mentioned in the introduction N activity is also controlled by several proteolytic cleavages (reviewed in Mumm and Kopan, 2000; Fortini, 2002; Selkoe and Kopan, 2003), which result in the translocation of the intracellular domain of N to the nucleus where it regulates expression of different target genes. Thus, a potential

ligand-independent mode of N activation may include inappropriate cleavage of N at the *vps25* endosome. Traditionally, it has been thought that after ligand binding S3 cleavage of N occurs at the plasma membrane (reviewed in Kaether et al., 2006). However, Presenilin and other subunits of the γ-secretase complex have largely been found to localize to an endosomal compartment (Ray et al., 1999; Pasternak et al., 2003). It is interesting that mutations in genes that control endosomal trafficking at an earlier step than ESCRT members such as *Rab5*, *avalanche* -a *Drosophila* syntaxin-, *β-arrestin* and *hrs* do not affect N signaling significantly (Jekely and Rorth, 2003; Lu and Bilder, 2005; Mukherjee et al., 2005; Vaccari et al., 2008). In stark contrast, disrupting the endosomal process just slightly more downstream by interfering with the function of members of the ESCRT-I and –II complexes such as *erupted* (*vps23*) and *vps25* leads to strong N activation (Moberg et al., 2005; Thompson et al., 2005; Vaccari and Bilder, 2005; Herz et al., 2006). Furthermore, elevated N activity in RNAi-treated cells against different ESCRT components is sensitive to a γ-secretase inhibitor (Thompson et al., 2005) even though the amount of cleaved N in *vps25* mutant tissue does not change compared to wild-type as judged by an *ex vivo* assay (Vaccari et al., 2008). However, the same assay detects a marked decrease in the levels of cleaved N for mutations in endosomal regulators that act more upstream such as *avalanche* and *shibire* (Vaccari et al., 2008). Taken together, a model emerges suggesting that at least for ligand-independent processes S3 cleavage of N occurs in a special environment at the early endosome. Interfering with the process of MVB formation by disruption of ESCRT function might therefore alter the kinetics of N transit through this specific endosomal 'activation compartment'. Whether this milieu for N cleavage is created accidentally and thus might actually have nothing to do with the *in vivo* activation of the N pathway remains to be elucidated for further

clarification. Nonetheless, it is possible that ligand-dependent S3 cleavage of N might not occur at the same location on the early endosome but rather more upstream or even at the plasma membrane.

6.4 Non-autonomous regulation of cell death by *vps25* and *vps36*

Paradoxically, although *vps22*, *vps25* and *vps36* clones die by apoptosis (Fig. 4A and 12F, G) we just identified *vps25* and *vps36* alleles as recessive suppressors of *GMR-hid*-induced cell death (Fig. 3B, C and 16C, D). Our analysis demonstrates that the wild-type tissue in *vps25* mosaics accounts for this suppression (Fig. 3K, L) although these cells are exposed to *GMR-hid*. However, these findings do not explain why *vps36* is a strong suppressor of *GMR-hid*, while *vps22* completely fails to suppress *GMR-hid* (Figure 16B, D). Thus, it does not appear that the phenotypic differences observed between *vps22* and *vps36* are due to allelic strength of the mutants. Rather, they appear to be caused by intrinsic differences of the endogenous genes which could function in endosomal independent processes as well (see also discussion under 'Shared and distinct genetic properties of ESCRT-II components').

Our initial explanation for this observation of non-autonomous resistance against apoptosis was that non-autonomous proliferation mediated by JAK/STAT signaling in *vps25* mosaics overrides the apoptotic activity of *GMR-hid*. However, over-expression of *upd*, the ligand of the JAK/STAT pathway, does not significantly suppress *GMR-hid* (Fig. 6F), although *GMR-upd* flies have a similar overgrowth

phenotype as *vps25* mosaics (Bach et al., 2003; Muller et al., 2005). This finding excludes non-autonomous proliferation through the JAK/STAT pathway for suppression of *GMR-hid* by *vps25*. However, Diap1 protein levels are increased in tissue abutting *vps25* clones (Fig. 7B). *GMR-hid* is sensitive to altered levels of Diap1 (Hay et al., 1995) suggesting that the increase of Diap1 outside of *vps25* clones may account for the suppression of *GMR-hid* even though it cannot be excluded that non-autonomous regulation of other apoptotic components causes the *GMR-hid* suppression phenotype. Thus, in addition to non-autonomous proliferation, *vps25* clones also increase the apoptotic resistance of adjacent wild-type tissue in a non-autonomous manner. The signaling pathway which can induce non-autonomous survival by increasing Diap1 protein levels is currently unknown. However, non-autonomous resistance against cell death might very well be dependent on N signaling as over-expression of the intracellular domain of *N* results in a very strong suppression of *GMR-hid* (Fig. 6G). This is very interesting, especially because N activation has been implicated to exert a pro-apoptotic function during retinal development of *Drosophila* (Miller and Cagan, 1998; Yu et al., 2002), but can have anti-apoptotic effects in other contexts as well (Deftos et al., 1998; Jehn et al., 1999). More recently, a mechanism has been proposed in which the intracellular domain of N can mediate the inhibition of apoptosis by binding to and preventing the auto-ubiquitinylation and thus degradation of XIAP, a mammalian inhibitor of apoptosis (Liu et al., 2007). Even though the results of these studies show that N activation can lead to even opposite effects depending on the developmental context and tissue in which N is functioning, they do not explain how N might mediate non-autonomous resistance against cell death. Possible mediators of this anti-apoptotic function of N signaling could be identified by performing a deficiency screen with the *GMR-hid*

GMR-Gal4/UAS-N^{intra} eye phenotype (Fig. 6G). Deficiencies which revert this phenotype (at least to a certain extend) would be further analyzed in order to identify the genes responsible for mediating the anti-apoptotic effect of the N pathway. In parallel, another deficiency screen that would make use of the *GMR-hid* suppression phenotype of *vps25* and *vps36* mosaics could lead to the identification of another set of genes as regulators of apoptosis. A significant overlap in these two sets of genes would imply that the non-autonomous resistance against cell death in *vps25* and *vps36* mosaics and the *GMR-hid* suppression by over-expression of N^{intra} are conveyed by the same factors.

6.5 Cell death in *vps* clones of ESCRT-II members

Our data also suggest that apoptosis in *vps25* mutant tissue is not only executed via the Hid/Diap1/Dronc/Ark-pathway. *vps25 ark* clones still died (Fig. 7F), suggesting that in addition to Ark at least one other pro-apoptotic component is activated in *vps25* clones. We showed previously that a Dronc/Ark-independent cell death pathway exists in *Drosophila*, but did not identify this pathway (Xu et al., 2005; Srivastava et al., 2007). Our data here implicate JNK as potential mediator of an alternative cell death pathway (Adachi-Yamada et al., 1999; Adachi-Yamada and O'Connor, 2002). *vps25 ark*/Puc mosaic eye discs are extremely overgrown and the clones occupy a large area of the disc (Fig. 8D). Caspase-3-dependent apoptosis is blocked in these clones (Fig. 8D). Only at the clonal boundaries, Caspase-3 activity is still detectable, suggesting that at the interface between *vps25* clones and wild-type tissue a potentially third apoptotic pathway is activated (Fig. 8D). Alternatively, the

surrounding wild-type cells could be outcompeted at the clonal margins and subsequently undergo cell death.

Our data show that cell competition is not sufficient to induce cell death in *vps25* clones (Fig. 9A, B). In contrast, given the extremely large size of cell death-inhibited *vps25* clones (Fig. 8D and 9D), it appears that *vps25* clones have no intrinsic growth disadvantage, and have the capability to overgrow and outcompete the surrounding wild-type tissue if cell death is blocked. Thus, cell competition does not contribute significantly to the apoptotic phenotype of *vps25* clones.

We show that Hippo signaling is increased in *vps25* clones (reviewed in Edgar, 2006; Harvey and Tapon, 2007; Pan, 2007; Saucedo and Edgar, 2007) Hippo signaling can induce cell death, and consistently, *hippo* mutants block cell death in *vps25* clones (Fig. 9D). Currently, it is unknown how Hippo signaling is activated in *vps25* clones. However, in analogy to N, a putative receptor that controls Hippo signaling may be deregulated in *vps25* clones and triggers Hippo signaling. This receptor has been postulated (Hamaratoglu et al., 2006) and lead to the identification of Fat, an atypical cadherin (Bennett and Harvey, 2006; Silva et al., 2006; Willecke et al., 2006). Even though Diap1 protein levels are upregulated in *fat* mutant clones (Bennett and Harvey, 2006; Silva et al., 2006; Willecke et al., 2006), *fat* eye mosaics do not result in suppression of *GMR-hid* (data not shown). Additionally, *fat* mutant tissue does not phenocopy *hippo* mutant clones in all aspects. Therefore, at least one other receptor still remains to be identified. This receptor might be responsible for mediating the pro-apoptotic signal in *vps22*, *vps25* and *vps36* mutant clones.

Alternatively, redundancy between several receptors that control the Hippo pathway may require the combined activation of all of them. However, it should also be pointed out that ESCRT components have additional functions outside of MVB protein sorting (see also 'Introduction'). Certain ESCRT-II members have been shown to bind to the transcriptional elongation factor ELL in order to derepress transcription by RNA polymerase II (Shilatifard, 1998; Schmidt et al., 1999; Kamura et al., 2001). Thus, in the absence of Vps25, transcriptional control of components of the Hippo pathway may be deregulated and contribute to cell death.

In summary, our data suggest that impaired ESCRT-II function leads to accumulation of N and Dl, and possibly of a receptor controlling the Hippo pathway. These receptors control non-autonomous proliferation and autonomous apoptosis, respectively. In addition, we postulate a signaling pathway that induces non-autonomous cell survival by controlling Diap1 protein levels or another anti-apoptotic factor. Further characterization of the *vps25* mutant phenotype may help identifying the postulated receptor of the Hippo pathway and the cell survival signaling pathway (for example by a screen as already mentioned above under 'Suppression of *GMR-hid* by non-autonomous increase of Diap1').

6.6 ESCRT-II components in *Drosophila*: a model for human cancer?

Human ESCRT components, most notably *Tsg101* (*vps23*), have been implicated in tumor suppression. NIH3T3 cells, depleted of *Tsg101* by an antisense

approach, formed colonies on soft agar and produced metastatic tumors in nude mice (Li and Cohen, 1996). However, the conditional *Tsg101* knockout in mouse mammary glands did not cause the formation of tumors over a period of two years, making a role of *Tsg101* as tumor suppressor controversial (Wagner et al., 2003). *Tsg101* mutant cells are very sensitive to apoptotic death (Wagner et al., 2003) implying that they die before they become harmful to the organism.

The phenotypic characterization of *vps25* mutants in *Drosophila* provides an explanation for the failure to confirm *Tsg101* as tumor suppressor. *vps25* clones need to survive over extended periods of time in order to sustain growth. Even though they induce non-autonomous proliferation, after they have died, N signaling is turned off and proliferation stops. Furthermore, the size of the adult eye of *vps25* mosaics is only slightly increased compared to wild-type, and does not match the strong overgrowth phenotype of larval imaginal discs which can be twice as large as wild-type discs (Fig. 3G-I). Thus, as long as *vps25* clones are not resistant to their own apoptotic death, tissue repair during pupal stages may partially regress the size of the imaginal disc back to almost normal. Instead, it appears that inhibition of cell death is the triggering event for a tumorous phenotype of *vps25* clones. *vps25*/Diap1 and *vps25 ark*/Puc clones can make up a large fraction of the tissue of imaginal discs, and the entire discs can be five times as large as wild-type discs (Fig. 7D and 8D).

Tumorigenesis requires multiple genetic alterations that transform normal cells progressively into malignant cancer cells (Hanahan and Weinberg, 2000). Thus, additional genetic ‘hits’ may be necessary to inhibit apoptosis of *Tsg101* mutant cells,

which may then be able to induce a similar growth phenotype as observed for *vps25*. The strong neoplastic transformation of *vps25* mutant tissue that we observe when cell death is blocked is also supported by a *Drosophila* model which shows the ability of transplanted cell death resistant *vps25* mutant tissue to form metastases (Thompson et al., 2005). Experiments that largely eliminate the surrounding wild-type tissue further support the neoplastic nature of *ept* and *vps25* mutant tissue (Moberg et al., 2005; Vaccari and Bilder, 2005). Thus, although a tumor suppressor function for *Tsg101* was not confirmed in a mouse model, it still is possible that *Tsg101* and other mammalian ESCRT members have tumor suppressor properties.

7 Significance of research and conclusion

For a long time the study of the major signaling pathways has been occupied with the identification of new components to gain a better understanding of the hierarchy of the proteins involved. In many instances this led to a more detailed picture of the activation and inhibition mechanisms of each signaling pathway. However, although our knowledge about the participating proteins in these pathways is as detailed as never before, many questions remain unanswered. For one thing because we do not know all components yet, for another thing it also increasingly becomes more obvious that there is a significant amount of cross talk and cross regulation going on between these pathways. Most importantly, accumulating evidence particularly over the past few years suggests that this lack of understanding how signaling pathways are regulated has much to do with our inadequate apprehension of the endocytic pathway. More and more researchers seem to recognize the fact that our insight into the regulation of signaling pathways can ultimately just be satisfied if we gain a better understanding of the regulatory mechanisms at the different endocytic compartments within the cell. It appears rather that probably all of the major signaling pathways are controlled in some way by the endocytic machinery.

Therefore, in this context the discovery of the ESCRT complexes in yeast (Katzmann et al., 2001; Babst et al., 2002a; Babst et al., 2002b) contributed largely to the progress in the field, giving us some answers to the mechanics of receptor turnover through regulation of MVB sorting at the early endosome and thus of the control of signaling itself. The general function of these complexes implies an interference with various signaling pathways which has been confirmed in various studies including ours (see also ‘Introduction’ and ‘Discussion’). As many of the

major signaling pathways are involved in developmental decisions including cell fate determination, differentiation, growth control and apoptosis it is to be expected that these processes are also impaired when certain components of the endocytic machinery are disrupted. In fact, this topic has been under extensive review (Sorkin and Von Zastrow, 2002; Gonzalez-Gaitan, 2003; Dudu et al., 2004; Le Roy and Wrana, 2005a; Fischer et al., 2006; Giebel and Wodarz, 2006; Hariharan and Bilder, 2006; Polo and Di Fiore, 2006; von Zastrow and Sorkin, 2007) and is supported by our findings that components of ESCRT-II in *Drosophila* regulate development through such diverse processes as differentiation, autonomous and non-autonomous proliferation, autonomous apoptosis and non-autonomous resistance against cell death. Whether all of these phenotypes are dependent on the endosomal functions of ESCRT or whether some of them are the result of regulatory control of endosomal independent mechanisms remains to be determined in the future.

8 Materials and Methods

8.1 Antibodies

8.1.1 Primary antibodies

Antigen used	Host	Source	Concentration
Armadillo	mouse	Hybridoma Bank (N2 7A1)	1:20
β-Galactosidase	mouse	Promega (Z378A)	1:1000
β-Galactosidase	rabbit	ICL (RGAL-45A)	1:500
Caspase-3	rabbit	Cell Signaling (9661)	1:100
Cut	mouse	Hybridoma Bank (2B10)	1:100
Delta	mouse	Hybridoma Bank (C594.9B)	1:20
Diap1	guinea pig	Pascal Meier (SK10)	1:400
Diap1	guinea pig	Pascal Meier (SK14)	1:400
Diap1	rabbit	Pascal Meier (227)	1:400
Diap1	rabbit	Pascal Meier (228)	1:400
Elav	mouse	Hybridoma Bank (9F8A9)	1:20
Elav	rat	Hybridoma Bank (7E8A10)	1:40
dpERK	mouse	Sigma (M-8159)	1:500
Expanded	rabbit	Allen Laughon	1:1500
GFP	mouse	Millipore (MAB 2510)	1:100
GFP	rabbit	Invitrogen (A11122)	1:100
Hid	guinea pig	Hong Don Ryoo	1:50

Hrs	guinea pig	Hugo Bellen	1:1000
pJNK	rabbit	Cell Signaling (9251)	1:100
N^{intra}	mouse	Hybridoma Bank (C17.9C6)	1:20
N^{extra}	mouse	Hybridoma Bank (C458.2H)	1:20
pSTAT92E	rabbit	Cell Signaling (9357)	1:100
Ubiquitin	rabbit	Sigma (U5379)	1:10
Ubiquitin (FK1)	mouse	Biomol Intern. (PW8805)	1:100
Ubiquitin (FK2)	mouse	Biomol Intern. (PW8810)	1:100
Wingless	mouse	Hybridoma Bank (4D4)	1:50

8.1.2 Secondary Antibodies

All secondary antibodies were obtained from Jackson ImmunoResearch. They were conjugated with either FITC-, Cy3- or Cy5-fluorophores and used at a dilution of 1:600.

8.2 Fly strains

Lines for P-element and deficiency mapping (Bloomington stock numbers and cytolocation included)

y w ; P{SUP or -P}KG01834	14580	43E11
y w ; P{SUP or -P}KG01035	13186	49D6
y w ; P{SUP or -P}KG04965	13534	56D1
y w ; P{SUP or -P}KG02448	13224	57A5
w ; Df(2R)H3C1/CyO	198	43F—44D8
w ; Df(2R)H3E1/CyO	201	44D1—44F12

w ; Df(2R)8047, P+Pbac{XP5.RB3}Exel8047/CyO 7863 44D4—44D5

w ; Df(2R)7098, P+Pbac{XP5.RB3}Exel7098/CyO 7864 44D5—44E3

Cell death genes

y w; FRT42D y^+ ark^{G8}*/CyO*

y w ; FRT42D y^+ ark^{H16}*/CyO*

y w ; FRT42D y^+ $hippo^{3D}$*/CyO*

***vps* alleles**

y w ; FRT42D y^+ $vps22^{2B6\text{-}3}$*/TM3, Ser, act-GFP* (Daniel St Johnston)

y w ; FRT42D y^+ $vps22^{5F8\text{-}3}$*/TM3, Ser, act-GFP* (Daniel St Johnston)

y w ; P{lacW}CG14750^{KG08904}*/CyO = y w ; P{lacW}vps25*^{KG08904}*/CyO* (Bloomington)

y w ; FRT42D y^+ $vps25^{K2}$*/CyO, act-GFP*

y w ; FRT42D y^+ $vps25^{K2}$ ark^{G8}*/CyO*

y w ; FRT42D y^+ $vps25^{N55}$*/CyO, act-GFP*

y w ; FRT42D y^+ $vps25^{N55}$ ark^{H16}*/CyO*

y w ; FRT42D y^+ $vps25^{N55}$ *UAS-*N^{DN}*/CyO*

y w ; $vps36^{L5212}$ *FRT2A/TM3, Ser, act-GFP* (Bloomington)

***FLP/FRT* lines**

w ; FRT42D y^+ (Barry Dickson)

y w ey-FLP ; ry (Bloomington)

y w GMR-hid ey-FLP

y w ey-FLP ; FRT42D w^+ (Barry Dickson)

y w ey-FLP ; FRT42D ubi-GFP (Georg Halder)

y w hs-FLP ; FRT42D ubi-GFP (Georg Halder)

y w hs-FLP UAS-GFP ; FRT42D tub-Gal80/CyO ; tub-Gal4/TM6B, Tb (Georg Halder)*(Irion and St Johnston, 2007)* (Lee and Luo, 2001)

y w hs-FLP ; FRT42D arm-lacz M(2)/CyO (Graeme Mardon)

y w GMR-hid ey-FLP ; FRT42D w^{+}

y w ey-FLP ; FRT42D w^{+}*/CyO ; GMR-hid*$^{w-}$

w ; ubi-GFP FRT2A (Bloomington)

w ; FRT82B/TM3, Sb (Bloomington)

y w ey-FLP ; FRT82B ubi-GFP (Georg Halder)

y w GMR-hid ey-FLP ; FRT82B ubi-GFP

GMR-hid lines

y w GMR-hid ey-FLP

y w ; GMR-hid GMR-Gal4/CyO, act-GFP

UAS constructs

y w UAS-diap1 (on X)

y w ; UAS-N^{DN}*/CyO* (Hugo Bellen)

y w hs-FLP ; UAS-N^{NEXT}*/CyO ; MKRS/TM2* (Gary Struhl)

y w hs-FLP ; UAS-$N^{751.6F}$*(full length)/CyO ; MKRS/TM2* (Gary Struhl)

y w ; UAS-N^{intra}*/CyO* (Hugo Bellen)

y w ; UAS-dMyc2.1/CyO (David Stein)

y w ; UAS-puc (on III) (Georg Halder)

y w ; UAS-upd26.2/CyO (Erika Bach)

Reporter lines

y w ; E(spl)m8 2.61-lacz/CyO (Kramatschek and Campos-Ortega, 1994)

y w ; brinker-lacz/TM3, Sb (Georg Halder)

8.3 Plasmids

pUAST

8.4 Primers

Primers are aligned in 5'-3' configuration. Restriction sites are depicted in bold and mentioned at the end of each primer.

vps25

CG14750.1: TGCTATTTAGCGCATATGGTCACTC (sense)

CG14750.2: CGAGACTGCAATGGCAGGTAA (antisense)

CG14750.3: G**GAATTC**ACAAATAAGTGTTTTCTTGGGATATT (sense)
EcoRI

CG14750.4: GC**TCTAGA**TCGTGTGGACAGGCTAACCAG (antisense) XbaI

CG14750.5: G**GAATTC**GCGCATATGGTCACTCTAGGC (sense) EcoRI

CG14750.6: GC**TCTAGA**ATGTACATTTTACAATACTTTACTCC (antisense)
XbaI

vps36

vps36.1: TGAATCGCTTCGCTTATGTG (sense)

vps36.2: CAGGCTACTGAAGTAGGCAGAA (antisense)

vps36.3: TCACCACACACCGACTGTTT (sense)

vps36.4: CGTGGGACTCCAGTTGTAGC (antisense)

vps36.5: AATGGCCTGAGTGTCGAGTT (sense)

vps36.6: CAGTCCCTCTACGGACTCGT (antisense)

actin5c

actin5c.1: TCAGCCTCGCCACTTGCG (sense)

actin5c.2: TGTTGTGCTGCACTCCAAACTTC (antisense)

8.5 Protocols

8.5.1 Antibody staining of embryos

Antibody stainings of embryos were performed using the Vectastain ABC Kit (Vector Laboratories, PK-6100).

Embryo fixation

1. Collect embryos from plate using a brush
2. Rinse embryos with water
3. Dechorionate embryos in 50% bleach (Clorox) for 3min
4. Rinse well with water
5. Fix embryos in 750µl heptane, 675µl PBS and 75µl formaldehyde (38%) for 20min on shaker with >400rpm
6. Remove as much of lower phase as possible
7. Add 750µl methanol
8. Devitellinize embryos by shaking vial vigorously by hand for 30s

9. Wash embryos 4 x in 500µl methanol
10. Store embryos in methanol at -20ºC until further processing

Antibody incubation

1. Rehydrate embryos through two washes each with 500µl PBT containing 90%, 70%, 50% and 25% methanol
2. Rinse 4 x in 500µl PBT
3. Transfer embryos in 500µl tube
4. Block embryos in 500µl PBT containing 5% normal donkey serum (NDS) for 20min
5. Prepare primary antibody solution in PBT containing 3% NDS
6. Aspirate primary antibody solution
7. Rinse 4 x with 500µl PBT
8. Wash embryos 4 x in 500µl PBT for 15min on shaker
9. Add 100µl of secondary antibody in PBT containing 3% NDS
10. Incubate for 90min at RT on shaker
11. Aspirate secondary antibody solution
12. Rinse 4 x with 500µl PBT
13. Wash 4 x in 500µl PBT for 15min on shaker
14. Prepare AB solution about 15-30min before adding to embryos: to 100µl of PBT add 1µl of component A and 1µl of component B from Vectastain ABC Kit (Vector Laboratories, PK-6100); mix and incubate for 15-30min at RT
15. Add 100µl of AB solution to embryos; incubate for 45-60min at RT on shaker
16. Aspirate AB solution
17. Rinse 4 x with 500µl PBT

18. Wash 4 x in 500µl PBT for 15min on shaker

Optional: TSA amplification

Occasionally it is necessary to amplify the signal even further. This can be accomplished by using the TSA Biotin System from PerkinElmer Life Sciences (NEL700A). The treatment will result in deposition of additional biotin moieties in the vicinity of the antigen. These can then be visualized using the Vectastain ABC Kit.

1. Rinse embryos 2 x in 50µl amplification diluent
2. Prepare TSA solution by diluting TSA reagent 1:50 in amplification diluent
3. Add 50µl TSA solution to embryos
4. Incubate for 10-15min at RT on shaker
5. Aspirate TSA solution
6. Rinse 4 x with 500µl PBT
7. Wash 2 x in 500µl PBT for 15min on shaker
8. Prepare AB solution about 15-30min before adding to embryos: to 100µl of PBT add 1µl of component A and 1µl of component B from Vectastain ABC Kit; mix and incubate for 15-30min at RT
9. Add 100µl of AB solution to embryos; incubate for 30min at RT on shaker
10. Aspirate AB solution
11. Rinse 4 x with 500µl PBT
12. Wash 4 x in 500µl PBT for 15min on shaker

Staining reaction

1. Dilute H_2O_2 (30%) from stock bottle 1:10 with PBT
2. Thaw 3, 3'-diaminobenzidine (DAB) stock solution (1%) (wear gloves)
3. Add 2µl of diluted H_2O_2 to 500µl of PBT
4. Add 500µl of H_2O_2-containing PBT to embryos
5. Transfer embryos and H_2O_2-containing PBT to a well of 24 micro titer plates
6. Dilute DAB from stock 1:10 with PBT (wear gloves)
7. Add 500µl diluted DAB to embryos (wear gloves)
8. Watch progress of reaction under dissecting scope and stop by washing embryos several times with PBT; discard DAB-containing solutions in 20-30% bleach
9. Transfer embryos to a 500µl eppendorf vial
10. Wash several times in 500µl PBT
11. Add 70% glycerol, let embryos settle, mount on slides, view and photograph

8.5.2 Antibody staining of imaginal discs

1. Dissect larval head in PBS pH 7.0 by pulling gently at the mouth hook to retrieve the larval brain with eye discs (for eye discs) or cut the anterior third of larvae off in PBS pH 7.0 and invert larval cuticle to expose the discs (for eye, wing and leg discs)
2. Remove extraneous tissue such as trachea, fat body, gut and salivary glands
3. Fix tissue in 300µl PBS pH 7.0 containing 4% paraformaldehyde for 20min at room temperature (RT)
4. Wash tissue in 300µl PBS pH 7.0 for 10min at RT
5. Incubate tissue in 300µl Block buffer for >30min at RT
6. Incubate tissue with primary antibody in wash buffer (100µl) over night at 4ºC

7. Wash tissue 3 x 20min in 300µl wash buffer at RT
8. Incubate tissue with secondary antibody in wash buffer (100µl) for 3 h at RT or over night at 4ºC
9. Wash tissue 3 x 20min in 300µl wash buffer at RT
10. Fix tissue in 300µl PBS pH 7.0 containing 4% paraformaldehyde for 20min at room temperature (RT)
11. Isolate discs from remaining tissue and add ~15µl of Vectashield (Vector Laboratories, H-1000)

8.5.3 BrdU staining of imaginal discs

Day 1

1. Dissect imaginal discs in cold Schneider's medium (Invitrogen, 11720) on ice, dissection should be done in less than 15min
2. Remove extraneous tissue such as trachea, fat body, gut and salivary glands
3. Incubate tissue in 0.5 mg/ml BrdU in Schneider's (1mg BrdU powder (Roche, 10280879) + 2ml Schneider's, dissolve well) for 1h at RT
4. Wash tissue 1 x fast and 1 x in 300µl Schneider's for 5min at 4ºC (RT)
5. Wash tissue 1 x fast and 2 x in 300µl PBS for 5min at 4ºC (RT)
6. Fix tissue in 300µl PBS containing 4% paraformaldehyde over night at 4ºC on shaker

Day 2

1. Wash tissue 3 x fast and 4 x in 300µl PBS for 10min at 4ºC (RT)
2. Incubate tissue in 5µl RQ1-DNAse (1µg/µl) (Promega, M6101) + 95µl DNAse buffer for 2h at 37ºC in water bath

3. Wash tissue 1 x fast and 3 x in 300µl PBT for 10min at 4ºC (RT)
4. Block tissue in 300µl PBTN for 1h at 4ºC (RT)
5. Incubate tissue with α-BrdU primary antibody (Becton Dickinson) in PBTN over night at 4ºC (RT)

Day 3

1. Wash tissue 3 x fast and 4 x in 300µl PBT for 20min at 4ºC (RT)
2. Incubate tissue with secondary antibody in PBTN for 4h or over night at 4ºC (RT)
3. Wash tissue 3 x fast and 6 x in 300µl PBT for 20min at 4ºC (RT)
4. Fix tissue in 300µl PBS pH 7.0 containing 4% paraformaldehyde for 20min at room temperature (RT)
5. Isolate discs from remaining tissue and add ~15µl of Vectashield (Vector Laboratories, H-1000)

8.5.4 TUNEL staining of imaginal discs

TUNEL staining was performed using the In Situ Cell Death Detection Kit TMR Red from Roche (12156792910) and Dilution Buffer from Roche (11966006001).

Day 1

1. Dissect larval head in PBS pH 7.0 by pulling gently at the mouth hook to retrieve the larval brain with eye discs (for eye discs) or cut the anterior third of larvae off in PBS pH 7.0 and invert larval cuticle to expose the discs (for eye, wing and leg discs)
2. Remove extraneous tissue such as trachea, fat body, gut and salivary glands

3. Fix tissue in 300µl PBS pH 7.0 containing 4% paraformaldehyde for 20min at room temperature (RT)
4. Wash tissue 3 x fast and 4 x in 300µl PBT for 15min at 4˚C (RT)
5. Block tissue in 300µl PBTN for 1h at 4˚C (if not performing antibody staining, block overnight and proceed to day 3: step #10)
6. Incubate tissue with primary antibody in PBTN (100µl) overnight at 4˚C

Day 2

1. Wash tissue 3 x fast and 6 x in 300µl PBT for 20min at 4˚C (RT)
2. Incubate tissue with secondary antibody [optional: TOPRO 1:2000] in PBTN for 4h at 4˚C
3. Wash tissue 3 x fast and 6 x in 300µl PBT for 20min at 4˚C (RT)
4. Block tissue in 300µl PBTN overnight at 4˚C

Day 3:

1. Incubate tissue in 495µl 100 mM NaCitrate + 5µl 10% Triton X-100 for 30min at 65˚C
2. Wash tissue 3 x fast in 300µl PBT at RT
3. Incubate tissue in 100µl of TUNEL Dilution Buffer (Roche, 11966006001), 2 x 5min each at RT
4. Incubate tissue in 50µl labeling solution (In Situ Cell Death Detection Kit TMR Red, Roche, 12156792910) for 30min at 37˚C in water bath
5. Add 5µl enzyme solution (In situ Cell Death Detection Kit TMR red), mix well, incubate for 2h at 37˚C in water bath

6. Wash tissue 3 x fast in 300µl PBT at 4˚C (RT)
7. Optional: Incubate tissue with TOPRO (1:2000) in PBTN for 30min at 4˚C
8. Wash tissue 3 x fast and 4 x in 300µl PBT for 15min at 4˚C (RT)
9. Isolate discs from remaining tissue and add ~15µl of Vectashield (Vector Laboratories, H-1000)

8.5.5 Preparation of competent E. coli

1. Inoculate a single colony of competent cells into 5ml of LB medium, shake at 37ºC overnight
2. Put 5ml of above cell culture into 1l of LB medium, shake at 37ºC (250rpm), follow OD_{550} till density reaches 0.5
3. Put cells for 10min on ice, keep everything cold
4. Spin down culture with 3500rpm for 10min at 4ºC
5. Remove supernatant from pellet
6. Gently resuspend pellet in 250ml cold, sterile, 0.1 M $MgCl_2$, keep on ice for 30min, spin with 3000rpm for 10min at 4ºC
7. Resuspend pellet in 250ml cold, sterile 0.1 M $CaCl_2$, keep on ice for 20min, spin with 3000rpm for 20min at 4ºC
8. Resuspend pellet in a total of 50ml cold, sterile 0.1 M $CaCl_2$ with 7ml of RT 100% Glycerol, mix gently, aliquot and freeze in dry ice/Ethanol bath, store at -80ºC

8.6 Solutions and growth media

8.6.1 Solutions for imaginal disc labeling

PBS (50ml): 150 mM NaCl (0.44g NaCl)

10 mM Na_3PO_4 pH 7.0 (2.89 ml 0.1 M Na_2HPO_4 + 2.11ml 0.1 M NaH_2PO_4)

ad 50ml ddH_2O

10 x PBS (50ml): 1.5 M NaCl (4.4g NaCl)

100 mM Na_3PO_4 pH 7.0 (28.9 ml 0.1 M Na_2HPO_4 + 21.1ml 0.1 M NaH_2PO_4)

ad 50ml ddH_2O

PBT (50ml): 150 mM NaCl (0.44g NaCl)

10 mM Na_3PO_4 pH 7.0 (2.89 ml 0.1 M Na_2HPO_4 + 2.11ml 0.1 M NaH_2PO_4)

0.3% Triton X-100 (30µl 100% Triton X-100)

ad 50ml ddH_2O

PBTN (50ml): 150 mM NaCl (0.44g NaCl)

10 mM Na_3PO_4 pH 7.0 (2.89 ml 0.1 M Na_2HPO_4 + 2.11ml 0.1 M NaH_2PO_4)

0.3% Triton X-100 (30µl 100% Triton X-100)

2mg/ml Normal Donkey Serum (NDS) (100mg NDS)

ad 50ml ddH_2O

Block Buffer (10ml): 50 mM Tris pH 6.8 (1ml 0.5 M Tris pH 6.8)

50 mM NaCl (300µl 5 M NaCl)

0.5% NP-40 (50µl 100% NP-40)

5mg/ml Bovine serum albumin (BSA) (50mg BSA)

ad 10ml ddH_2O

Wash Buffer (50ml): 50 mM Tris pH 6.8 (5ml 0.5 M Tris pH 6.8)

150 mM NaCl (1.5ml 5 M NaCl)

0.5% NP-40 (250µl 100% NP-40)

1mg/ml BSA (50mg BSA)

ad 50ml ddH_2O

Fix Solution (40ml): 4ml 10 x PBS

10ml 16% paraformaldehyde (Electron Microscopy Sciences, 15710)

ad 40ml ddH_2O

8.6.2 Solutions for gel electrophoresis

50 x TAE (1l): 242g Tris base pH 8.5

57.1ml Acetic acid

100ml 0.5M EDTA

ad 1l ddH_2O

8.6.3 Solutions for genomic DNA isolation

TE: 10 mM Tris-HCl pH 7.5

1 mM EDTA

Solution A: 0.1 M Tris-HCl pH 9.0

0.1 M EDTA

1% SDS

8.6.4 Growth media

LB: 10g NaCl

10g Tryptone (DIFCO, 211705)

5g yeast extract (DIFCO, 212750)

ad 1l ddH_2O

LB plates: LB components

15g agar (DIFCO, 214510)

(alternatively 50mg Ampicillin = 50µg/ml)

ad 1l ddH_2O

8.7 Techniques

8.7.1 Gel electrophoresis

Gels were prepared with 150ml TAE and 1.5g of agarose (1%). Agarose was dissolved in a microwave and cooled at RT for 10min. 10µl ethidium bromide was added and Gels poured in chambers. Gels were run with 100V for 35min.

8.7.2 Isolation of genomic DNA

The following protocol describes the isolation of DNA from adult flies but can be used equally well to extract DNA from other developmental stages. DNA prepared according to this method is readily digested by restriction enzymes and has an average size of 40-60kb. In order to remove RNA contaminating the DNA preparations DNase-free RNase should be included when digesting with restriction enzymes.

1. Anaesthetize flies with CO2 and put 30 flies in an eppendorf tube, keep on ice until next step
2. Add solution A and 0.5-1% DEPC (added directly before use) and homogenize gently with a glass or metal rod. Use 100µl of solution A for extracting DNA from 1-5 flies, 200µl for 6-10 flies and 500µl for up to 50 flies. Incubate for 20-30min at 70ºC
3. Add 14µl of 8 M potassium acetate for each 100µl homogenate and leave on ice for 30min.
4. Spin at full speed for 15min at 4ºC. Transfer the supernatant into a fresh eppendorf tube being careful not to disturb the pellet. If you get flakes in the supernatant respin.

5. Precipitate DNA by adding 0.5 volumes of isopropanol at RT and spin at full speed for 5min at RT. Wash the pellet carefully with 70% ethanol, respin at full speed for 5min at RT, dry and dissolve pellet in 10µl (1 fly) to 100µl (50 flies) ddH_2O (TE)

8.7.3 RNA isolation

10mg of *vps36*^{L5212} or *y w* first instar larvae were collected. RNA isolation was performed using the RNeasy Mini Kit from Qiagen (74104) following the description in the manual.

8.7.4 RT PCR (Invitrogen)

RT PCR was performed following the description for the Super Script First-Strand Synthesis System for RT-PCR from Invitrogen (12371-019).

1. Heat to 65ºC for 5min, put on ice
2. Prepare reaction mix: x µl 10 x RT buffer (2 x total # of reactions)
   x µl 25 mM $MgCl_2$ (4 x total # of reactions)
   x µl 0.1 M DTT (2 x total # of reactions)
   x µl RNAse OUT (1 x total # of reactions)
3. Add 9µl reaction mix to each tube, spin down, incubate for 2min at RT
4. Add 1µl reverse transcriptase (RT) to each tube, incubate for 10min at RT
5. Incubate for 1h at 42ºC
6. Incubate for 15min at 70ºC, put on ice
7. Spin down briefly, add 1µl RNAse H

8. Incubate for 20min at 37ºC
9. Store cDNA at -20ºC

8.7.5 PCR amplification of genomic DNA and cDNA

Primers *CG14750.3* together with *CG14750.4* and *CG14750.5* together with *CG14750.6* were used for PCR amplification of genomic *vps25* DNA. cDNA amplification was performed with primer pairs *vps36.1* and *vps36.2*, *vps36.3* and *vps36.4*, *vps36.5* and *vps36.6*, *CG14750.3* and *CG14750.4*, *actin5c.1* and *actin5c.2*.

PCR reaction for genomic DNA

1µl primer1 (30 µM)

1µl primer2 (30 µM)

2µl dNTPs (10 mM)

5µl 10 x PCR buffer

1µl $MgCl_2$ (25 mM)

1µl genomic DNA

1µl Taq polymerase

38µl ddH_2O

PCR reaction for cDNA

1µl primer1 (30 µM)

1µl primer2 (30 µM)

2µl dNTPs (10 mM)

5µl 10 x PCR buffer

1µl $MgCl_2$ (25 mM)

20µl cDNA

1µl Taq polymerase

19µl ddH_2O

PCR program

5min 94ºC

30s 94ºC (melting)

1min annealing temperature of primers

1min 30s 72ºC

10min 72ºC (final extension)

∞ 4ºC

30 cycles were run for genomic DNA and 35 cycles for cDNA.

8.7.6 Purification of PCR-amplified DNA

Plasmids and PCR-amplified DNA were purified using either the QIAquick PCR Purification Kit (28106) or QIAquick Gel Extraction Kit (28704) from Qiagen following the description in the manuals, respectively.

8.7.7 Sequencing of amplified DNA

Primers *CG14750.1*, *CG14750.2*, *CG14750.3*, *CG14750.4*, *CG14750.5* and *CG14750.6* were used for sequence analysis of $vps25^{K2}$ and $vps25^{N55}$ and the genomic rescue constructs (see also 'Genomic rescue construct'). Sequencing of amplified

DNA was performed by the 'DNA Analysis Core Facility' of M.D. Anderson Cancer Center.

http://inside.mdanderson.org/departments/dna/index.html

8.7.8 Amplification of plasmids and constructs

Plasmids and constructs were amplified using either the QIAprep Spin Mini Prep Kit (12243) or QIAfilter Plasmid Midi Kit (28704) from Qiagen following the description in the manuals, respectively.

8.7.9 Bacterial transformation

1. Thaw competent bacteria on ice
2. Add 0.5µl of plasmid or construct DNA (1mg/ml)
3. Incubate on ice for 30min
4. Heat shock for 1min at 42ºC
5. Add 1ml of LB
6. Shake for 1h at 37ºC
7. Plate 50µl and rest on Ampicillin-containing (50µg/ml) LB plates
8. Incubate plates at 37ºC overnight

8.7.10 Genomic rescue construct

DNA was extracted via the 'Isolation of genomic DNA' protocol from *w ; FRT42D y+* flies and PCR-amplified with the primer pairs *CG14750.3*, *CG14750.4* and *CG14750.5*, *CG14750.6* as described under 'PCR amplification of genomic DNA and

cDNA'. Purification was obtained as reported under 'Purification of PCR-amplified DNA'. The resulting PCR products were digested with EcoRI and XbaI and cloned into a pUAST plasmid. The genomic rescue construct was transformed into competent E. coli as described under 'Bacterial transformation' and amplified following 'Amplification of plasmids and constructs'. Correct *vps25* sequences were confirmed as described under 'Sequencing of amplified DNA'. The genomic rescue constructs were injected with self-pulled glass needles in preblastoderm embryos using an Axiovert 25 platform from Zeiss and the FemtoJet injection apparatus from Eppendorf.

8.8 Genetic methods

8.8.1 EMS screen

1. Starve 50-100 males per empty bottle for 12h
2. Prepare 25mM ethyl methane sulfonate (EMS) (240µl) suspension in 5% Sucrose (100ml)
3. For inactivation of EMS use 10% Sodiumthiosulfate (500ml)
4. Fold Kleenex towels to fit in empty bottles
5. Fix Kleenex towels with pipette tip at bottom of bottle
6. Add ~9ml of EMS suspension on Kleenex towel
7. Transfer starved flies in prepared bottle
8. Incubate flies for 24h
9. Cross EMS treated males to ~double number of females
10. Transfer flies every day to new bottle (about 10 days)

8.8.2 Recombination mapping

See Fig. 2 for a detailed description of recombination mapping of the *K2/N55* alleles according to the method described in (Zhai et al., 2003).

8.8.3 Gal4-UAS system

The Gal4-UAS system was used for over-expression of various genes of interest. Gal4 is a transcriptional activator from yeast that targets genes which contain *UAS* sequences. By combining the *Gal4* gene with tissue specific promoters (i. e. in this study *Glass Multimer Reporter GMR*) targeted over-expression of *UAS*-linked genes of interest can be achieved (Fischer et al., 1988).

8.8.4 FLP/FRT system

The *FLP/FRT* system was designed to create mutant tissue in a wild-type environment to be able to comparatively study the effects of certain genes of interest (in our case *vps25*). Tissue-specific (in our study the *eyeless* promoter) or heat shock-driven activation of Flippase induces mitotic recombination at FLP recombinase targets (FRTs) resulting in two different clones. One clone is mutant for the gene of interest and the other clone homozygous wild-type. Tissue that has not undergone mitotic recombination is heterozygous mutant. The phenotypes of the various clones can be visualized by appropriate markers (for example *GFP* and w^+) located distally to the respective FRT (Xu and Rubin, 1993).

8.9 Photography

8.9.1 Fly eye and head images

To be prepared for photography, flies were anaesthetized with CO_2 and frozen for 20min at -80ºC. Flies were simply turned on their sides for photography of fly eyes. For pictures that were taken from the top the abdomen was glued (superglue) to the surface of a paper card. In order to prevent light reflection on the cuticle of the fly a 2.5cm high ring was cut out of a white styrofoam cup and placed around the specimen. The two ends of a ‘goose neck’ light source ‘goose neck’ light source (KL 1500 LCD from Leica or KL 2500 LCD from Zeiss) were pointed from the outside from opposite directions on the inside of the cup, allowing the light to reflect of the cup and onto the fly. Pictures were taken using the Z16 APO from Leica or the Imager.Z1 from Zeiss. Cameras were either the DFC 300 FX from Leica or tha AxioCam HRc from Zeiss. Software used was ImagePro Plus 6.1 for Leica or AxioVision Rel. 4.5 for Zeiss applications. For Zeiss applications individual pictures of one Z-stack were merged using the CZ Focus software.

8.9.2 Fluorescence images

Fluorescence pictures were taken using the confocal microscope Fluoview FV500 with Fluoview software from Olympus or especially for lower magnification images the Imager.Z1 light microscope with Apotome technology, AxioVision Rel. 4.5 software and the camera AxioCam MRm from Zeiss. For Zeiss applications individual pictures of one Z-stack were merged using the CZ Focus software.

8.9.3 Gel images

Gel images were acquired with the AlphaImager 2200 from Alpha Innotech with AlphaImager 2200 software.

9 References

Abrams, J. M. (2002). Competition and compensation: coupled to death in development and cancer. *Cell* **110**, 403-6.

Adachi-Yamada, T., Fujimura-Kamada, K., Nishida, Y. and Matsumoto, K. (1999). Distortion of proximodistal information causes JNK-dependent apoptosis in Drosophila wing. *Nature* **400**, 166-9.

Adachi-Yamada, T. and O'Connor, M. B. (2002). Morphogenetic apoptosis: a mechanism for correcting discontinuities in morphogen gradients. *Dev Biol* **251**, 74-90.

Agromayor, M. and Martin-Serrano, J. (2006). Interaction of AMSH with ESCRT-III and deubiquitination of endosomal cargo. *J Biol Chem* **281**, 23083-91.

Alam, S. L., Langelier, C., Whitby, F. G., Koirala, S., Robinson, H., Hill, C. P. and Sundquist, W. I. (2006). Structural basis for ubiquitin recognition by the human ESCRT-II EAP45 GLUE domain. *Nat Struct Mol Biol* **13**, 1029-30.

Alam, S. L., Sun, J., Payne, M., Welch, B. D., Blake, B. K., Davis, D. R., Meyer, H. H., Emr, S. D. and Sundquist, W. I. (2004). Ubiquitin interactions of NZF zinc fingers. *Embo J* **23**, 1411-21.

Allenspach, E. J., Maillard, I., Aster, J. C. and Pear, W. S. (2002). Notch signaling in cancer. *Cancer Biol Ther* **1**, 466-76.

Amerik, A. Y., Nowak, J., Swaminathan, S. and Hochstrasser, M. (2000). The Doa4 deubiquitinating enzyme is functionally linked to the vacuolar protein-sorting and endocytic pathways. *Mol Biol Cell* **11**, 3365-80.

Azmi, I., Davies, B., Dimaano, C., Payne, J., Eckert, D., Babst, M. and Katzmann, D. J. (2006). Recycling of ESCRTs by the AAA-ATPase Vps4 is regulated by a conserved VSL region in Vta1. *J Cell Biol* **172**, 705-17.

Azmi, I. F., Davies, B. A., Xiao, J., Babst, M., Xu, Z. and Katzmann, D. J. (2008). ESCRT-III family members stimulate Vps4 ATPase activity directly or via Vta1. *Dev Cell* **14**, 50-61.

Babst, M. (2005). A protein's final ESCRT. *Traffic* **6**, 2-9.

Babst, M., Katzmann, D. J., Estepa-Sabal, E. J., Meerloo, T. and Emr, S. D. (2002a). Escrt-III: an endosome-associated heterooligomeric protein complex required for mvb sorting. *Dev Cell* **3**, 271-82.

Babst, M., Katzmann, D. J., Snyder, W. B., Wendland, B. and Emr, S. D. (2002b). Endosome-associated complex, ESCRT-II, recruits transport machinery for protein sorting at the multivesicular body. *Dev Cell* **3**, 283-9.

Babst, M., Odorizzi, G., Estepa, E. J. and Emr, S. D. (2000). Mammalian tumor susceptibility gene 101 (TSG101) and the yeast homologue, Vps23p, both function in late endosomal trafficking. *Traffic* **1**, 248-58.

Babst, M., Sato, T. K., Banta, L. M. and Emr, S. D. (1997). Endosomal transport function in yeast requires a novel AAA-type ATPase, Vps4p. *Embo J* **16**, 1820-31.

Babst, M., Wendland, B., Estepa, E. J. and Emr, S. D. (1998). The Vps4p AAA ATPase regulates membrane association of a Vps protein complex required for normal endosome function. *Embo J* **17**, 2982-93.

Bach, E. A., Vincent, S., Zeidler, M. P. and Perrimon, N. (2003). A sensitized genetic screen to identify novel regulators and components of the Drosophila janus kinase/signal transducer and activator of transcription pathway. *Genetics* **165**, 1149-66.

Bache, K. G., Brech, A., Mehlum, A. and Stenmark, H. (2003a). Hrs regulates multivesicular body formation via ESCRT recruitment to endosomes. *J Cell Biol* **162**, 435-42.

Bache, K. G., Raiborg, C., Mehlum, A. and Stenmark, H. (2003b). STAM and Hrs are subunits of a multivalent ubiquitin-binding complex on early endosomes. *J Biol Chem* **278**, 12513-21.

Bache, K. G., Slagsvold, T., Cabezas, A., Rosendal, K. R., Raiborg, C. and Stenmark, H. (2004). The growth-regulatory protein HCRP1/hVps37A is a subunit of mammalian ESCRT-I and mediates receptor down-regulation. *Mol Biol Cell* **15**, 4337-46.

Baehrecke, E. H. (2002). How death shapes life during development. *Nat Rev Mol Cell Biol* **3**, 779-87.

Bailey, A. M. and Posakony, J. W. (1995). Suppressor of hairless directly activates transcription of enhancer of split complex genes in response to Notch receptor activity. *Genes Dev* **9**, 2609-22.

Bennett, F. C. and Harvey, K. F. (2006). Fat Cadherin Modulates Organ Size in Drosophila via the Salvador/Warts/Hippo Signaling Pathway. *Curr Biol* **16**, 2101-10.

Bergmann, A., Yang, A. Y. and Srivastava, M. (2003). Regulators of IAP function: coming to grips with the grim reaper. *Curr Opin Cell Biol* **15**, 717-24.

Bilodeau, P. S., Urbanowski, J. L., Winistorfer, S. C. and Piper, R. C. (2002). The Vps27p Hse1p complex binds ubiquitin and mediates endosomal protein sorting. *Nat Cell Biol* **4**, 534-9.

Bilodeau, P. S., Winistorfer, S. C., Kearney, W. R., Robertson, A. D. and Piper, R. C. (2003). Vps27-Hse1 and ESCRT-I complexes cooperate to increase efficiency of sorting ubiquitinated proteins at the endosome. *J Cell Biol* **163**, 237-43.

Bishop, N. and Woodman, P. (2000). ATPase-defective mammalian VPS4 localizes to aberrant endosomes and impairs cholesterol trafficking. *Mol Biol Cell* **11**, 227-39.

Bonifacino, J. S. (2004). The GGA proteins: adaptors on the move. *Nat Rev Mol Cell Biol* **5**, 23-32.

Bonifacino, J. S. and Traub, L. M. (2003). Signals for sorting of transmembrane proteins to endosomes and lysosomes. *Annu Rev Biochem* **72**, 395-447.

Bouamr, F., Houck-Loomis, B. R., De Los Santos, M., Casaday, R. J., Johnson, M. C. and Goff, S. P. (2007). The C-terminal portion of the Hrs protein interacts with Tsg101 and interferes with human immunodeficiency virus type 1 Gag particle production. *J Virol* **81**, 2909-22.

Bowers, K., Lottridge, J., Helliwell, S. B., Goldthwaite, L. M., Luzio, J. P. and Stevens, T. H. (2004). Protein-protein interactions of ESCRT complexes in the yeast Saccharomyces cerevisiae. *Traffic* **5**, 194-210.

Bray, S. J. (2006). Notch signalling: a simple pathway becomes complex. *Nat Rev Mol Cell Biol* **7**, 678-89.

Brou, C., Logeat, F., Gupta, N., Bessia, C., LeBail, O., Doedens, J. R., Cumano, A., Roux, P., Black, R. A. and Israel, A. (2000). A novel proteolytic cleavage involved in Notch signaling: the role of the disintegrin-metalloprotease TACE. *Mol Cell* **5**, 207-16.

Brown, S., Hu, N. and Hombria, J. C. (2001). Identification of the first invertebrate interleukin JAK/STAT receptor, the Drosophila gene domeless. *Curr Biol* **11**, 1700-5.

Bucci, C., Parton, R. G., Mather, I. H., Stunnenberg, H., Simons, K., Hoflack, B. and Zerial, M. (1992). The small GTPase rab5 functions as a regulatory factor in the early endocytic pathway. *Cell* **70**, 715-28.

Burd, C. G. and Emr, S. D. (1998). Phosphatidylinositol(3)-phosphate signaling mediated by specific binding to RING FYVE domains. *Mol Cell* **2**, 157-62.

Burgdorf, S., Leister, P. and Scheidtmann, K. H. (2004). TSG101 interacts with apoptosis-antagonizing transcription factor and enhances androgen receptor-mediated transcription by promoting its monoubiquitination. *J Biol Chem* **279**, 17524-34.

Cabezas, A., Bache, K. G., Brech, A. and Stenmark, H. (2005). Alix regulates cortical actin and the spatial distribution of endosomes. *J Cell Sci* **118**, 2625-35.

Carlton, J. G. and Martin-Serrano, J. (2007). Parallels between cytokinesis and retroviral budding: a role for the ESCRT machinery. *Science* **316**, 1908-12.

Carstens, M. J., Krempler, A., Triplett, A. A., Van Lohuizen, M. and Wagner, K. U. (2004). Cell cycle arrest and cell death are controlled by p53-dependent and p53-independent mechanisms in Tsg101-deficient cells. *J Biol Chem* **279**, 35984-94.

Cashio, P., Lee, T. V. and Bergmann, A. (2005). Genetic control of programmed cell death in Drosophila melanogaster. *Semin Cell Dev Biol* **16**, 225-35.

Chao, J. L., Tsai, Y. C., Chiu, S. J. and Sun, Y. H. (2004). Localized Notch signal acts through eyg and upd to promote global growth in Drosophila eye. *Development* **131**, 3839-47.

Chen, H. W., Chen, X., Oh, S. W., Marinissen, M. J., Gutkind, J. S. and Hou, S. X. (2002). mom identifies a receptor for the Drosophila JAK/STAT signal transduction pathway and encodes a protein distantly related to the mammalian cytokine receptor family. *Genes Dev* **16**, 388-98.

Chen, M. S., Obar, R. A., Schroeder, C. C., Austin, T. W., Poodry, C. A., Wadsworth, S. C. and Vallee, R. B. (1991). Multiple forms of dynamin are encoded by shibire, a Drosophila gene involved in endocytosis. *Nature* **351**, 583-6.

Chen, P., Nordstrom, W., Gish, B. and Abrams, J. M. (1996). grim, a novel cell death gene in Drosophila. *Genes Dev* **10**, 1773-82.

Childress, J. L., Acar, M., Tao, C. and Halder, G. (2006). Lethal Giant Discs, a Novel C2-Domain Protein, Restricts Notch Activation during Endocytosis. *Curr Biol* **16**, 2228-33.

Chu, T., Sun, J., Saksena, S. and Emr, S. D. (2006). New component of ESCRT-I regulates endosomal sorting complex assembly. *J Cell Biol* **175**, 815-23.

Cornell, M., Evans, D. A., Mann, R., Fostier, M., Flasza, M., Monthatong, M., Artavanis-Tsakonas, S. and Baron, M. (1999). The Drosophila melanogaster Suppressor of deltex gene, a regulator of the Notch receptor signaling pathway, is an E3 class ubiquitin ligase. *Genetics* **152**, 567-76.

Curtiss, M., Jones, C. and Babst, M. (2007). Efficient cargo sorting by ESCRT-I and the subsequent release of ESCRT-I from multivesicular bodies requires the subunit Mvb12. *Mol Biol Cell* **18**, 636-45.

Danial, N. N. and Korsmeyer, S. J. (2004). Cell death: critical control points. *Cell* **116**, 205-19.

de Celis, J. F. and Bray, S. (1997). Feed-back mechanisms affecting Notch activation at the dorsoventral boundary in the Drosophila wing. *Development* **124**, 3241-51.

de Celis, J. F., Garcia-Bellido, A. and Bray, S. J. (1996). Activation and function of Notch at the dorsal-ventral boundary of the wing imaginal disc. *Development* **122**, 359-69.

de Gassart, A., Geminard, C., Hoekstra, D. and Vidal, M. (2004). Exosome secretion: the art of reutilizing nonrecycled proteins? *Traffic* **5**, 896-903.

De Strooper, B., Annaert, W., Cupers, P., Saftig, P., Craessaerts, K., Mumm, J. S., Schroeter, E. H., Schrijvers, V., Wolfe, M. S., Ray, W. J. et al. (1999). A

presenilin-1-dependent gamma-secretase-like protease mediates release of Notch intracellular domain. *Nature* **398**, 518-22.

Deblandre, G. A., Lai, E. C. and Kintner, C. (2001). Xenopus neuralized is a ubiquitin ligase that interacts with XDelta1 and regulates Notch signaling. *Dev Cell* **1**, 795-806.

Deftos, M. L., He, Y. W., Ojala, E. W. and Bevan, M. J. (1998). Correlating notch signaling with thymocyte maturation. *Immunity* **9**, 777-86.

Demirov, D. G. and Freed, E. O. (2004). Retrovirus budding. *Virus Res* **106**, 87-102.

Diederich, R. J., Matsuno, K., Hing, H. and Artavanis-Tsakonas, S. (1994). Cytosolic interaction between deltex and Notch ankyrin repeats implicates deltex in the Notch signaling pathway. *Development* **120**, 473-81.

Dorstyn, L., Colussi, P. A., Quinn, L. M., Richardson, H. and Kumar, S. (1999). DRONC, an ecdysone-inducible Drosophila caspase. *Proc Natl Acad Sci U S A* **96**, 4307-12.

Dudu, V., Pantazis, P. and Gonzalez-Gaitan, M. (2004). Membrane traffic during embryonic development: epithelial formation, cell fate decisions and differentiation. *Curr Opin Cell Biol* **16**, 407-14.

Dukes, J. D., Richardson, J. D., Simmons, R. and Whitley, P. (2008). A dominant-negative ESCRT-III protein perturbs cytokinesis and trafficking to lysosomes. *Biochem J* **411**, 233-9.

Duncan, L. M., Piper, S., Dodd, R. B., Saville, M. K., Sanderson, C. M., Luzio, J. P. and Lehner, P. J. (2006). Lysine-63-linked ubiquitination is required for endolysosomal degradation of class I molecules. *Embo J* **25**, 1635-45.

Edgar, B. A. (2006). From cell structure to transcription: Hippo forges a new path. *Cell* **124**, 267-73.

Ellisen, L. W., Bird, J., West, D. C., Soreng, A. L., Reynolds, T. C., Smith, S. D. and Sklar, J. (1991). TAN-1, the human homolog of the Drosophila notch gene, is broken by chromosomal translocations in T lymphoblastic neoplasms. *Cell* **66**, 649-61.

Fan, Y. and Bergmann, A. (2008). Distinct mechanisms of apoptosis-induced compensatory proliferation in proliferating and differentiating tissues in the Drosophila eye. *Dev Cell* **14**, 399-410.

Fehon, R. G., Kooh, P. J., Rebay, I., Regan, C. L., Xu, T., Muskavitch, M. A. and Artavanis-Tsakonas, S. (1990). Molecular interactions between the protein products of the neurogenic loci Notch and Delta, two EGF-homologous genes in Drosophila. *Cell* **61**, 523-34.

Felder, S., Miller, K., Moehren, G., Ullrich, A., Schlessinger, J. and Hopkins, C. R. (1990). Kinase activity controls the sorting of the epidermal growth factor receptor within the multivesicular body. *Cell* **61**, 623-34.

Feng, G. H., Lih, C. J. and Cohen, S. N. (2000). TSG101 protein steady-state level is regulated posttranslationally by an evolutionarily conserved COOH-terminal sequence. *Cancer Res* **60**, 1736-41.

Filimonenko, M., Stuffers, S., Raiborg, C., Yamamoto, A., Malerod, L., Fisher, E. M., Isaacs, A., Brech, A., Stenmark, H. and Simonsen, A. (2007). Functional multivesicular bodies are required for autophagic clearance of protein aggregates associated with neurodegenerative disease. *J Cell Biol* **179**, 485-500.

Fischer, J. A., Eun, S. H. and Doolan, B. T. (2006). Endocytosis, endosome trafficking, and the regulation of Drosophila development. *Annu Rev Cell Dev Biol* **22**, 181-206.

Fischer, J. A., Giniger, E., Maniatis, T. and Ptashne, M. (1988). GAL4 activates transcription in Drosophila. *Nature* **332**, 853-6.

Fiuza, U. M. and Arias, A. M. (2007). Cell and molecular biology of Notch. *J Endocrinol* **194**, 459-74.

Fortini, M. E. (2002). Gamma-secretase-mediated proteolysis in cell-surface-receptor signalling. *Nat Rev Mol Cell Biol* **3**, 673-84.

Fortini, M. E. and Artavanis-Tsakonas, S. (1994). The suppressor of hairless protein participates in notch receptor signaling. *Cell* **79**, 273-82.

Fostier, M., Evans, D. A., Artavanis-Tsakonas, S. and Baron, M. (1998). Genetic characterization of the Drosophila melanogaster Suppressor of deltex gene: A regulator of notch signaling. *Genetics* **150**, 1477-85.

Fraser, A. G. and Evan, G. I. (1997). Identification of a Drosophila melanogaster ICE/CED-3-related protease, drICE. *Embo J* **16**, 2805-13.

Fraser, A. G., McCarthy, N. J. and Evan, G. I. (1997). drICE is an essential caspase required for apoptotic activity in Drosophila cells. *Embo J* **16**, 6192-9.

Fujii, K., Hurley, J. H. and Freed, E. O. (2007). Beyond Tsg101: the role of Alix in 'ESCRTing' HIV-1. *Nat Rev Microbiol* **5**, 912-6.

Fujimuro, M., Sawada, H. and Yokosawa, H. (1994). Production and characterization of monoclonal antibodies specific to multi-ubiquitin chains of polyubiquitinated proteins. *FEBS Lett* **349**, 173-80.

Fujimuro, M., Sawada, H. and Yokosawa, H. (1997). Dynamics of ubiquitin conjugation during heat-shock response revealed by using a monoclonal antibody specific to multi-ubiquitin chains. *Eur J Biochem* **249**, 427-33.

Fujita, H., Yamanaka, M., Imamura, K., Tanaka, Y., Nara, A., Yoshimori, T., Yokota, S. and Himeno, M. (2003). A dominant negative form of the AAA ATPase SKD1/VPS4 impairs membrane trafficking out of endosomal/lysosomal compartments: class E vps phenotype in mammalian cells. *J Cell Sci* **116**, 401-14.

Gallagher, C. M. and Knoblich, J. A. (2006). The conserved c2 domain protein lethal (2) giant discs regulates protein trafficking in Drosophila. *Dev Cell* **11**, 641-53.

Gallahan, D. and Callahan, R. (1987). Mammary tumorigenesis in feral mice: identification of a new int locus in mouse mammary tumor virus (Czech II)-induced mammary tumors. *J Virol* **61**, 66-74.

Garrus, J. E., von Schwedler, U. K., Pornillos, O. W., Morham, S. G., Zavitz, K. H., Wang, H. E., Wettstein, D. A., Stray, K. M., Cote, M., Rich, R. L. et al. (2001). Tsg101 and the vacuolar protein sorting pathway are essential for HIV-1 budding. *Cell* **107**, 55-65.

Gayther, S. A., Barski, P., Batley, S. J., Li, L., de Foy, K. A., Cohen, S. N., Ponder, B. A. and Caldas, C. (1997). Aberrant splicing of the TSG101 and FHIT genes occurs frequently in multiple malignancies and in normal tissues and mimics alterations previously described in tumours. *Oncogene* **15**, 2119-26.

Giebel, B. and Wodarz, A. (2006). Tumor suppressors: control of signaling by endocytosis. *Curr Biol* **16**, R91-2.

Gill, D. J., Teo, H., Sun, J., Perisic, O., Veprintsev, D. B., Emr, S. D. and Williams, R. L. (2007). Structural insight into the ESCRT-I/-II link and its role in MVB trafficking. *Embo J* **26**, 600-12.

Glittenberg, M., Pitsouli, C., Garvey, C., Delidakis, C. and Bray, S. (2006). Role of conserved intracellular motifs in Serrate signalling, cis-inhibition and endocytosis. *Embo J* **25**, 4697-706.

Gonzalez-Gaitan, M. (2003). Signal dispersal and transduction through the endocytic pathway. *Nat Rev Mol Cell Biol* **4**, 213-24.

Gorvel, J. P., Chavrier, P., Zerial, M. and Gruenberg, J. (1991). rab5 controls early endosome fusion in vitro. *Cell* **64**, 915-25.

Grabher, C., von Boehmer, H. and Look, A. T. (2006). Notch 1 activation in the molecular pathogenesis of T-cell acute lymphoblastic leukaemia. *Nat Rev Cancer* **6**, 347-59.

Grether, M. E., Abrams, J. M., Agapite, J., White, K. and Steller, H. (1995). The head involution defective gene of Drosophila melanogaster functions in programmed cell death. *Genes Dev* **9**, 1694-708.

Gruenberg, J. and Stenmark, H. (2004). The biogenesis of multivesicular endosomes. *Nat Rev Mol Cell Biol* **5**, 317-23.

Gruenberg, J. and van der Goot, F. G. (2006). Mechanisms of pathogen entry through the endosomal compartments. *Nat Rev Mol Cell Biol* **7**, 495-504.

Gupta-Rossi, N., Six, E., LeBail, O., Logeat, F., Chastagner, P., Olry, A., Israel, A. and Brou, C. (2004). Monoubiquitination and endocytosis direct gamma-secretase cleavage of activated Notch receptor. *J Cell Biol* **166**, 73-83.

Haas, T. J., Sliwinski, M. K., Martinez, D. E., Preuss, M., Ebine, K., Ueda, T., Nielsen, E., Odorizzi, G. and Otegui, M. S. (2007). The Arabidopsis AAA ATPase SKD1 is involved in multivesicular endosome function and interacts with its positive regulator LYST-INTERACTING PROTEIN5. *Plant Cell* **19**, 1295-312.

Haglund, K. and Dikic, I. (2005). Ubiquitylation and cell signaling. *Embo J* **24**, 3353-9.

Hamaratoglu, F., Willecke, M., Kango-Singh, M., Nolo, R., Hyun, E., Tao, C., Jafar-Nejad, H. and Halder, G. (2006). The tumour-suppressor genes NF2/Merlin and Expanded act through Hippo signalling to regulate cell proliferation and apoptosis. *Nat Cell Biol* **8**, 27-36.

Hanahan, D. and Weinberg, R. A. (2000). The hallmarks of cancer. *Cell* **100**, 57-70.

Hariharan, I. K. and Bilder, D. (2006). Regulation of imaginal disc growth by tumor-suppressor genes in Drosophila. *Annu Rev Genet* **40**, 335-61.

Harrison, D. A., McCoon, P. E., Binari, R., Gilman, M. and Perrimon, N. (1998). Drosophila unpaired encodes a secreted protein that activates the JAK signaling pathway. *Genes Dev* **12**, 3252-63.

Harvey, K. and Tapon, N. (2007). The Salvador-Warts-Hippo pathway - an emerging tumour-suppressor network. *Nat Rev Cancer* **7**, 182-91.

Harvey, K. F., Pfleger, C. M. and Hariharan, I. K. (2003). The Drosophila Mst ortholog, hippo, restricts growth and cell proliferation and promotes apoptosis. *Cell* **114**, 457-67.

Hawkins, C. J., Wang, S. L. and Hay, B. A. (1999). A cloning method to identify caspases and their regulators in yeast: identification of Drosophila IAP1 as an inhibitor of the Drosophila caspase DCP-1. *Proc Natl Acad Sci U S A* **96**, 2885-90.

Hay, B. A., Huh, J. R. and Guo, M. (2004). The genetics of cell death: approaches, insights and opportunities in Drosophila. *Nat Rev Genet* **5**, 911-22.

Hay, B. A., Wassarman, D. A. and Rubin, G. M. (1995). Drosophila homologs of baculovirus inhibitor of apoptosis proteins function to block cell death. *Cell* **83**, 1253-62.

Hengartner, M. O. (2000). The biochemistry of apoptosis. *Nature* **407**, 770-6.

Herz, H. M., Chen, Z., Scherr, H., Lackey, M., Bolduc, C. and Bergmann, A. (2006). vps25 mosaics display non-autonomous cell survival and overgrowth, and autonomous apoptosis. *Development* **133**, 1871-80.

Hicke, L. and Dunn, R. (2003). Regulation of membrane protein transport by ubiquitin and ubiquitin-binding proteins. *Annu Rev Cell Dev Biol* **19**, 141-72.

Hicke, L., Schubert, H. L. and Hill, C. P. (2005). Ubiquitin-binding domains. *Nat Rev Mol Cell Biol* **6**, 610-21.

Hierro, A., Sun, J., Rusnak, A. S., Kim, J., Prag, G., Emr, S. D. and Hurley, J. H. (2004). Structure of the ESCRT-II endosomal trafficking complex. *Nature* **431**, 221-5.

Hinshaw, J. E. (2000). Dynamin and its role in membrane fission. *Annu Rev Cell Dev Biol* **16**, 483-519.

Hipfner, D. R. and Cohen, S. M. (2004). Connecting proliferation and apoptosis in development and disease. *Nat Rev Mol Cell Biol* **5**, 805-15.

Hirano, S., Suzuki, N., Slagsvold, T., Kawasaki, M., Trambaiolo, D., Kato, R., Stenmark, H. and Wakatsuki, S. (2006). Structural basis of ubiquitin recognition by mammalian Eap45 GLUE domain. *Nat Struct Mol Biol* **13**, 1031-2.

Holley, C. L., Olson, M. R., Colon-Ramos, D. A. and Kornbluth, S. (2002). Reaper eliminates IAP proteins through stimulated IAP degradation and generalized translational inhibition. *Nat Cell Biol* **4**, 439-44.

Howard, T. L., Stauffer, D. R., Degnin, C. R. and Hollenberg, S. M. (2001). CHMP1 functions as a member of a newly defined family of vesicle trafficking proteins. *J Cell Sci* **114**, 2395-404.

Huang, F., Kirkpatrick, D., Jiang, X., Gygi, S. and Sorkin, A. (2006). Differential regulation of EGF receptor internalization and degradation by multiubiquitination within the kinase domain. *Mol Cell* **21**, 737-48.

Huh, J. R., Guo, M. and Hay, B. A. (2004). Compensatory proliferation induced by cell death in the Drosophila wing disc requires activity of the apical cell death caspase Dronc in a nonapoptotic role. *Curr Biol* **14**, 1262-6.

Hurley, J. H. (2008). ESCRT complexes and the biogenesis of multivesicular bodies. *Curr Opin Cell Biol* **20**, 4-11.

Hurley, J. H. and Emr, S. D. (2006). The ESCRT complexes: structure and mechanism of a membrane-trafficking network. *Annu Rev Biophys Biomol Struct* **35**, 277-98.

Igaki, T., Yamamoto-Goto, Y., Tokushige, N., Kanda, H. and Miura, M. (2002). Down-regulation of DIAP1 triggers a novel Drosophila cell death pathway mediated by Dark and DRONC. *J Biol Chem* **277**, 23103-6.

Irion, U. and St Johnston, D. (2007). bicoid RNA localization requires specific binding of an endosomal sorting complex. *Nature* **445**, 554-8.

Itoh, M., Kim, C. H., Palardy, G., Oda, T., Jiang, Y. J., Maust, D., Yeo, S. Y., Lorick, K., Wright, G. J., Ariza-McNaughton, L. et al. (2003). Mind bomb is a ubiquitin ligase that is essential for efficient activation of Notch signaling by Delta. *Dev Cell* **4**, 67-82.

Jacobsen, T. L., Brennan, K., Arias, A. M. and Muskavitch, M. A. (1998). Cis-interactions between Delta and Notch modulate neurogenic signalling in Drosophila. *Development* **125**, 4531-40.

Jacobson, M. D., Weil, M. and Raff, M. C. (1997). Programmed cell death in animal development. *Cell* **88**, 347-54.

Jaekel, R. and Klein, T. (2006). The Drosophila Notch inhibitor and tumor suppressor gene lethal (2) giant discs encodes a conserved regulator of endosomal trafficking. *Dev Cell* **11**, 655-69.

Jehn, B. M., Bielke, W., Pear, W. S. and Osborne, B. A. (1999). Cutting edge: protective effects of notch-1 on TCR-induced apoptosis. *J Immunol* **162**, 635-8.

Jehn, B. M., Dittert, I., Beyer, S., von der Mark, K. and Bielke, W. (2002). c-Cbl binding and ubiquitin-dependent lysosomal degradation of membrane-associated Notch1. *J Biol Chem* **277**, 8033-40.

Jekely, G. and Rorth, P. (2003). Hrs mediates downregulation of multiple signalling receptors in Drosophila. *EMBO Rep* **4**, 1163-8.

Jennings, B., Preiss, A., Delidakis, C. and Bray, S. (1994). The Notch signalling pathway is required for Enhancer of split bHLH protein expression during neurogenesis in the Drosophila embryo. *Development* **120**, 3537-48.

Johnson, M. C., Spidel, J. L., Ako-Adjei, D., Wills, J. W. and Vogt, V. M. (2005). The C-terminal half of TSG101 blocks Rous sarcoma virus budding and sequesters Gag into unique nonendosomal structures. *J Virol* **79**, 3775-86.

Kaether, C., Haass, C. and Steiner, H. (2006). Assembly, trafficking and function of gamma-secretase. *Neurodegener Dis* **3**, 275-83.

Kaiser, W. J., Vucic, D. and Miller, L. K. (1998). The Drosophila inhibitor of apoptosis D-IAP1 suppresses cell death induced by the caspase drICE. *FEBS Lett* **440**, 243-8.

Kamura, T., Burian, D., Khalili, H., Schmidt, S. L., Sato, S., Liu, W. J., Conrad, M. N., Conaway, R. C., Conaway, J. W. and Shilatifard, A. (2001). Cloning and characterization of ELL-associated proteins EAP45 and EAP20. a role for yeast EAP-like proteins in regulation of gene expression by glucose. *J Biol Chem* **276**, 16528-33.

Kastan, M. B. and Bartek, J. (2004). Cell-cycle checkpoints and cancer. *Nature* **432**, 316-23.

Katzmann, D. J., Babst, M. and Emr, S. D. (2001). Ubiquitin-dependent sorting into the multivesicular body pathway requires the function of a conserved endosomal protein sorting complex, ESCRT-I. *Cell* **106**, 145-55.

Katzmann, D. J., Odorizzi, G. and Emr, S. D. (2002). Receptor downregulation and multivesicular-body sorting. *Nat Rev Mol Cell Biol* **3**, 893-905.

Katzmann, D. J., Stefan, C. J., Babst, M. and Emr, S. D. (2003). Vps27 recruits ESCRT machinery to endosomes during MVB sorting. *J Cell Biol* **162**, 413-23.

Khoury, C. M., Yang, Z., Ismail, S. and Greenwood, M. T. (2007). Characterization of a novel alternatively spliced human transcript encoding an N-terminally truncated Vps24 protein that suppresses the effects of Bax in an ESCRT independent manner in yeast. *Gene* **391**, 233-41.

Klein, T., Brennan, K. and Arias, A. M. (1997). An intrinsic dominant negative activity of serrate that is modulated during wing development in Drosophila. *Dev Biol* **189**, 123-34.

Kopan, R., Schroeter, E. H., Weintraub, H. and Nye, J. S. (1996). Signal transduction by activated mNotch: importance of proteolytic processing and its regulation by the extracellular domain. *Proc Natl Acad Sci U S A* **93**, 1683-8.

Kostelansky, M. S., Schluter, C., Tam, Y. Y., Lee, S., Ghirlando, R., Beach, B., Conibear, E. and Hurley, J. H. (2007). Molecular architecture and functional model of the complete yeast ESCRT-I heterotetramer. *Cell* **129**, 485-98.

Kostelansky, M. S., Sun, J., Lee, S., Kim, J., Ghirlando, R., Hierro, A., Emr, S. D. and Hurley, J. H. (2006). Structural and functional organization of the ESCRT-I trafficking complex. *Cell* **125**, 113-26.

Kramatschek, B. and Campos-Ortega, J. A. (1994). Neuroectodermal transcription of the Drosophila neurogenic genes E(spl) and HLH-m5 is regulated by proneural genes. *Development* **120**, 815-26.

Kramer, H. and Phistry, M. (1996). Mutations in the Drosophila hook gene inhibit endocytosis of the boss transmembrane ligand into multivesicular bodies. *J Cell Biol* **133**, 1205-15.

Kranz, A., Kinner, A. and Kolling, R. (2001). A family of small coiled-coil-forming proteins functioning at the late endosome in yeast. *Mol Biol Cell* **12**, 711-23.

Krempler, A., Henry, M. D., Triplett, A. A. and Wagner, K. U. (2002). Targeted deletion of the Tsg101 gene results in cell cycle arrest at G1/S and p53-independent cell death. *J Biol Chem* **277**, 43216-23.

Kuranaga, E., Kanuka, H., Igaki, T., Sawamoto, K., Ichijo, H., Okano, H. and Miura, M. (2002). Reaper-mediated inhibition of DIAP1-induced DTRAF1 degradation results in activation of JNK in Drosophila. *Nat Cell Biol* **4**, 705-10.

Kyuuma, M., Kikuchi, K., Kojima, K., Sugawara, Y., Sato, M., Mano, N., Goto, J., Takeshita, T., Yamamoto, A., Sugamura, K. et al. (2007). AMSH, an ESCRT-III associated enzyme, deubiquitinates cargo on MVB/late endosomes. *Cell Struct Funct* **31**, 159-72.

Ladi, E., Nichols, J. T., Ge, W., Miyamoto, A., Yao, C., Yang, L. T., Boulter, J., Sun, Y. E., Kintner, C. and Weinmaster, G. (2005). The divergent DSL ligand Dll3 does not activate Notch signaling but cell autonomously attenuates signaling induced by other DSL ligands. *J Cell Biol* **170**, 983-92.

Lai, E. C., Deblandre, G. A., Kintner, C. and Rubin, G. M. (2001). Drosophila neuralized is a ubiquitin ligase that promotes the internalization and degradation of delta. *Dev Cell* **1**, 783-94.

Lai, E. C., Roegiers, F., Qin, X., Jan, Y. N. and Rubin, G. M. (2005). The ubiquitin ligase Drosophila Mind bomb promotes Notch signaling by regulating the localization and activity of Serrate and Delta. *Development* **132**, 2319-32.

Lambert, C., Doring, T. and Prange, R. (2007). Hepatitis B virus maturation is sensitive to functional inhibition of ESCRT-III, Vps4, and gamma 2-adaptin. *J Virol* **81**, 9050-60.

Langelier, C., von Schwedler, U. K., Fisher, R. D., De Domenico, I., White, P. L., Hill, C. P., Kaplan, J., Ward, D. and Sundquist, W. I. (2006). Human ESCRT-II

complex and its role in human immunodeficiency virus type 1 release. *J Virol* **80**, 9465-80.

Le Borgne, R. (2006). Regulation of Notch signalling by endocytosis and endosomal sorting. *Curr Opin Cell Biol* **18**, 213-22.

Le Borgne, R., Bardin, A. and Schweisguth, F. (2005). The roles of receptor and ligand endocytosis in regulating Notch signaling. *Development* **132**, 1751-62.

Le Borgne, R. and Schweisguth, F. (2003a). Notch signaling: endocytosis makes delta signal better. *Curr Biol* **13**, R273-5.

Le Borgne, R. and Schweisguth, F. (2003b). Unequal segregation of Neuralized biases Notch activation during asymmetric cell division. *Dev Cell* **5**, 139-48.

Le Roy, C. and Wrana, J. L. (2005a). Clathrin- and non-clathrin-mediated endocytic regulation of cell signalling. *Nat Rev Mol Cell Biol* **6**, 112-26.

Le Roy, C. and Wrana, J. L. (2005b). Signaling and endocytosis: a team effort for cell migration. *Dev Cell* **9**, 167-8.

Lee, J. A., Beigneux, A., Ahmad, S. T., Young, S. G. and Gao, F. B. (2007). ESCRT-III Dysfunction Causes Autophagosome Accumulation and Neurodegeneration. *Curr Biol* **17**, 1561-7.

Lee, J. A. and Gao, F. B. (2008). Roles of ESCRT in autophagy-associated neurodegeneration. *Autophagy* **4**, 230-2.

Lee, M. P. and Feinberg, A. P. (1997). Aberrant splicing but not mutations of TSG101 in human breast cancer. *Cancer Res* **57**, 3131-4.

Lee, T. and Luo, L. (2001). Mosaic analysis with a repressible cell marker (MARCM) for Drosophila neural development. *Trends Neurosci* **24**, 251-4.

Lee, T. V., Ding, T., Chen, Z., Rajendran, V., Scherr, H., Lackey, M., Bolduc, C. and Bergmann, A. (2008). The E1 ubiquitin-activating enzyme Uba1 in Drosophila controls apoptosis autonomously and tissue growth non-autonomously. *Development* **135**, 43-52.

Levine, B. and Kroemer, G. (2008). Autophagy in the pathogenesis of disease. *Cell* **132**, 27-42.

Li, L. and Cohen, S. N. (1996). Tsg101: a novel tumor susceptibility gene isolated by controlled homozygous functional knockout of allelic loci in mammalian cells. *Cell* **85**, 319-29.

Li, L., Li, X., Francke, U. and Cohen, S. N. (1997). The TSG101 tumor susceptibility gene is located in chromosome 11 band p15 and is mutated in human breast cancer. *Cell* **88**, 143-54.

Li, L., Liao, J., Ruland, J., Mak, T. W. and Cohen, S. N. (2001). A TSG101/MDM2 regulatory loop modulates MDM2 degradation and MDM2/p53 feedback control. *Proc Natl Acad Sci U S A* **98**, 1619-24.

Li, Y. and Baker, N. E. (2004). The roles of cis-inactivation by Notch ligands and of neuralized during eye and bristle patterning in Drosophila. *BMC Dev Biol* **4**, 5.

Licata, J. M., Simpson-Holley, M., Wright, N. T., Han, Z., Paragas, J. and Harty, R. N. (2003). Overlapping motifs (PTAP and PPEY) within the Ebola virus VP40

protein function independently as late budding domains: involvement of host proteins TSG101 and VPS-4. *J Virol* **77**, 1812-9.

Lin, S. Y., Chen, Y. J. and Chang, J. G. (1998). Multiple truncated transcripts of TSG101 in gastrointestinal cancers. *J Gastroenterol Hepatol* **13**, 1111-4.

Liu, W. H., Hsiao, H. W., Tsou, W. I. and Lai, M. Z. (2007). Notch inhibits apoptosis by direct interference with XIAP ubiquitination and degradation. *Embo J* **26**, 1660-9.

Lloyd, T. E., Atkinson, R., Wu, M. N., Zhou, Y., Pennetta, G. and Bellen, H. J. (2002). Hrs regulates endosome membrane invagination and tyrosine kinase receptor signaling in Drosophila. *Cell* **108**, 261-9.

Lohi, O. and Lehto, V. P. (2001). STAM/EAST/Hbp adapter proteins--integrators of signalling pathways. *FEBS Lett* **508**, 287-90.

Lottridge, J. M., Flannery, A. R., Vincelli, J. L. and Stevens, T. H. (2006). Vta1p and Vps46p regulate the membrane association and ATPase activity of Vps4p at the yeast multivesicular body. *Proc Natl Acad Sci U S A* **103**, 6202-7.

Lowe, S. W., Cepero, E. and Evan, G. (2004). Intrinsic tumour suppression. *Nature* **432**, 307-15.

Lu, H. and Bilder, D. (2005). Endocytic control of epithelial polarity and proliferation in Drosophila. *Nat Cell Biol* **7**, 1232-9.

Lu, Q., Hope, L. W., Brasch, M., Reinhard, C. and Cohen, S. N. (2003). TSG101 interaction with HRS mediates endosomal trafficking and receptor down-regulation. *Proc Natl Acad Sci U S A* **100**, 7626-31.

Luhtala, N. and Odorizzi, G. (2004). Bro1 coordinates deubiquitination in the multivesicular body pathway by recruiting Doa4 to endosomes. *J Cell Biol* **166**, 717-29.

Luzio, J. P., Pryor, P. R. and Bright, N. A. (2007). Lysosomes: fusion and function. *Nat Rev Mol Cell Biol* **8**, 622-32.

Ma, Y. M., Boucrot, E., Villen, J., Affar el, B., Gygi, S. P., Gottlinger, H. G. and Kirchhausen, T. (2007). Targeting of AMSH to endosomes is required for epidermal growth factor receptor degradation. *J Biol Chem* **282**, 9805-12.

Mahul-Mellier, A. L., Hemming, F. J., Blot, B., Fraboulet, S. and Sadoul, R. (2006). Alix, making a link between apoptosis-linked gene-2, the endosomal sorting complexes required for transport, and neuronal death in vivo. *J Neurosci* **26**, 542-9.

Maiuri, M. C., Zalckvar, E., Kimchi, A. and Kroemer, G. (2007). Self-eating and self-killing: crosstalk between autophagy and apoptosis. *Nat Rev Mol Cell Biol* **8**, 741-52.

Mao, Y., Nickitenko, A., Duan, X., Lloyd, T. E., Wu, M. N., Bellen, H. and Quiocho, F. A. (2000). Crystal structure of the VHS and FYVE tandem domains of Hrs, a protein involved in membrane trafficking and signal transduction. *Cell* **100**, 447-56.

Martin-Blanco, E., Gampel, A., Ring, J., Virdee, K., Kirov, N., Tolkovsky, A. M. and Martinez-Arias, A. (1998). puckered encodes a phosphatase that mediates a feedback loop regulating JNK activity during dorsal closure in Drosophila. *Genes Dev* **12**, 557-70.

Martin-Serrano, J. (2007). The role of ubiquitin in retroviral egress. *Traffic* **8**, 1297-303.

Martin-Serrano, J., Yarovoy, A., Perez-Caballero, D. and Bieniasz, P. D. (2003a). Divergent retroviral late-budding domains recruit vacuolar protein sorting factors by using alternative adaptor proteins. *Proc Natl Acad Sci U S A* **100**, 12414-9.

Martin-Serrano, J., Zang, T. and Bieniasz, P. D. (2001). HIV-1 and Ebola virus encode small peptide motifs that recruit Tsg101 to sites of particle assembly to facilitate egress. *Nat Med* **7**, 1313-9.

Martin-Serrano, J., Zang, T. and Bieniasz, P. D. (2003b). Role of ESCRT-I in retroviral budding. *J Virol* **77**, 4794-804.

Massague, J. (2004). G1 cell-cycle control and cancer. *Nature* **432**, 298-306.

Mathew, R., Karantza-Wadsworth, V. and White, E. (2007). Role of autophagy in cancer. *Nat Rev Cancer* **7**, 961-7.

Matsuno, K., Diederich, R. J., Go, M. J., Blaumueller, C. M. and Artavanis-Tsakonas, S. (1995). Deltex acts as a positive regulator of Notch signaling through interactions with the Notch ankyrin repeats. *Development* **121**, 2633-44.

McCullough, J., Clague, M. J. and Urbe, S. (2004). AMSH is an endosome-associated ubiquitin isopeptidase. *J Cell Biol* **166**, 487-92.

McCullough, J., Row, P. E., Lorenzo, O., Doherty, M., Beynon, R., Clague, M. J. and Urbe, S. (2006). Activation of the endosome-associated ubiquitin isopeptidase AMSH by STAM, a component of the multivesicular body-sorting machinery. *Curr Biol* **16**, 160-5.

Medina, G., Zhang, Y., Tang, Y., Gottwein, E., Vana, M. L., Bouamr, F., Leis, J. and Carter, C. A. (2005). The functionally exchangeable L domains in RSV and HIV-1 Gag direct particle release through pathways linked by Tsg101. *Traffic* **6**, 880-94.

Meier, P., Finch, A. and Evan, G. (2000a). Apoptosis in development. *Nature* **407**, 796-801.

Meier, P., Silke, J., Leevers, S. J. and Evan, G. I. (2000b). The Drosophila caspase DRONC is regulated by DIAP1. *Embo J* **19**, 598-611.

Micchelli, C. A., Rulifson, E. J. and Blair, S. S. (1997). The function and regulation of cut expression on the wing margin of Drosophila: Notch, Wingless and a dominant negative role for Delta and Serrate. *Development* **124**, 1485-95.

Miele, L., Golde, T. and Osborne, B. (2006). Notch signaling in cancer. *Curr Mol Med* **6**, 905-18.

Miller, D. T. and Cagan, R. L. (1998). Local induction of patterning and programmed cell death in the developing Drosophila retina. *Development* **125**, 2327-35.

Misra, S. and Hurley, J. H. (1999). Crystal structure of a phosphatidylinositol 3-phosphate-specific membrane-targeting motif, the FYVE domain of Vps27p. *Cell* **97**, 657-66.

Mizushima, N. (2007). Autophagy: process and function. *Genes Dev* **21**, 2861-73.

Moberg, K. H., Schelble, S., Burdick, S. K. and Hariharan, I. K. (2005). Mutations in erupted, the Drosophila ortholog of mammalian tumor susceptibility gene 101, elicit non-cell-autonomous overgrowth. *Dev Cell* **9**, 699-710.

Morata, G. and Ripoll, P. (1975). Minutes: mutants of drosophila autonomously affecting cell division rate. *Dev Biol* **42**, 211-21.

Moreno, E., Basler, K. and Morata, G. (2002). Cells compete for decapentaplegic survival factor to prevent apoptosis in Drosophila wing development. *Nature* **416**, 755-9.

Morita, E., Sandrin, V., Chung, H. Y., Morham, S. G., Gygi, S. P., Rodesch, C. K. and Sundquist, W. I. (2007). Human ESCRT and ALIX proteins interact with proteins of the midbody and function in cytokinesis. *Embo J* **26**, 4215-27.

Morita, E. and Sundquist, W. I. (2004). Retrovirus budding. *Annu Rev Cell Dev Biol* **20**, 395-425.

Mukherjee, A., Veraksa, A., Bauer, A., Rosse, C., Camonis, J. and Artavanis-Tsakonas, S. (2005). Regulation of Notch signalling by non-visual beta-arrestin. *Nat Cell Biol* **7**, 1191-201.

Muller, P., Kuttenkeuler, D., Gesellchen, V., Zeidler, M. P. and Boutros, M. (2005). Identification of JAK/STAT signalling components by genome-wide RNA interference. *Nature* **436**, 871-5.

Mumm, J. S. and Kopan, R. (2000). Notch signaling: from the outside in. *Dev Biol* **228**, 151-65.

Mumm, J. S., Schroeter, E. H., Saxena, M. T., Griesemer, A., Tian, X., Pan, D. J., Ray, W. J. and Kopan, R. (2000). A ligand-induced extracellular cleavage regulates gamma-secretase-like proteolytic activation of Notch1. *Mol Cell* **5**, 197-206.

Muziol, T., Pineda-Molina, E., Ravelli, R. B., Zamborlini, A., Usami, Y., Gottlinger, H. and Weissenhorn, W. (2006). Structural basis for budding by the ESCRT-III factor CHMP3. *Dev Cell* **10**, 821-30.

Newsome, T. P., Asling, B. and Dickson, B. J. (2000). Analysis of Drosophila photoreceptor axon guidance in eye-specific mosaics. *Development* **127**, 851-60.

Nickerson, D. P., Russell, M. R. and Odorizzi, G. (2007). A concentric circle model of multivesicular body cargo sorting. *EMBO Rep* **8**, 644-50.

Nickerson, D. P., West, M. and Odorizzi, G. (2006). Did2 coordinates Vps4-mediated dissociation of ESCRT-III from endosomes. *J Cell Biol* **175**, 715-20.

Nikko, E. and Andre, B. (2007). Split-ubiquitin two-hybrid assay to analyze protein-protein interactions at the endosome: application to Saccharomyces cerevisiae Bro1 interacting with ESCRT complexes, the Doa4 ubiquitin hydrolase, and the Rsp5 ubiquitin ligase. *Eukaryot Cell* **6**, 1266-77.

Nishi, T. and Forgac, M. (2002). The vacuolar (H+)-ATPases--nature's most versatile proton pumps. *Nat Rev Mol Cell Biol* **3**, 94-103.

Obita, T., Saksena, S., Ghazi-Tabatabai, S., Gill, D. J., Perisic, O., Emr, S. D. and Williams, R. L. (2007). Structural basis for selective recognition of ESCRT-III by the AAA ATPase Vps4. *Nature* **449**, 735-9.

Odorizzi, G., Babst, M. and Emr, S. D. (1998). Fab1p PtdIns(3)P 5-kinase function essential for protein sorting in the multivesicular body. *Cell* **95**, 847-58.

Odorizzi, G., Katzmann, D. J., Babst, M., Audhya, A. and Emr, S. D. (2003). Bro1 is an endosome-associated protein that functions in the MVB pathway in Saccharomyces cerevisiae. *J Cell Sci* **116**, 1893-903.

Oestreich, A. J., Davies, B. A., Payne, J. A. and Katzmann, D. J. (2007). Mvb12 is a novel member of ESCRT-I involved in cargo selection by the multivesicular body pathway. *Mol Biol Cell* **18**, 646-57.

Oh, H., Mammucari, C., Nenci, A., Cabodi, S., Cohen, S. N. and Dotto, G. P. (2002). Negative regulation of cell growth and differentiation by TSG101 through association with p21(Cip1/WAF1). *Proc Natl Acad Sci U S A* **99**, 5430-5.

Oh, K. B., Stanton, M. J., West, W. W., Todd, G. L. and Wagner, K. U. (2007). Tsg101 is upregulated in a subset of invasive human breast cancers and its targeted overexpression in transgenic mice reveals weak oncogenic properties for mammary cancer initiation. *Oncogene* **26**, 5950-9.

Overstreet, E., Fitch, E. and Fischer, J. A. (2004). Fat facets and Liquid facets promote Delta endocytosis and Delta signaling in the signaling cells. *Development* **131**, 5355-66.

Pan, D. (2007). Hippo signaling in organ size control. *Genes Dev* **21**, 886-97.

Panin, V. M., Papayannopoulos, V., Wilson, R. and Irvine, K. D. (1997). Fringe modulates Notch-ligand interactions. *Nature* **387**, 908-12.

Pantalacci, S., Tapon, N. and Leopold, P. (2003). The Salvador partner Hippo promotes apoptosis and cell-cycle exit in Drosophila. *Nat Cell Biol* **5**, 921-7.

Parkinson, N., Ince, P. G., Smith, M. O., Highley, R., Skibinski, G., Andersen, P. M., Morrison, K. E., Pall, H. S., Hardiman, O., Collinge, J. et al. (2006). ALS phenotypes with mutations in CHMP2B (charged multivesicular body protein 2B). *Neurology*.

Pasternak, S. H., Bagshaw, R. D., Guiral, M., Zhang, S., Ackerley, C. A., Pak, B. J., Callahan, J. W. and Mahuran, D. J. (2003). Presenilin-1, nicastrin, amyloid precursor protein, and gamma-secretase activity are co-localized in the lysosomal membrane. *J Biol Chem* **278**, 26687-94.

Pavlopoulos, E., Pitsouli, C., Klueg, K. M., Muskavitch, M. A., Moschonas, N. K. and Delidakis, C. (2001). neuralized Encodes a peripheral membrane protein involved in delta signaling and endocytosis. *Dev Cell* **1**, 807-16.

Peck, J. W., Bowden, E. T. and Burbelo, P. D. (2004). Structure and function of human Vps20 and Snf7 proteins. *Biochem J* **377**, 693-700.

Perez-Garijo, A., Martin, F. A. and Morata, G. (2004). Caspase inhibition during apoptosis causes abnormal signalling and developmental aberrations in Drosophila. *Development* **131**, 5591-8.

Petcherski, A. G. and Kimble, J. (2000). LAG-3 is a putative transcriptional activator in the C. elegans Notch pathway. *Nature* **405**, 364-8.

Philips, J. A., Porto, M. C., Wang, H., Rubin, E. J. and Perrimon, N. (2008). ESCRT factors restrict mycobacterial growth. *Proc Natl Acad Sci U S A* **105**, 3070-5.

Polo, S. and Di Fiore, P. P. (2006). Endocytosis conducts the cell signaling orchestra. *Cell* **124**, 897-900.

Poodry, C. A. (1990). shibire, a neurogenic mutant of Drosophila. *Dev Biol* **138**, 464-72.

Pornillos, O., Alam, S. L., Davis, D. R. and Sundquist, W. I. (2002a). Structure of the Tsg101 UEV domain in complex with the PTAP motif of the HIV-1 p6 protein. *Nat Struct Biol* **9**, 812-7.

Pornillos, O., Alam, S. L., Rich, R. L., Myszka, D. G., Davis, D. R. and Sundquist, W. I. (2002b). Structure and functional interactions of the Tsg101 UEV domain. *Embo J* **21**, 2397-406.

Pornillos, O., Garrus, J. E. and Sundquist, W. I. (2002c). Mechanisms of enveloped RNA virus budding. *Trends Cell Biol* **12**, 569-79.

Pornillos, O., Higginson, D. S., Stray, K. M., Fisher, R. D., Garrus, J. E., Payne, M., He, G. P., Wang, H. E., Morham, S. G. and Sundquist, W. I. (2003). HIV Gag mimics the Tsg101-recruiting activity of the human Hrs protein. *J Cell Biol* **162**, 425-34.

Prag, G., Watson, H., Kim, Y. C., Beach, B. M., Ghirlando, R., Hummer, G., Bonifacino, J. S. and Hurley, J. H. (2007). The Vps27/Hse1 complex is a GAT domain-based scaffold for ubiquitin-dependent sorting. *Dev Cell* **12**, 973-86.

Qi, H., Rand, M. D., Wu, X., Sestan, N., Wang, W., Rakic, P., Xu, T. and Artavanis-Tsakonas, S. (1999). Processing of the notch ligand delta by the metalloprotease Kuzbanian. *Science* **283**, 91-4.

Radtke, F. and Raj, K. (2003). The role of Notch in tumorigenesis: oncogene or tumour suppressor? *Nat Rev Cancer* **3**, 756-67.

Raiborg, C., Bache, K. G., Gillooly, D. J., Madshus, I. H., Stang, E. and Stenmark, H. (2002). Hrs sorts ubiquitinated proteins into clathrin-coated microdomains of early endosomes. *Nat Cell Biol* **4**, 394-8.

Raiborg, C., Bache, K. G., Mehlum, A., Stang, E. and Stenmark, H. (2001a). Hrs recruits clathrin to early endosomes. *Embo J* **20**, 5008-21.

Raiborg, C., Bremnes, B., Mehlum, A., Gillooly, D. J., D'Arrigo, A., Stang, E. and Stenmark, H. (2001b). FYVE and coiled-coil domains determine the specific localisation of Hrs to early endosomes. *J Cell Sci* **114**, 2255-63.

Raiborg, C., Rusten, T. E. and Stenmark, H. (2003). Protein sorting into multivesicular endosomes. *Curr Opin Cell Biol* **15**, 446-55.

Ray, W. J., Yao, M., Mumm, J., Schroeter, E. H., Saftig, P., Wolfe, M., Selkoe, D. J., Kopan, R. and Goate, A. M. (1999). Cell surface presenilin-1 participates in the gamma-secretase-like proteolysis of Notch. *J Biol Chem* **274**, 36801-7.

Raymond, C. K., Howald-Stevenson, I., Vater, C. A. and Stevens, T. H. (1992). Morphological classification of the yeast vacuolar protein sorting mutants: evidence for a prevacuolar compartment in class E vps mutants. *Mol Biol Cell* **3**, 1389-402.

Reid, E., Connell, J., Edwards, T. L., Duley, S., Brown, S. E. and Sanderson, C. M. (2005). The hereditary spastic paraplegia protein spastin interacts with the ESCRT-III complex-associated endosomal protein CHMP1B. *Hum Mol Genet* **14**, 19-38.

Reynolds-Kenneally, J. and Mlodzik, M. (2005). Notch signaling controls proliferation through cell-autonomous and non-autonomous mechanisms in the Drosophila eye. *Dev Biol* **285**, 38-48.

Reynolds, T. C., Smith, S. D. and Sklar, J. (1987). Analysis of DNA surrounding the breakpoints of chromosomal translocations involving the beta T cell receptor gene in human lymphoblastic neoplasms. *Cell* **50**, 107-17.

Richter, C., West, M. and Odorizzi, G. (2007). Dual mechanisms specify Doa4-mediated deubiquitination at multivesicular bodies. *Embo J* **26**, 2454-64.

Rodriguez, A., Oliver, H., Zou, H., Chen, P., Wang, X. and Abrams, J. M. (1999). Dark is a Drosophila homologue of Apaf-1/CED-4 and functions in an evolutionarily conserved death pathway. *Nat Cell Biol* **1**, 272-9.

Row, P. E., Liu, H., Hayes, S., Welchman, R., Charalabous, P., Hofmann, K., Clague, M. J., Sanderson, C. M. and Urbe, S. (2007). The MIT domain of UBPY constitutes a CHMP binding and endosomal localization signal required for efficient epidermal growth factor receptor degradation. *J Biol Chem* **282**, 30929-37.

Ruland, J., Sirard, C., Elia, A., MacPherson, D., Wakeham, A., Li, L., de la Pompa, J. L., Cohen, S. N. and Mak, T. W. (2001). p53 accumulation, defective cell proliferation, and early embryonic lethality in mice lacking tsg101. *Proc Natl Acad Sci U S A* **98**, 1859-64.

Russell, D. G. (2001). Mycobacterium tuberculosis: here today, and here tomorrow. *Nat Rev Mol Cell Biol* **2**, 569-77.

Rusten, T. E., Filimonenko, M., Rodahl, L. M., Stenmark, H. and Simonsen, A. (2007a). ESCRTing autophagic clearance of aggregating proteins. *Autophagy* **4**.

Rusten, T. E., Vaccari, T., Lindmo, K., Rodahl, L. M., Nezis, I. P., Sem-Jacobsen, C., Wendler, F., Vincent, J. P., Brech, A., Bilder, D. et al. (2007b). ESCRTs and Fab1 regulate distinct steps of autophagy. *Curr Biol* **17**, 1817-25.

Ryoo, H. D., Bergmann, A., Gonen, H., Ciechanover, A. and Steller, H. (2002). Regulation of Drosophila IAP1 degradation and apoptosis by reaper and ubcD1. *Nat Cell Biol* **4**, 432-8.

Ryoo, H. D., Gorenc, T. and Steller, H. (2004). Apoptotic cells can induce compensatory cell proliferation through the JNK and the Wingless signaling pathways. *Dev Cell* **7**, 491-501.

Sachse, M., Urbe, S., Oorschot, V., Strous, G. J. and Klumperman, J. (2002). Bilayered clathrin coats on endosomal vacuoles are involved in protein sorting toward lysosomes. *Mol Biol Cell* **13**, 1313-28.

Sakamoto, K., Ohara, O., Takagi, M., Takeda, S. and Katsube, K. (2002). Intracellular cell-autonomous association of Notch and its ligands: a novel mechanism of Notch signal modification. *Dev Biol* **241**, 313-26.

Sakata, T., Sakaguchi, H., Tsuda, L., Higashitani, A., Aigaki, T., Matsuno, K. and Hayashi, S. (2004). Drosophila Nedd4 regulates endocytosis of notch and suppresses its ligand-independent activation. *Curr Biol* **14**, 2228-36.

Saksena, S., Sun, J., Chu, T. and Emr, S. D. (2007). ESCRTing proteins in the endocytic pathway. *Trends Biochem Sci* **32**, 561-73.

Saucedo, L. J. and Edgar, B. A. (2007). Filling out the Hippo pathway. *Nat Rev Mol Cell Biol* **8**, 613-21.

Scheuring, S., Bodor, O., Rohricht, R. A., Muller, S., Beyer, A. and Kohrer, K. (1999). Cloning, characterisation, and functional expression of the Mus musculus SKD1 gene in yeast demonstrates that the mouse SKD1 and the yeast VPS4 genes are orthologues and involved in intracellular protein trafficking. *Gene* **234**, 149-59.

Scheuring, S., Rohricht, R. A., Schoning-Burkhardt, B., Beyer, A., Muller, S., Abts, H. F. and Kohrer, K. (2001). Mammalian cells express two VPS4 proteins both of which are involved in intracellular protein trafficking. *J Mol Biol* **312**, 469-80.

Schmidt, A. E., Miller, T., Schmidt, S. L., Shiekhattar, R. and Shilatifard, A. (1999). Cloning and characterization of the EAP30 subunit of the ELL complex that confers derepression of transcription by RNA polymerase II. *J Biol Chem* **274**, 21981-5.

Schmidt, M. H., Chen, B., Randazzo, L. M. and Bogler, O. (2003). SETA/CIN85/Ruk and its binding partner AIP1 associate with diverse cytoskeletal elements, including FAKs, and modulate cell adhesion. *J Cell Sci* **116**, 2845-55.

Schroeter, E. H., Kisslinger, J. A. and Kopan, R. (1998). Notch-1 signalling requires ligand-induced proteolytic release of intracellular domain. *Nature* **393**, 382-6.

Schweisguth, F. (2004). Regulation of notch signaling activity. *Curr Biol* **14**, R129-38.

Scott, A., Chung, H. Y., Gonciarz-Swiatek, M., Hill, G. C., Whitby, F. G., Gaspar, J., Holton, J. M., Viswanathan, R., Ghaffarian, S., Hill, C. P. et al. (2005a). Structural and mechanistic studies of VPS4 proteins. *Embo J* **24**, 3658-69.

Scott, A., Gaspar, J., Stuchell-Brereton, M. D., Alam, S. L., Skalicky, J. J. and Sundquist, W. I. (2005b). Structure and ESCRT-III protein interactions of the MIT domain of human VPS4A. *Proc Natl Acad Sci U S A* **102**, 13813-8.

Selkoe, D. and Kopan, R. (2003). Notch and Presenilin: regulated intramembrane proteolysis links development and degeneration. *Annu Rev Neurosci* **26**, 565-97.

Sen, A., Reddy, G. V. and Rodrigues, V. (2003). Combinatorial expression of Prospero, Seven-up, and Elav identifies progenitor cell types during sense-organ differentiation in the Drosophila antenna. *Dev Biol* **254**, 79-92.

Seto, E. S. and Bellen, H. J. (2004). The ins and outs of Wingless signaling. *Trends Cell Biol* **14**, 45-53.

Seto, E. S. and Bellen, H. J. (2006). Internalization is required for proper Wingless signaling in Drosophila melanogaster. *J Cell Biol* **173**, 95-106.

Seugnet, L., Simpson, P. and Haenlin, M. (1997). Requirement for dynamin during Notch signaling in Drosophila neurogenesis. *Dev Biol* **192**, 585-98.

Sevrioukov, E. A., Moghrabi, N., Kuhn, M. and Kramer, H. (2005). A mutation in dVps28 reveals a link between a subunit of the endosomal sorting complex required for transport-I complex and the actin cytoskeleton in Drosophila. *Mol Biol Cell* **16**, 2301-12.

Shih, S. C., Katzmann, D. J., Schnell, J. D., Sutanto, M., Emr, S. D. and Hicke, L. (2002). Epsins and Vps27p/Hrs contain ubiquitin-binding domains that function in receptor endocytosis. *Nat Cell Biol* **4**, 389-93.

Shilatifard, A. (1998). Identification and purification of the Holo-ELL complex. Evidence for the presence of ELL-associated proteins that suppress the transcriptional inhibitory activity of ELL. *J Biol Chem* **273**, 11212-7.

Silva, E., Tsatskis, Y., Gardano, L., Tapon, N. and McNeill, H. (2006). The Tumor-Suppressor Gene fat Controls Tissue Growth Upstream of Expanded in the Hippo Signaling Pathway. *Curr Biol* **16**, 2081-9.

Simpson, P. and Morata, G. (1981). Differential mitotic rates and patterns of growth in compartments in the Drosophila wing. *Dev Biol* **85**, 299-308.

Skibinski, G., Parkinson, N. J., Brown, J. M., Chakrabarti, L., Lloyd, S. L., Hummerich, H., Nielsen, J. E., Hodges, J. R., Spillantini, M. G., Thusgaard, T. et al. (2005). Mutations in the endosomal ESCRTIII-complex subunit CHMP2B in frontotemporal dementia. *Nat Genet* **37**, 806-8.

Slagsvold, T., Aasland, R., Hirano, S., Bache, K. G., Raiborg, C., Trambaiolo, D., Wakatsuki, S. and Stenmark, H. (2005). Eap45 in mammalian ESCRT-II binds ubiquitin via a phosphoinositide-interacting GLUE domain. *J Biol Chem* **280**, 19600-6.

Slagsvold, T., Pattni, K., Malerod, L. and Stenmark, H. (2006). Endosomal and non-endosomal functions of ESCRT proteins. *Trends Cell Biol* **16**, 317-26.

Song, Z., McCall, K. and Steller, H. (1997). DCP-1, a Drosophila cell death protease essential for development. *Science* **275**, 536-40.

Sorkin, A. and Von Zastrow, M. (2002). Signal transduction and endocytosis: close encounters of many kinds. *Nat Rev Mol Cell Biol* **3**, 600-14.

Spitzer, C., Schellmann, S., Sabovljevic, A., Shahriari, M., Keshavaiah, C., Bechtold, N., Herzog, M., Muller, S., Hanisch, F. G. and Hulskamp, M. (2006). The Arabidopsis elch mutant reveals functions of an ESCRT component in cytokinesis. *Development* **133**, 4679-89.

Srivastava, M., Scherr, H., Lackey, M., Xu, D., Chen, Z., Lu, J. and Bergmann, A. (2007). ARK, the Apaf-1 related killer in Drosophila, requires diverse domains for its apoptotic activity. *Cell Death Differ* **14**, 92-102.

Stauffer, D. R., Howard, T. L., Nyun, T. and Hollenberg, S. M. (2001). CHMP1 is a novel nuclear matrix protein affecting chromatin structure and cell-cycle progression. *J Cell Sci* **114**, 2383-93.

Steiner, P., Barnes, D. M., Harris, W. H. and Weinberg, R. A. (1997). Absence of rearrangements in the tumour susceptibility gene TSG101 in human breast cancer. *Nat Genet* **16**, 332-3.

Struhl, G. and Adachi, A. (2000). Requirements for presenilin-dependent cleavage of notch and other transmembrane proteins. *Mol Cell* **6**, 625-36.

Struhl, G. and Greenwald, I. (1999). Presenilin is required for activity and nuclear access of Notch in Drosophila. *Nature* **398**, 522-5.

Stuchell-Brereton, M. D., Skalicky, J. J., Kieffer, C., Karren, M. A., Ghaffarian, S. and Sundquist, W. I. (2007). ESCRT-III recognition by VPS4 ATPases. *Nature* **449**, 740-4.

Stuchell, M. D., Garrus, J. E., Muller, B., Stray, K. M., Ghaffarian, S., McKinnon, R., Krausslich, H. G., Morham, S. G. and Sundquist, W. I. (2004). The human endosomal sorting complex required for transport (ESCRT-I) and its role in HIV-1 budding. *J Biol Chem* **279**, 36059-71.

Sun, Z., Pan, J., Bubley, G. and Balk, S. P. (1997). Frequent abnormalities of TSG101 transcripts in human prostate cancer. *Oncogene* **15**, 3121-5.

Sun, Z., Pan, J., Hope, W. X., Cohen, S. N. and Balk, S. P. (1999). Tumor susceptibility gene 101 protein represses androgen receptor transactivation and interacts with p300. *Cancer* **86**, 689-96.

Sweeney, N. T., Brenman, J. E., Jan, Y. N. and Gao, F. B. (2006). The coiled-coil protein shrub controls neuronal morphogenesis in Drosophila. *Curr Biol* **16**, 1006-11.

Tamura, K., Taniguchi, Y., Minoguchi, S., Sakai, T., Tun, T., Furukawa, T. and Honjo, T. (1995). Physical interaction between a novel domain of the receptor Notch and the transcription factor RBP-J kappa/Su(H). *Curr Biol* **5**, 1416-23.

Tanaka, N., Kyuuma, M. and Sugamura, K. (2008). Endosomal sorting complex required for transport proteins in cancer pathogenesis, vesicular transport, and non-endosomal functions. *Cancer Sci*.

Tarassishin, L., Yin, Y. I., Bassit, B. and Li, Y. M. (2004). Processing of Notch and amyloid precursor protein by gamma-secretase is spatially distinct. *Proc Natl Acad Sci U S A* **101**, 17050-5.

Taylor, R. C., Cullen, S. P. and Martin, S. J. (2008). Apoptosis: controlled demolition at the cellular level. *Nat Rev Mol Cell Biol* **9**, 231-41.

Teo, H., Gill, D. J., Sun, J., Perisic, O., Veprintsev, D. B., Vallis, Y., Emr, S. D. and Williams, R. L. (2006). ESCRT-I core and ESCRT-II GLUE domain structures reveal role for GLUE in linking to ESCRT-I and membranes. *Cell* **125**, 99-111.

Teo, H., Perisic, O., Gonzalez, B. and Williams, R. L. (2004). ESCRT-II, an endosome-associated complex required for protein sorting: crystal structure and interactions with ESCRT-III and membranes. *Dev Cell* **7**, 559-69.

ter Haar, E., Harrison, S. C. and Kirchhausen, T. (2000). Peptide-in-groove interactions link target proteins to the beta-propeller of clathrin. *Proc Natl Acad Sci U S A* **97**, 1096-100.

Thery, C., Zitvogel, L. and Amigorena, S. (2002). Exosomes: composition, biogenesis and function. *Nat Rev Immunol* **2**, 569-79.

Thompson, B. J., Mathieu, J., Sung, H. H., Loeser, E., Rorth, P. and Cohen, S. M. (2005). Tumor suppressor properties of the ESCRT-II complex component Vps25 in Drosophila. *Dev Cell* **9**, 711-20.

Tian, X., Hansen, D., Schedl, T. and Skeath, J. B. (2004). Epsin potentiates Notch pathway activity in Drosophila and C. elegans. *Development* **131**, 5807-15.

Toyoshima, M., Tanaka, N., Aoki, J., Tanaka, Y., Murata, K., Kyuuma, M., Kobayashi, H., Ishii, N., Yaegashi, N. and Sugamura, K. (2007). Inhibition of tumor growth and metastasis by depletion of vesicular sorting protein Hrs: its regulatory role on E-cadherin and beta-catenin. *Cancer Res* **67**, 5162-71.

Trajkovic, K., Hsu, C., Chiantia, S., Rajendran, L., Wenzel, D., Wieland, F., Schwille, P., Brugger, B. and Simons, M. (2008). Ceramide triggers budding of exosome vesicles into multivesicular endosomes. *Science* **319**, 1244-7.

Tsai, Y. C. and Sun, Y. H. (2004). Long-range effect of upd, a ligand for Jak/STAT pathway, on cell cycle in Drosophila eye development. *Genesis* **39**, 141-53.

Tsang, H. T., Connell, J. W., Brown, S. E., Thompson, A., Reid, E. and Sanderson, C. M. (2006). A systematic analysis of human CHMP protein interactions: additional MIT domain-containing proteins bind to multiple components of the human ESCRT III complex. *Genomics* **88**, 333-46.

Udan, R. S., Kango-Singh, M., Nolo, R., Tao, C. and Halder, G. (2003). Hippo promotes proliferation arrest and apoptosis in the Salvador/Warts pathway. *Nat Cell Biol* **5**, 914-20.

Urbanowski, J. L. and Piper, R. C. (2001). Ubiquitin sorts proteins into the intralumenal degradative compartment of the late-endosome/vacuole. *Traffic* **2**, 622-30.

Uyttendaele, H., Marazzi, G., Wu, G., Yan, Q., Sassoon, D. and Kitajewski, J. (1996). Notch4/int-3, a mammary proto-oncogene, is an endothelial cell-specific mammalian Notch gene. *Development* **122**, 2251-9.

Vaccari, T. and Bilder, D. (2005). The Drosophila tumor suppressor vps25 prevents nonautonomous overproliferation by regulating notch trafficking. *Dev Cell* **9**, 687-98.

Vaccari, T., Lu, H., Kanwar, R., Fortini, M. E. and Bilder, D. (2008). Endosomal entry regulates Notch receptor activation in Drosophila melanogaster. *J Cell Biol* **180**, 755-62.

Vajjhala, P. R., Catchpoole, E., Nguyen, C. H., Kistler, C. and Munn, A. L. (2007). Vps4 regulates a subset of protein interactions at the multivesicular endosome. *Febs J* **274**, 1894-907.

van der Bliek, A. M. and Meyerowitz, E. M. (1991). Dynamin-like protein encoded by the Drosophila shibire gene associated with vesicular traffic. *Nature* **351**, 411-4.

Vetrivel, K. S., Cheng, H., Lin, W., Sakurai, T., Li, T., Nukina, N., Wong, P. C., Xu, H. and Thinakaran, G. (2004). Association of gamma-secretase with lipid rafts in post-Golgi and endosome membranes. *J Biol Chem* **279**, 44945-54.

Vieira, O. V., Harrison, R. E., Scott, C. C., Stenmark, H., Alexander, D., Liu, J., Gruenberg, J., Schreiber, A. D. and Grinstein, S. (2004). Acquisition of Hrs, an essential component of phagosomal maturation, is impaired by mycobacteria. *Mol Cell Biol* **24**, 4593-604.

von Schwedler, U. K., Stuchell, M., Muller, B., Ward, D. M., Chung, H. Y., Morita, E., Wang, H. E., Davis, T., He, G. P., Cimbora, D. M. et al. (2003). The protein network of HIV budding. *Cell* **114**, 701-13.

von Zastrow, M. and Sorkin, A. (2007). Signaling on the endocytic pathway. *Curr Opin Cell Biol* **19**, 436-45.

Wagner, K. U., Krempler, A., Qi, Y., Park, K., Henry, M. D., Triplett, A. A., Riedlinger, G., Rucker, I. E. and Hennighausen, L. (2003). Tsg101 is essential for cell growth, proliferation, and cell survival of embryonic and adult tissues. *Mol Cell Biol* **23**, 150-62.

Wang, W. and Struhl, G. (2004). Drosophila Epsin mediates a select endocytic pathway that DSL ligands must enter to activate Notch. *Development* **131**, 5367-80.

Weijzen, S., Rizzo, P., Braid, M., Vaishnav, R., Jonkheer, S. M., Zlobin, A., Osborne, B. A., Gottipati, S., Aster, J. C., Hahn, W. C. et al. (2002). Activation of Notch-1 signaling maintains the neoplastic phenotype in human Ras-transformed cells. *Nat Med* **8**, 979-86.

Wells, B. S., Yoshida, E. and Johnston, L. A. (2006). Compensatory Proliferation in Drosophila Imaginal Discs Requires Dronc-Dependent p53 Activity. *Curr Biol* **16**, 1606-15.

Welsch, S., Muller, B. and Krausslich, H. G. (2007). More than one door - Budding of enveloped viruses through cellular membranes. *FEBS Lett* **581**, 2089-97.

Weng, A. P., Ferrando, A. A., Lee, W., Morris, J. P. t., Silverman, L. B., Sanchez-Irizarry, C., Blacklow, S. C., Look, A. T. and Aster, J. C. (2004). Activating mutations of NOTCH1 in human T cell acute lymphoblastic leukemia. *Science* **306**, 269-71.

Wernimont, A. K. and Weissenhorn, W. (2004). Crystal structure of subunit VPS25 of the endosomal trafficking complex ESCRT-II. *BMC Struct Biol* **4**, 10.

Weston, C. R. and Davis, R. J. (2007). The JNK signal transduction pathway. *Curr Opin Cell Biol* **19**, 142-9.

White, K., Grether, M. E., Abrams, J. M., Young, L., Farrell, K. and Steller, H. (1994). Genetic control of programmed cell death in Drosophila. *Science* **264**, 677-83.

Wilkin, M. B., Carbery, A. M., Fostier, M., Aslam, H., Mazaleyrat, S. L., Higgs, J., Myat, A., Evans, D. A., Cornell, M. and Baron, M. (2004). Regulation of notch endosomal sorting and signaling by Drosophila Nedd4 family proteins. *Curr Biol* **14**, 2237-44.

Willecke, M., Hamaratoglu, F., Kango-Singh, M., Udan, R., Chen, C. L., Tao, C., Zhang, X. and Halder, G. (2006). The Fat Cadherin Acts through the Hippo Tumor-Suppressor Pathway to Regulate Tissue Size. *Curr Biol* **16**, 2090-100.

Williams, R. L. and Urbe, S. (2007). The emerging shape of the ESCRT machinery. *Nat Rev Mol Cell Biol* **8**, 355-68.

Wirblich, C., Bhattacharya, B. and Roy, P. (2006). Nonstructural protein 3 of bluetongue virus assists virus release by recruiting ESCRT-I protein Tsg101. *J Virol* **80**, 460-73.

Wolfe, M. S., Xia, W., Ostaszewski, B. L., Diehl, T. S., Kimberly, W. T. and Selkoe, D. J. (1999). Two transmembrane aspartates in presenilin-1 required for presenilin endoproteolysis and gamma-secretase activity. *Nature* **398**, 513-7.

Wu, L., Aster, J. C., Blacklow, S. C., Lake, R., Artavanis-Tsakonas, S. and Griffin, J. D. (2000). MAML1, a human homologue of Drosophila mastermind, is a transcriptional co-activator for NOTCH receptors. *Nat Genet* **26**, 484-9.

Wu, S., Huang, J., Dong, J. and Pan, D. (2003). hippo encodes a Ste-20 family protein kinase that restricts cell proliferation and promotes apoptosis in conjunction with salvador and warts. *Cell* **114**, 445-56.

Xie, W., Li, L. and Cohen, S. N. (1998). Cell cycle-dependent subcellular localization of the TSG101 protein and mitotic and nuclear abnormalities associated with TSG101 deficiency. *Proc Natl Acad Sci U S A* **95**, 1595-600.

Xie, Z. and Klionsky, D. J. (2007). Autophagosome formation: core machinery and adaptations. *Nat Cell Biol* **9**, 1102-9.

Xu, D., Li, Y., Arcaro, M., Lackey, M. and Bergmann, A. (2005). The CARD-carrying caspase Dronc is essential for most, but not all, developmental cell death in Drosophila. *Development* **132**, 2125-34.

Xu, T. and Rubin, G. M. (1993). Analysis of genetic mosaics in developing and adult Drosophila tissues. *Development* **117**, 1223-37.

Yamada, M., Takeshita, T., Miura, S., Murata, K., Kimura, Y., Ishii, N., Nose, M., Sakagami, H., Kondo, H., Tashiro, F. et al. (2001). Loss of hippocampal CA3 pyramidal neurons in mice lacking STAM1. *Mol Cell Biol* **21**, 3807-19.

Ye, Y., Lukinova, N. and Fortini, M. E. (1999). Neurogenic phenotypes and altered Notch processing in Drosophila Presenilin mutants. *Nature* **398**, 525-9.

Yeh, E., Dermer, M., Commisso, C., Zhou, L., McGlade, C. J. and Boulianne, G. L. (2001). Neuralized functions as an E3 ubiquitin ligase during Drosophila development. *Curr Biol* **11**, 1675-9.

Yoo, S. J., Huh, J. R., Muro, I., Yu, H., Wang, L., Wang, S. L., Feldman, R. M., Clem, R. J., Muller, H. A. and Hay, B. A. (2002). Hid, Rpr and Grim negatively regulate DIAP1 levels through distinct mechanisms. *Nat Cell Biol* **4**, 416-24.

Yorikawa, C., Shibata, H., Waguri, S., Hatta, K., Horii, M., Katoh, K., Kobayashi, T., Uchiyama, Y. and Maki, M. (2005). Human CHMP6, a myristoylated ESCRT-III protein, interacts directly with an ESCRT-II component EAP20 and regulates endosomal cargo sorting. *Biochem J* **387**, 17-26.

Yoshimori, T., Yamagata, F., Yamamoto, A., Mizushima, N., Kabeya, Y., Nara, A., Miwako, I., Ohashi, M., Ohsumi, M. and Ohsumi, Y. (2000). The mouse SKD1, a homologue of yeast Vps4p, is required for normal endosomal trafficking and morphology in mammalian cells. *Mol Biol Cell* **11**, 747-63.

Yu, S. Y., Yoo, S. J., Yang, L., Zapata, C., Srinivasan, A., Hay, B. A. and Baker, N. E. (2002). A pathway of signals regulating effector and initiator caspases in the developing Drosophila eye. *Development* **129**, 3269-78.

Zamborlini, A., Usami, Y., Radoshitzky, S. R., Popova, E., Palu, G. and Gottlinger, H. (2006). Release of autoinhibition converts ESCRT-III components into potent inhibitors of HIV-1 budding. *Proc Natl Acad Sci U S A* **103**, 19140-5.

Zhai, R. G., Hiesinger, P. R., Koh, T. W., Verstreken, P., Schulze, K. L., Cao, Y., Jafar-Nejad, H., Norga, K. K., Pan, H., Bayat, V. et al. (2003). Mapping Drosophila mutations with molecularly defined P element insertions. *Proc Natl Acad Sci U S A* **100**, 10860-5.

Zhou, L., Song, Z., Tittel, J. and Steller, H. (1999). HAC-1, a Drosophila homolog of APAF-1 and CED-4 functions in developmental and radiation-induced apoptosis. *Mol Cell* **4**, 745-55.

Zhou, S., Fujimuro, M., Hsieh, J. J., Chen, L., Miyamoto, A., Weinmaster, G. and Hayward, S. D. (2000). SKIP, a CBF1-associated protein, interacts with the ankyrin repeat domain of NotchIC To facilitate NotchIC function. *Mol Cell Biol* **20**, 2400-10.